THE UNIVERSITY OF ALBERTA

RADIOLYSIS OF METHYLCYCLOPENTANE

BY

ELEANOR DIANE STOVER

A THESIS

SUBMITTED TO THE FACULTY OF GRADUATE STUDIES

IN PARTIAL FULFILMENT OF THE REQUIREMENTS FOR THE DEGREE

OF DOCTOR OF PHILOSOPHY

DEPARTMENT OF CHEMISTRY

EDMONTON, ALBERTA

AUGUST, 1967

UNIVERSITY OF ALBERTA

FACULTY OF GRADUATE STUDIES

The undersigned certify that they have read, and recommend to the Faculty of Graduate Studies for acceptance, a thesis entitled RADIOLYSIS OF METHYLCYCLOPENTANE submitted by ELEANOR DIANE STOVER in partial fulfilment of the requirements for the degree of Doctor of Philosophy.

ABSTRACT

The ^{60}Co γ radiolysis of methylcyclopentane has been studied in the pure state and with various additives. The G values of the major products extrapolated to zero dose are hydrogen (4.2), methane (0.12), 1-methylcyclopentene (2.7), 3-methylcyclopentene (0.8), hexene (1.0), bimethylcyclopentyl (0.9) and methylcyclopentylmethylcyclopentene (0.2). The dimers and most of the methylcyclopentenes are formed by the combination and disproportionation of methylcyclopentyl radicals.

The yields of all of these major products are decreased by the addition of 1,3-cyclohexadiene and of benzene to methylcyclopentane. For the liquid products and methane most of this decrease is due to radical scavenging by the additives. The liquid products and hydrogen yields were also decreased by the addition of CO_2. Methane was unaffected. When ND_3 was added, all liquid products except hexene increased in yield. This is probably due to positive ion scavenging by ND_3 to form more methylcyclopentyl radicals than are present in the pure system.

Nonhomogeneous kinetics were applied to the hydrogen yields of all systems containing additives and to the nitrogen yields from N_2O addition. From the values of the parameters needed to fit curves to the experimental results it was found that N_2O, CO_2, SF_6 and 1,3-cyclohexadiene were electron scavengers while ND_3 and benzene scavenge positive ions. In addition to ion scavenging, 1,3-cyclohexadiene and

benzene reduce the hydrogen yield further by either H atom scavenging or energy transfer mechanisms.

The hydrogen yield is thus composed of three parts, g = 1.8 from ions, g = 1.72 to 1.90 from hydrogen atoms or energy transfer and g = 0.5 to 0.68 of molecular hydrogen which is unscavengeable.

From the positive ion scavenging by ND_3 it was found that the total yield of ions formed on radiolysis is between 2.9 and 3.6 g units.

ACKNOWLEDGEMENTS

The author would like to thank Dr. G. R. Freeman for his guidance and interest during this study.

The author wishes to express her gratitude to her mother, Mrs. V. L. Stover, for her help in proof-reading and her patience and understanding throughout the project.

The author also wishes to thank Mrs. Gail Conway for typing the final draft of the thesis.

The assistance of and many helpful discussions with the members of the radiation chemistry group is gratefully acknowledged.

TABLE OF CONTENTS

LIST OF FIGURES

LIST OF TABLES

I. INTRODUCTION

A. Radiation Chemistry

1. Definition

Radiation chemistry is the study of the chemical effects of ionizing radiation on matter. The ionizing radiation used includes radiation produced by radioactive nuclei (alpha, beta and gamma rays), high energy charged particles (electrons, protons, etc.) and x-rays. The energy of the radiation is spent in exciting or ionizing a large number of molecules along the paths of charged particles and forming a mixture of excited molecules, ions and radicals.

2. Radiation Source

Gamma radiation from ^{60}Co was used in this study. ^{60}Co is formed in a nuclear reactor from ^{59}Co by the absorption of a neutron (1). It decays to ^{60}Ni with the emission of a β ray of maximum energy 0.314 MeV and two γ rays of energy 1.33 MeV and 1.17 MeV. The range of a 0.314 MeV β ray in glass is 0.5 mm (2) so that no β rays penetrate the sample cell and the radiation effects are due solely to γ rays of average energy 1.25 MeV.

3. History

Radiation chemistry came into existence as a field of investigation shortly after the discovery of x-rays by Roentgen (1895) and of radio-activity by Becquerel (1896). The first chemical effects of radiation were observed in water by Curie and by Debierne (3). It was thought

that radiation affected the water as an electrolysis, since the products were hydrogen and oxygen gases. Later Mme. Curie suggested that the primary act of radiation was ionization. During his studies of the amount of ozone produced by alpha particles from radon acting on O_2, Lind defined the ion pair yield, M/N, which is the number of molecules converted per ion pair formed (4). He found that M/N was frequently greater than unity and interpreted this as being the result of ion clustering in which a single molecule ion would be surrounded by one or more molecules, adhering to it through induced dipole forces. The ion cluster, on neutralization with an electron, could produce several products from the single ion. In 1936, Eyring, Hirschfelder and Taylor (5) calculated that in hydrogen gas at 1 atmosphere pressure, clusters involving a large number of hydrogen molecules were not probable. They proposed the existence of ion molecule reactions and the decomposition of excited molecules into free radicals which could then take part in chain reactions. This would explain the very high product yield in the conversion of para to ortho hydrogen.

Since free radical mechanisms could account for the results obtained from most hydrocarbon radiolyses, for many years the importance of ions in the system was overlooked. However, lately a number of investigators (6-8) have been studying the role of ions in radiolytic systems.

Interest in radiation chemistry increased greatly in the middle

1940's with the development of atomic reactors.

B.   Stages of the Radiolytic Process

It is possible to set up a time scale for the reactions occurring in a radiolytic system (Fig. I-1).   The events have been divided into three stages by Platzman (9) and Kupperman (10).

1.   Physical Stage

This stage concerns the processes by which radiant energy is transferred to the system.   Ions and excited atoms and molecules are produced in less than about 10^{-15} sec.   During this time, secondary electrons of varying energies are formed through ionization by primary (Compton) electrons.   These secondary electrons may cause further ionization and excitation.   This stage will be discussed more fully in section C.

2.   Physicochemical Stage

During this stage, which lasts about 10^{-12} sec, excited species reach thermal equilibrium.   Dissociation of excited molecules, ion molecule reactions and energy transfer occur.   The fate of the secondary electrons is also determined within this period.   There have been two divergent theories proposed concerning these electrons in water. Samuel and Magee (11) use a classical model to calculate that the electron, upon losing energy by inelastic collisions, will return to the parent ion in less than 10^{-13} sec, forming an excited neutral molecule.   These excited molecules could then decompose into H and OH radicals in close

Figure I-1

Time Scale for Reactions Occurring in a Radiolytic System

Physical Stage
Ions and excited atoms and molecules are formed
(Spur formation)

Physicochemical Stage
Free radical formation
Ion molecule reactions

Chemical Stage
Diffusion of spurs
Reactions in spurs
Reactions in bulk

-15   -12   -7

$\text{Log} \left[\text{time (sec)} \right]$

proximity. According to Platzman (12), the electron loses energy by causing bond dipole vibration and rotation of solvent molecules until it has travelled at least 50 $\overset{o}{A}$ from the parent ion in 10^{-12} sec. It then becomes solvated and reacts to form H atoms while the parent ion undergoes reaction 50 $\overset{o}{A}$ away to form OH radicals. Various experimental results tend to support either mechanism so that the actual mechanism remains unsettled.

3. Chemical Stage

The third stage consists of chemical reaction of the reactive species in the spurs (small regions of high local concentration of reactive species) and later in the bulk solution. Diffusion of the reactive species within and away from the spurs also occurs. Radicals in a spur may react in about 10^{-12} to 10^{-8} seconds, however, by the time that the spur has increased by two orders of magnitude in volume, about 10^{-7} seconds have elapsed. Following this expansion of the spur , reactions continue to take place in the bulk solution. The reactions of ions and free radicals will be discussed in a later section.

C. Interaction of γ Radiation with Matter (Physical Stage)

1. Energy Transfer from Electromagnetic Radiation

Photons lose a large part of their energy with each interaction. The reduction in intensity of the photon beam as it passes through the absorber is given, in integrated form, by

$$I = I_o e^{-\mu x}$$

[1]

where I_0 and I are the beam intensities before and after passage through the absorber of thickness x and μ is the linear absorption coefficient. This absorption coefficient is the sum of several coefficients representing various processes. The particular processes of absorption taking place depend on the energy of the incident photons. In radiolytic studies the most important of these processes are the photoelectric effect, the Compton effect and pair production.

a. Photoelectric Effect

The photoelectric effect is important at photon energies less than 0.1 MeV in light atoms. In this process, the incident photon transfers all of its energy to a single atom or molecule, which may then eject an electron with an energy equal to that of the incident photon less the binding energy of the electron in the atom or molecule. The electron ejected will be the one with a binding energy nearest to, but below, the energy of the photon. Thus for photon energies greater than the K shell binding energy, about 80% of the electrons ejected will be from the K shell with most of the remainder from the L shell (13). Empirically, the atomic absorption coefficient, $_a\tau$, is approximately proportional to the fourth power of the atomic number and decreases rapidly with increasing energy.

b. The Compton Effect

The Compton effect is important for photon energies between about 0.01 and 100 MeV. The photon interacts with an electron, giving

up part of its energy to the electron and ejecting it while being deflected with a reduced energy. The kinetic energy of the ejected electron is given by

$$T = h(\Delta \nu) - w \qquad [2]$$

where $\Delta \nu$ is the change in frequency of the photon during the interaction and w is the binding energy of the electron. Unlike the photoelectric effect, the Compton process may occur with either a bound or a free electron. The atomic Compton absorption coefficient, $_a\sigma$, is proportional to the atomic number or the number of electrons in the atom, thus the relative amount of absorption by different compounds is proportional to their electron densities. The absorption coefficient may be divided into two parts. One part, σ_a, represents the energy transferred to the ejected electron and the other part, σ_s, the energy remaining with the scattered photon. At low photon energy, σ_a is approximately zero since the photons are scattered but transfer little energy to the electrons. At high photon energies $\sigma_a \sim 3\sigma_s$ and in the region of ^{60}Co γ rays (i.e. 1.25 MeV), $\sigma_a = \sigma_s$ and the average energy of the ejected electron is 0.625 MeV.

    c. Pair Production

Pair production is of importance at energies above about 5 MeV. In this process a photon interacts with the nuclear field of an atom producing an electron and a positron. The sum of the kinetic energies of the positron and electron is the energy of the incident photon less the

rest energies of the two electrons, $2m_oc^2 = 1.02$ MeV. The positron

is slowed down and finally annihilated by an electron producing two

0.51 MeV γ rays. The atomic pair production absorption coefficient,

$_a K$, is proportional to the square of the atomic number.

The composition of the total mass absorption coefficient, μ/ρ,

for all three processes in water is shown in Figure I-2 (14). It is

given by

$$\mu/\rho = \sigma_a/\rho + \sigma_s/\rho + \tau/\rho + K/\rho \qquad [3]$$

where σ_a/ρ is the true Compton mass absorption coefficient,

σ_s/ρ is the scattering Compton mass absorption coefficient,

τ/ρ is the Photoelectric mass absorption coefficient,

K/ρ is the pair production mass absorption coefficient,

and ρ is the density of the medium.

It is evident from Fig. I-2 that for the 1.25 MeV γ rays used in this

investigation, the only process of importance is the Compton effect.

2. Energy Transfer from Compton Electrons

a. Energy loss by inelastic collision

The recoil electrons produced by the Compton effect lose their

energy mainly by inelastic collisions with molecules in the medium.

The products of the collisions are excited and ionized molecules which

are formed along the path or track of the Compton electrons. The

rate of energy loss of a high energy electron per unit path length was

derived by Bethe (15) to be:

Figure I-2

The Composition of the Total Mass Absorption Coefficient

Water

Mass Absorption Coefficient (cm²/gm)

Photon Energy (MeV)

$$-\left(\frac{dT}{dx}\right)_{coll} = \frac{2\pi e^4 ZN}{m_0 v^2}\left[\ln\frac{m_0 v^2 T}{2I^2(1-\beta^2)} - (2\sqrt{1-\beta^2}-1+\beta^2)\ln 2 + (1-\beta^2)\right.$$

$$\left. + \frac{1}{8}(1-\sqrt{1-\beta^2})^2\right] \tag{4}$$

where Z is the number of electrons/atom, N is the number of atoms/cc, m_0 is the rest mass of the electron, v is the velocity of the electron, I is the average excitation potential of the atom, $\beta = v/c$ and c is the velocity of light and T is the relativistic kinetic energy of the electron. The equation assumes that the velocity of the incident electron is greater than that of the orbital electrons.

b. Energy loss by radiation

The production of x-rays (Bremsstrahlung) by the negative acceleration of electrons is an inefficient process at energies below 1 MeV so that this process is negligible for Compton electrons produced by ^{60}Co γ rays.

D. Reactions of Excited Molecules, Ions and Free Radicals (Chemical Stage)

1. Excited Molecules

Excited molecules may be formed by the direct action of radiation or by the neutralization of ions formed. There are a number of paths by which these excited molecules may lose their excess energy.

a. Photoemission

Electronically excited molecules may lose energy by emitting radiation and returning to the ground state.

$$M* \longrightarrow M + h\nu \qquad\qquad [5]$$

b. Unimolecular reactions

i. Dissociation to free radicals

The excited molecules may, if they have greater than the bond

dissociation energy, dissociate to give free radicals,

$$MN* \longrightarrow M\cdot + \cdot N \qquad\qquad [6]$$

The radicals formed usually contain an excess of energy.   Possible

reactions of these radicals will be discussed later.

ii. Dissociation to molecules

New molecules may be formed by the dissociation of an excited

molecule.   One example of this is the formation of part of the "mole-

cular" yields of hydrogen and low molecular weight products in alkane

radiolyses.   For example, Dorfman (16, 17) has found that about

half of the hydrogen yield in ethane radiolysis of mixtures of C_2H_6

and C_2D_6 is due to molecular detachment of H_2 (or D_2).   In the liquid

phase, Dyne (18) has postulated the following reactions in the radiolysis

of $c\text{-}C_6H_{12} - c\text{-}C_6D_{12}$ mixtures.

$$c\text{-}C_6D_{12}* \longrightarrow c\text{-}C_6D_{10} + D_2 \qquad\qquad [7]$$

and $\quad c\text{-}C_6H_{12}* \longrightarrow c\text{-}C_6H_{10} + H_2 \qquad\qquad [8]$

iii. Isomerization

Intramolecular rearrangement is possible in polyatomic excited

molecules.   The most common type studied is cis-trans isomerism in

olefins.   For example, in the radiolysis of trans stilbene in benzene,

isomerization occurs via the triplet state of stilbene (19).

C. Bimolecular reactions

If the acceptor has an energy level the same as or below the excited level of the donor, energy transfer can occur. This process has been postulated for the "protecting" action of benzene in the radiolysis of cyclohexane-benzene mixtures (20). Generally, compounds containing π bonds have lower excitation potentials than ones containing only σ bonds so that olefins might also be expected to be involved in energy transfer mechanisms.

Quenching also involves the conversion of an excited molecule to the ground state or to a more stable excited state. Electronic excitation energy may be converted to vibrational energy in the ground electronic state of the originally excited molecule. The quencher itself may become electronically excited.

Stern-Volmer reactions involving the interchange of atoms between two molecules, at least one of which is excited, may occur to form products.

2. Ions

a. Unimolecular ionic reactions

i. Isomerization

Unimolecular isomerization has been proposed in some radiolytic systems (21) to explain the products formed. However, absolute evidence for this mechanism has not been obtained. In solutions of methylcyclo-

pentane containing a strongly electrophilic reagent, the isomerization

of the tertiary carbonium ion has been postulated (22) to account for

the formation of cyclohexane.

$$[9]$$

followed by

$$[10]$$

ii. Dissociation

Most positive ions formed by ionizing radiation will be vibration-

ally excited and some may dissociate into smaller ions and molecules

or radical ions and radicals. This reaction is observed in the mass

spectrometer in the gas phase. Futrell (23) has proposed this mechanism

to explain some of the products of hexane radiolysis.

b. Bimolecular ionic reactions

i. Ion molecule reactions

Ion molecule reactions may be observed in the mass spectrometer

at higher pressures than normal. These reactions in the gas phase are

of the type (24)

$$C_4H_6^+ + C_4H_6 = C_7H_9^+ + CH_3 \qquad [11]$$
$$= C_6H_8^+ + C_2H_4 \qquad [12]$$
$$= C_6H_7^+ + C_2H_5 \qquad [13]$$
$$= C_6H_6^+ + C_2H_6 \qquad [14]$$

In the liquid phase, ion molecule reactions of the sort

$$C_5H_{12}^+ \; + \; (CD_2)_3 \; = \; CD_2HCD_2CD_2H \; + \; C_5H_{10}^+ \qquad [15]$$

have been postulated by Scala et al (25).

ii. Charge transfer

This reaction may occur if the ionization potential of the neutral molecule is less than or equal to the ionization potential of the neutral form of the ion. An example of this is given by Hardwick (26)

$$n\text{-}C_6H_{14}^+ \; + \; neo\text{-}C_6H_{14} \; \longrightarrow \; n\text{-}C_6H_{14} + neo\text{-}C_6H_{14}^+ \qquad [16]$$

and more recently by Stone et al (27).

$$R_1H^+ \; + \; R_2D \; \longrightarrow \; R_1H \; + \; R_2D^+ \qquad [17]$$

iii. Electron addition

In saturated hydrocarbon systems, the capture of an electron to form a negatively charged ion does not occur.

3. **Free Radicals**

Free radicals are formed by the dissociation of excited species. If the radicals are able to escape their "cage" of formation they may react in a number of ways. The cyclohexyl radical may undergo the following reactions:

a. Abstraction

$$c\text{-}C_6H_{11}\cdot \; + \; RH \; \longrightarrow \; c\text{-}C_6H_{12} \; + \; R\cdot \qquad [18]$$

b. Combination

$$2 \, c\text{-}C_6H_{11}\cdot \; \longrightarrow \; (c\text{-}C_6H_{11})_2 \qquad [19]$$

c. Disproportionation

$$2 \; c\text{-}C_6H_{11}\text{\textbullet} \quad \longrightarrow \quad c\text{-}C_6H_{10} \; + \; c\text{-}C_6H_{12} \qquad [20]$$

d. Addition to an olefin double bond

$$c\text{-}C_6H_{11}\text{\textbullet} + \quad \text{\textbackslash}C\text{-}C\text{/} \quad \longrightarrow \quad c\text{-}C_6H_{11}\text{-}C\text{-}C\text{/} \text{\textbullet} \qquad [21]$$

E. Alkane Radiolysis

1. General Features

An excellent review on liquid hydrocarbon radiolysis has recently appeared in the literature (28).

a. Products

The products formed during the radiolysis of alkanes may generally be divided into groups. In most cases, the product groups are hydrogen, lower molecular weight saturated and unsaturated hydrocarbons, congruent olefins and higher molecular weight saturated and unsaturated hydro- carbons including dimers. For cyclic alkanes, ring scission depends upon the size of the ring. In less strained rings, the radiolysis products are mainly hydrogen, congruent olefin and dimer.

b. Dose dependence

Experimentally, the results of increasing the dose are a decrease in hydrogen and congruent olefin yields, and increase in yield of total higher molecular weight products and no change in the yields of lower molecular weight hydrocarbons. The increase in total higher mole- cular weight products yields is due to an increase in the yield of olefins of molecular weight greater than the congruent olefins.

c. Dose rate dependence

An increase in dose rate would increase the concentration of radicals in the bulk solution. Radical-radical reactions would then be favored over addition and abstraction reactions. This hypothesis has been supported by Schuler and Muccini (29) in their work with mixtures of cyclopentane and cyclohexane. In pure cyclohexane, no dose rate effect would be expected since at both low and high dose rates, the only reactions which produce the major products, cyclo-hexene and bicyclohexyl, are radical-radical reactions. This has been supported by Dewhurst's work on cyclohexane (30). Other work demonstrating the decrease of yields of products from radical abstraction with decreasing dose rate has been done by Holroyd (31), and Schuler and Kuntz (32).

2. Detection of Intermediates

a. Effect of Additives

One of the earliest used methods for measuring radicals formed during radiolysis was the addition of a scavenger which would produce a unique product. The most common scavenger used was I_2 which can react according to

$$R \cdot + I_2 \longrightarrow RI + I \cdot \qquad [22]$$

followed by the combination of two iodine atoms. The alkyl iodides formed were then measured. Schuler and Kuntz (32) have used this method to determine radical yields. In the case of methyl radicals no

problems are encountered, however for higher carbon numbered radicals

the possibility exists of the formation of alkyl iodides by addition of

HI to "molecular" olefins. Unfortunately iodine also reacts with

electrons

$$e^- + I_2 \longrightarrow I^- + I\cdot \qquad [23]$$

so that the results obtained with this additive are not entirely unambiguous.

Some information can be gained by adding a solute which will

react with a specific type of intermediate, for example free radicals,

electrons or positive ions, and studying the reduction in yield of

various products. In the case of hydrogen, Hardwick (33) developed a

kinetic method for determining the "molecular" and free radical yields.

The general mechanism may be written

$$RH \xrightarrow{G_1} H_2 + products \qquad [24]$$
$$\xrightarrow{G_2} H + R \qquad [25]$$
$$H + RH \xrightarrow{k_3} H_2 + R \qquad [26]$$
$$H + S \xrightarrow{k_4} SH \qquad [27]$$
$$\xrightarrow{k_5} H_2 + M \qquad [28]$$

where RH is an alkane, S is the added solute, R and M are radicals.

Applying a steady state kinetic treatment for hydrogen atoms gives

the expression

$$\frac{1}{G_{H_2(O)} - G_{H_2(S)}} = \frac{1}{\Delta G_{H_2}} = \frac{k_3[RH]}{k_4[S] G_2} + \frac{1}{G_2}\left(\frac{k_5}{k_4} + 1\right) \qquad [29]$$

where $G_{H_2(O)}$ and $G_{H_2(S)}$ are the yields of H_2 in the absence and in the

presence of solute of concentration $[S]$. Plotting $1/\Delta G_{H_2}$ against

$[RH] / [S]$ gives a straight line of slope $k_3/k_4 G_2$ and intercept

$(k_5/k_4 + 1)/G_2$. This expression may be simplified and the value of

G_2 found if a solute is used which will not undergo reaction [28]. Also

if k_3 is known, k_4 and k_5 may be calculated. Hardwick has done this

for a number of compounds (34, 35).

Other hydrogen atom scavengers which have been used include

monoolefins (35), diolefins (36, 37) and benzene (38). Since these

compounds generally have lower excitation potentials than alkanes,

they may react with the system by energy transfer (39) as well as by

hydrogen atom scavenging (38).

Certain additives will scavenge electrons in alkane solutions.

Nitrous oxide has been used by a number of investigators (40, 41, 42,

43). The main reaction has been suggested to be

$$e^- + N_2O \longrightarrow N_2 + O^- \qquad [30]$$

with the negative ion reacting further with alkane cations. Sulfur

hexafluoride has been used by Lee and Armstrong (44) and Stone et al

(27) as an efficient electron scavenger. The reaction occurring would

probably be

$$e^- + SF_6 \longrightarrow SF_6^- \qquad [31]$$

Several investigators (45, 46, 47) have studied the effects of

CO_2 on the radiolysis of aqueous solutions and find CO_2 to be an

efficient electron scavenger with little or no reaction of hydrogen

atoms with CO_2 (47). The radiolysis of CO_2-hydrocarbon mixtures with

an analysis of the oxygen containing products has been studied by Kalyazin

and co-workers (48, 49) who also propose that CO_2 scavenges electrons

as part of the mechanism for product formation. The liquid oxygen

containing products found included carboxylic acids, ketones, aldehydes

and esters.

Since positive ions are present in irradiated hydrocarbons, it

should be possible to scavenge these with appropriate additives. The

yields of freely diffusing ions have been determined (50, 51, 7) by

measuring the conductivity of irradiated solutions. The yield of free

ions appears to be about 0.1 G units (51) which agrees with the yields

deduced from mechanism studies on the polymerization of cyclopenta-

diene inhibited by ammonia (53). Williams (6) has used ND_3 as a

positive ion scavenger in cyclohexane radiolysis. A mechanism given

by Freeman (55) for the reactions involved is

$$\left[C_6H_{13}^+ + e_{solv}^- \right] \rightarrow \left[C_6H_{12} + H \right] \tag{32}$$

$$\rightarrow C_6H_{13}^+ + e_{solv}^- \text{ (free ions)} \tag{33}$$

$$\left[C_6H_{13}^+ + ND_3 \right] \rightarrow \left[C_6H_{12} + ND_3H^+ \right] \tag{34}$$

$$C_6H_{13}^+ + ND_3 \rightarrow C_6H_{12} + ND_3H^+ \tag{35}$$

$$\left[ND_3H^+ + e_{solv}^- \right] \rightarrow \left[D + ND_2H \right] \tag{36}$$

$$\rightarrow \left[H + ND_3 \right] \tag{37}$$

$$ND_3H^+ + e_{solv}^- \rightarrow D + ND_2H \tag{38}$$

$$\rightarrow H + ND_3 \tag{39}$$

$$D + C_6H_{12} \longrightarrow HD + C_6H_{11} \qquad [40]$$

$$H + C_6H_{12} \longrightarrow H_2 + C_6H_{11} \qquad [41]$$

The square brackets indicate that the species are in spurs. Using this mechanism, Freeman has devised a kinetic scheme to describe the scavenging of positive ions in the radiolysis of liquids.

b. Physical methods

Since free radicals contain unpaired electrons, two methods of measurement available to detect them are magnetic susceptibility measurements and electron spin resonance. If the radicals formed are stable, they may be detected by magnetic susceptibility measurements. Since relatively high concentrations of radicals are needed for measurement, this method is limited. A more direct method is electron spin resonance. This method may be used for stable free radicals and for reactive radicals frozen in media for stability. Hardwick (56) has determined the total radical yields in irradiated alkanes by this method.

One method of producing high concentrations of radicals is pulse radiolysis. The radicals formed by this method are detected by spectrophotometric means. So far pulse radiolysis studies have been mostly confined to aqueous systems, however Dillon and Burton (57) have studied excitation transfer in cyclohexane-benzene systems with p-ter-phenyl present as a scintillator. Bühler and Gäumann (58) have investigated the carbon tetrachloride-benzene system. Radical

ion yields in the pulse radiolysis of cyclohexane solutions have been

measured by Keene, Land and Swallow (59).

3. Liquid Cycloalkanes

The radiolysis of the three cycloalkanes most closely related

to methylcyclopentane will be briefly reviewed.

a. Cyclohexane

A great deal of work has been done on the radiolysis of cyclo-

hexane and binary cyclohexane-additive systems. The main products

from radiolysis of pure cyclohexane are hydrogen (G_i = 5.6), cyclo-

hexene (G_i = 3.2) and bicyclohexyl (G_i = 1.76) where G_i is the initial

yield (60). One possible mechanism by which the liquid products may

be formed is the disproportionation and combination of cyclohexyl

radicals

$$2 \ c\text{-}C_6H_{11} \xrightarrow{k_d} c\text{-}C_6H_{12} + c\text{-}C_6H_{10} \qquad [42]$$

$$\xrightarrow{k_c} (c\text{-}C_6H_{11})_2 \qquad [43]$$

However cyclohexene may also be formed in reactions such as

$$c\text{-}C_6H_{12}^* \longrightarrow H_2 + c\text{-}C_6H_{10} \qquad [44]$$

or $\quad (H + c\text{-}C_6H_{11})_{spur} \longrightarrow H_2 + c\text{-}C_6H_{10} \qquad [45]$

The ratio of the rate constants for disproportionation and combination,

k_d/k_c, for cyclohexyl radicals has a lower limit of 1.1 ± 0.3 as deter-

mined from the decrease in the respective product yields. Other

products are the results of a small degree of ring cleavage. The

yields of the major products decrease to a limiting value with increasing

dose, perhaps due to reactions such as

$$H \quad + \quad c\text{-}C_6H_{10} \quad \longrightarrow \quad c\text{-}C_6H_{11} \qquad [46]$$

$$\longrightarrow \quad H_2 \quad + \quad c\text{-}C_6H_9 \qquad [47]$$

Since there is a limiting value however, this suggests that the products

are also formed by "molecular" processes. In fact, Dyne and Jenkinson

(61) have suggested from the results of irradiated mixtures of $c\text{-}C_6H_{12}$

and $c\text{-}C_6D_{12}$ that 10 to 20% of the hydrogen yield is due to a unimolecular

process (Eq. [44]). However despite the great amount of work done

on the cyclohexane system, the exact mechanism for product formation

has not been established.

b. Cyclopentane

Lepley (62) used gas chromatography to analyze the hydrocarbon

products of the radiolysis of cyclopentane. The most abundant hydro-

carbons were found to be cyclopentene and bicyclopentyl, which agrees

with the results of Hughes and Hanrahan (63) who found the G values of

the major products to be hydrogen 5.20, cyclopentene 3.10 and bicyclo-

pentyl 1.22. These authors also found larger yields of fragmentation

products than in cyclohexane radiolysis and attributed this to a greater

ring strain in cyclopentane than in cyclohexane. Walker (64) has also

measured the yields of the major and minor products in liquid cyclo-

pentane radiolysis. His yields for the major products agree within 5%

with those of Hughes and Hanrahan. Hardwick (56) has reported a

hydrogen yield of 5.78 G units and a congruent olefin yield of 4.24 G units,

both of which are substantially higher than the values obtained by Walker

and by Hughes and Hanrahan. The latter two authors give a reaction

mechanism which corresponds to that of cyclohexane.

A number of investigators (65, 66) have studied cyclohexane-

cyclopentane mixtures and found that the results could be explained by

postulating the radical abstraction reaction

$$C_6H_{11} + C_5H_{10} \longrightarrow C_6H_{12} + C_5H_9 \qquad [48]$$

c. Methylcyclohexane

Very little work has been done on liquid methylcyclohexane.

Freeman (67, 68) has studied the radiolysis of pure methylcyclohexane

and methylcyclohexane with benzene added. The product spectrum is

more complicated than for an unsubstituted cycloalkane, with the major

products being hydrogen ($G_i = 4.80$), 1-methylcyclohexene plus methylene

cyclohexane ($G_i = 2.65$), and bimethylcyclohexyl plus methylcyclohexyl

heptene ($G_i = 0.88$). The major portions of the congruent olefins and

dimers were formed by the disproportionation and combination of

radicals. The methane yield ($G_i = 0.08$) was higher than in the unsub-

stituted cycloalkanes. Hardwick (56) agrees with Freeman's hydrogen

yield although his congruent olefin yield is less than Freeman's. Schuler

and Kuntz (32) reported a methyl radical yield of 0.038 G units. Based

on their assumption that the ratio of the yield of molecular methane to

that of methyl radicals is in the range 0.6 to 0.9, the methane yield to

be expected would be 0.06 to 0.08 G units which agrees with Freeman's

results.

When benzene was added to methylcyclohexane the dominant

effect at low benzene concentrations appeared to be hydrogen atom

scavenging, while at higher concentrations energy transfer occurred

from excited methylcyclohexane to benzene.

F. Previous Work on Methylcyclopentane

Little work has been done on the methylcyclopentane system.

A few papers have dealt with certain aspects of this compound.

1. Mercury Photosensitization

The only photolytic study of methylcyclopentane has been the

investigation of its reaction with Hg-6($^3P_1$) atoms by Schlochauer

and Gunning (69). The products identified were hydrogen, dimer

($C_{12}H_{22}$) and methylcyclopentenes. The mechanism given by these

authors for the reaction was

$$C_6H_{12} + Hg\ 6\ (^3P_1) \longrightarrow C_6H_{11} + H + Hg\ 6\ (^1S_0)$$ [49]

$$H + C_6H_{12} \longrightarrow C_6H_{11} + H_2$$ [50]

$$H + C_6H_{11} \longrightarrow C_6H_{12}$$ [51]

$$H + C_6H_{11} \longrightarrow C_6H_{10} + H_2$$ [52]

$$2\ C_6H_{11} \longrightarrow C_{12}H_{22}$$ [53]

$$H_2 + Hg\ 6\ (^3P_1) \longrightarrow 2\ H + Hg\ 6\ (^1S_0)$$ [54]

C_6H_{10} refers primarily to methylcyclopentenes although it was possible

that methylene cyclopentane was also present. No evidence of ring

splitting was found.

2. Radiolysis

Hardwick (56) measured certain products from the radiolysis of methylcyclopentane. He found an initial hydrogen yield of 4.62 G units and from his scavenger studies using methylmethacrylate, the hydrogen atom yield (i.e. scavengeable hydrogen) was 2.63 G units. He also measured an initial yield of congruent olefin of 3.89 G units and a "molecular" (unscavengeable) congruent olefin yield of 1.67 G units. Using electron spin resonance methods he determined the total radical yield to be 6.9 G units for methylcyclopentane. Methane was found in the products with a G value of 0.11 in pure methylcyclopentane and 0.06 when 1.25% methyl methacrylate was present. Schuler and Kuntz (32), using I_2, have determined the methyl radical yield from methylcyclopentane radiolysis to be 0.06 G units and, based on their ratio of the yield of molecular methane to that of methyl radicals of 0.6 to 0.9, this gives an expected methane yield of 0.10 or 0.11 G units which agrees well with Hardwick's values. Hardwick gives a free radical mechanism as an explanation of the method of formation of products.

G. Scope of Present Work

Prior to the commencement of this study, the radiolysis of cyclohexane and methylcyclohexane liquids had been carried out in this laboratory. Work on methylcyclopentane began as a study of the effect of molecular structure on the radiolysis mechanism. The yields of

hydrogen, methane and liquid products were studied as a function of

dose. In order to gain insight into the type of reactive intermediates

formed by radiolysis, and hence the mechanism of formation of products,

various scavengers were added to the methylcyclopentane. The

scavengers included 1,3-cyclohexadiene, benzene, nitrous oxide,

carbon dioxide, sulfur hexafluoride and perdeutero ammonia. Hydrogen

and methane yields were determined for all additives and liquid products

were measured for binary solutions of methylcyclopentane and 1,3-

cyclohexadiene, benzene, CO_2 and ND_3.

II.   EXPERIMENTAL

A.   Materials

1.   Materials for Irradiation

a. Methylcyclopentane (MCP)

Phillips Petroleum Co. (Pure Grade) MCP contains traces of olefins as impurities.   Since these unsaturated compounds could affect the radiolysis, the MCP used for most of the samples was purified by the following method.   About 200 ml of MCP and 50 ml of H_2SO_4 were stirred by a glass covered magnetic stirrer for 48 hours.   The H_2SO_4 was changed once during this time.   The MCP was then washed 5 or 6 times with about 25 ml portions of doubly distilled water and left to dry over anhydrous $MgSO_4$ overnight. Before use it was distilled at atmospheric pressure.   The purified MCP contained < 0.001% olefin, < 0.095% n-hexane and < 0.10% cyclo-hexane.   The amount of cyclohexane in the MCP varied from lot to lot since it was formed by the isomerization of MCP during the H_2SO_4 treatment.   The purity of MCP was determined by gas chromatography.

b. 1,3-Cyclohexadiene

Aldrich Chemical Co. 1,3-cyclohexadiene was first distilled at atmospheric pressure to remove dimer and polymers, then purified by gas chromatography.   A β,β'-oxydipropionitrile column was used and the liquid was trapped in a Dry Ice-ethanol trap placed between the column and the detector.   The impurities remaining were 0.36% cyclo-

hexane, 0.55% benzene and a trace of 1,4-cyclohexadiene.

c. Benzene

Phillips Petroleum Co. (Research Grade) benzene was distilled at atmospheric pressure before use, the middle third being retained.

d. Gases used as additives.

Gas	Source	Minimum Purity
CO_2	Air Reduction Canada, Ltd.	99.9%
HCl	Matheson of Canada Ltd.	99.0%
N_2O	Matheson of Canada Ltd.	99.61%
SF_6	Matheson of Canada Ltd.	98.0%
ND_3	Merck, Sharp and Dohme	98% isotopic purity

The CO_2 was used as supplied in a glass bulb. The HCl, N_2O and SF_6 were purified by trap to trap distillation, the first portion being pumped away. The ND_3 was also purified in this manner, however the walls of the trapping system and storage bulb had previously been equilibrated with D_2O before the final evacuation.

2. Materials for calibration and identification

The materials used for purposes other than irradiation are given in Table II-1. Unless otherwise stated, they were used without further purification.

TABLE II-1

Materials Used

Name	Source	Remarks (see after Table)
1. Apiezon Greases (L and N)	Metropolitan-Vickers Electrical Co. , Ltd.	-
2. Bimethylcyclopentyl	Prepared as described	ii
3. Biphenyl	British Drug House, Ltd.	-
4. Carbon monoxide	Air Reduction Co. Matheson of Canada	-
5. Celite (Kromat CE)	Burrell Corporation	-
6. Charcoal (High activity)	Burrell Corporation	-
7. 1,3-Cyclohexadiene Dimer	Prepared as described	i
8. Cyclohexane (Spectrograde)	Eastman Kodak Co.	-
9. Diethyl ether	Mallinckrodt	-
10. Di-n-decyl phthalate	Eastman Kodak Co.	-
11. Di-t-butyl peroxide	Matheson, Coleman and Bell	-
12. Drierite (8 mesh)	W. A. Hammond Drierite Co.	-
13. Ethanol	Reliance Chemical Co.	-
14. Ferrous ammonium sulfate	Mallinckrodt	-
15. Firebrick (Kromat FB)	Burrell Corporation	-

TABLE II-1, continued

	Name	Source	Remarks
16.	Helium	Air Reduction Canada, Ltd. Canadian Helium Limited	-
17.	n-Hexane (Spectroquality)	Matheson, Coleman and Bell	-
18.	Hexene-1 (Research grade)	Phillips Petroleum Co.	iii
19.	Hexene-2 (Research grade)	Phillips Petroleum Co.	-
20.	H_2, HD, D_2 mixture	Merck, Sharp and Dohme	-
21.	Magnesium Sulfate	Baker and Adamson Allied Chemical Corporation	-
22.	Mercury (Triple distilled)	Mallinckrodt	-
23.	Methane (Research grade)	Phillips Petroleum Co.	-
24.	1-Methylcyclo-pentene	Aldrich Chemical Co., Inc. Columbia Organic Chemicals	iv
25.	3-Methylcyclo-pentene	Prepared as described	v
26.	2-Methyl pentane (Research grade)	Phillips Petroleum Co.	-
27.	3-Methyl pentane (Research grade)	Phillips Petroleum Co.	-
28.	2-Methyl pentene-1	Matheson, Coleman and Bell	-
29.	4-Methyl pentene-1	Matheson, Coleman and Bell	-
30.	4-Methyl pentene-2	Matheson, Coleman and Bell	-

TABLE II-1, continued

	Name	Source	Remarks
31.	Molecular sieve (No. 13X)	Burrell Corporation	-
32.	Nitric acid	Baker and Adamson Allied Chemical Co.	-
33.	Potassium hydroxide	McArthur Chemical Co.	-
34.	Potassium permanganate	Mallinckrodt	-
35.	Silica gel (Medium activity)	Burrell Corporation	-
36.	Silicone grease	Dow Corning	-
37.	Silicone oil - 710	Dow Corning	-
38.	Silicone rubber	Wilkins Instrument and Research, Inc.	-
39.	Sodium chloride	Fisher Scientific Co.	-
40.	Squalane	Eastman Kodak Co.	-
41.	Sulfuric acid	Baker and Adamson Allied Chemical Co.	-
42.	Tricresyl phosphate	Eastman Kodak Co.	-
43.	Tris(cyano-ethoxy) propane	F & M Scientific Corp.	-
44.	Ucon (75-H-1400)	Union Carbide Chemical Co.	-
45.	Water	Doubly distilled	vi

Remarks from Table II-1:

i. 1,3-Cyclohexadiene dimer was prepared by R. Schutte by the following method. 1,3-Cyclohexadiene was degassed and heated at 200°C in a sealed tube for approximately 24 hours and then vacuum distilled. The purity of the liquid used was 99.6%.

ii. Bimethylcyclopentyl was prepared by the method of Farmer and Moore (70). MCP and di-tert-butyl peroxide were heated in a sealed tube in the presence of N_2 for approximately 24 hours at 145°. After distillation at atmospheric pressure and then vacuum distillation of the product, the collected portion (b.p. 97°-105°/12 mm) contained at least two dimers, as shown by gas chromatography on a silica gel column. The larger peak (bimethylcyclopentyl) was 99.7% of the total.

iii. Hexene-1 was used as a calibration standard for the straight chain olefin products. It was vacuum distilled before use and from gas chromatography appeared to be 100% pure.

iv. 1-Methylcyclopentene was also used as a calibration standard. The liquid used was always freshly vacuum distilled. Its purity was >99.2%.

v. 3-Methylcyclopentene was prepared by J. van Dyke by the following method. 2-Methylcyclopentanone was reduced to 2-methylcyclopentanol and converted to the acetate by acetic anhydride. The acetate was then heated to 450° in a sealed tube to form a mixture of 1-methylcyclopentene and 3-methylcyclopentene in a ratio of approximately 1 to 2. This mixture was separated and purified by gas chromatography.

vi. The doubly distilled water was prepared by distillation from a solution containing $KMnO_4$ and KOH followed by a second distillation. This water was used for the Fricke dosimeter and for rinsing glassware used in preparing samples.

B. Apparatus

1. High Vacuum System

The high vacuum system used was made of Pyrex glass clamped to a rigid frame. The frame was constructed from Dexion angle iron and metal rods and was bolted to a wooden table. The system was evacuated by a Welch Duo Seal two stage vacuum pump and mercury diffusion pump. The approximate pressure of the system was measured with a Pirani gauge (Consolidated Electrodynamics Type GP-110). Pressures less than 5 microns were measured by the combination Toepler-McLeod gauge shown in Fig. II-4.

a. Main Manifold

A schematic diagram of the main manifold is shown in Fig. II-1. Apiezon N grease was used on the standard taper joints of the traps T1 and T2 and on stopcocks 1, 2, 3, 4, 5, and 6. On all other joints and stopcocks silicone grease was used as a lubricant. When the vacuum line was in use, traps T1 and T2 were always cooled with liquid nitrogen to prevent impairment of the efficiency of the pumps. Stopcocks 2, 3, 5 and 6 were 10 mm high vacuum stopcocks. All other stopcocks were 4 mm bore.

Figure II-1

Main Manifold

b. Liquid Sample System

Radiolysis samples of pure MCP and of MCP with benzene and with 1,3-cyclohexadiene added were made up by similar methods. The required volume of liquid was put into the sample tube by pipet or syringe. The system is shown in Fig. II-2.

c. Gas Sample System

This portion of the vacuum system shown in Fig. II-3 was used to make up samples containing MCP and a gaseous additive. Each gas used was stored in a gas reservoir and the MCP was stored, after purification, in the liquid reservoir. The required volume of gas was measured in the appropriate calibrated bulb and the gas pressure was measured by the manometer. The volume of liquid needed was measured in the measuring tube.

TABLE II-2

Calibrated Volumes of Gas Measuring Bulbs

Bulb	Volume (ml)
B1	202.9
B2	100.2
B3	12.12
B4	1.647

d. Gas Analysis System

Fig. II-4 shows the sample breaking traps, distillation traps,

Figure II-2

Liquid Sample System

Figure II-3

Gas Sample System

Figure II-4

Gas Analysis System

TO MECHANICAL PUMP

MAIN MANIFOLD

GAS SAMPLER G2

TO MAIN MANIFOLD

26 25 M1 M2 M3 M4 FLOAT VALVE

TO AIR 27 TRAP

MERCURY

TOEPLER McLEOD GAUGE

24

DISTILLATION TRAPS

23

GAS SAMPLER G1

22 21 20 19 18

17 16 15 14

TO MAIN MANIFOLD

TO AIR

BREAKING TRAPS

combined Toepler-McLeod gauge and the gas sampler, G2, for collecting the gas fractions of the irradiated samples. This sampler was attached to the system by 12/2 ball joints.

The standard volumes in the Toepler-McLeod gauge were calibrated and these volumes are given in Table II-3.

The sampler G1 for introducing gases for calibration purposes is also shown. A portion of the gas from this sampler was expanded into a series of volumes before an aliquot was taken and measured in the Toepler-McLeod gauge and transferred to gas sampler G2. All gas samples were injected into the gas chromatograph by transferring sampler G2 to the gas chromatographic unit, attaching it by means of the 12/2 ball joints and turning the two fourway stopcocks, 26 and 48 (Figure II-5).

When the liquid products of irradiation were not to be retained, the sample breaking traps used were as pictured in Figure II-4. When it was desired to keep the liquids for further analysis, a side arm was attached to these traps which was then sealed off with the liquid in it after the gases had been removed. During sealing, the liquid was kept at $-196^{\circ}C$.

The mechanical pump for evacuating the Toepler-McLeod gauge was a Welch Duo Seal, two stage vacuum pump. The trap preceeding it was uncooled.

TABLE II-3

Calibrated Volumes of the Toepler-McLeod Gauge

(Figure II-4)

Mark (from stopcock)	Volume (ml)
to M1	0.09651
to M2	0.5466
to M3	5.020
to M4	36.35

2. Analytical Systems

a. Gow Mac gas chromatograph

This chromatograph was constructed from component parts.

The schematic representation is given in Fig. II-5. The hot wire

detector (Model TR II B) and power supply (Model 9999C) units were

obtained from Gow Mac Instrument Co. and the recorder (Cat. no.

347-01-25) was made by E. H. Sargent Co. The needle valve (Type

LB1A) to control the flow rate was manufactured by Edwards High

Vacuum Ltd. Copper tubing of inside diameter 1/8" was used to

connect the helium tank to the drying tubes and to join the outlet of the

reference side to the needle valve. To connect the needle valve to

stopcock 48 and from there to the column, copper tubing of 3/16"

inside diameter was used. From the sample outlet to stopcock 49,

copper tubing of inside diameter 5/16" was used. All other tubing

was Pyrex glass. The chromatographic columns used were either

Figure II-5

Gow Mac Gas Chromatographic Unit

$2\frac{1}{2}$ meters or 1 meter long and were made of 3/8" heavy walled Pyrex

tubing wound with nichrome wire for heating purposes. These columns

were housed in a rectangular metal box lined with glass wool. The

temperature of the sample before it entered the detector cell was

measured by a thermocouple obtained from Thermoelectric (Canada)

Ltd. (Model 29).

The helium used as a carrier gas was introduced at about

20 p.s.i. from the cylinder and its flow rate regulated by the needle

valve. The flow rate was measured by timing the rise of soap bubbles

between marks M5 and M6. The volume of the tube between these

marks was 20 ml.

The detector was operated at $200^{\circ}C$ and a cell current of 250 ma.

b. Burrell gas chromatograph

Some of the liquid analyses were done on a Burrell Kromo-Tog

(Model K2). The columns used were similar to those used for the

Gow Mac. The detector was operated at $200^{\circ}C$ and a cell current

of 235 ma.

c. Ultraviolet spectroscopy

A Cary recording spectrophotometer (Model 14M) was used

during the dosimetry determinations.

d.   Mass spectrometer

The MCP samples containing ND_3 were analyzed for H_2, HD,

D_2 and CH_4 by mass spectrometer. The instrument used was a modified

Consolidated Electrodynamics Corporation Residual Gas Analyzer

(Model 21-614).

3. Cobalt 60 Irradiation Sources

a. Source 1

The first irradiations were done with a 300 curie ^{60}Co source

contained in a lead and steel shield and housed in a specially built room

(cave). During irradiation the source was extended along a steel

track to a predetermined position, the reproducibility of which was

insured by a rigidly fixed pin along the track. This procedure was

controlled from outside the room.

The sample cells were placed in a sample block (Block A) which

consisted of a rectangular aluminum frame containing rows of rigidly

fixed glass tubes, slightly larger in diameter than the sample tubes.

This block was constructed, in part, by a colleage, J. Myron.

This source was used for the pure liquid MCP samples analyzed

for H_2 and CH_4.

b. Source 2

The latter irradiations were carried out in a Gamma Cell

(Model 220) ^{60}Co source. This source had a strength of approximately

12,300 curies and contained its own shielding. The block used in

this source (Block B) was a cylindrically shaped aluminum can about

2" in height and 6" in diameter. It contained three horizontal plates

in which holes were drilled to hold the samples rigidly in position.

This source was used for the major portion of irradiations.

C. Procedure

1. Dosimetry

To determined the dose rate for the two radiation sources the

Fricke dosimeter was used. The solution irradiated was 10^{-3}M in

$FeSO_4(NH_4)_2SO_4 \cdot 6H_2O$, 10^{-3}M in NaCl and 0.8 N in H_2SO_4. Covered

round bottomed glass tubes of the same diameter as the MCP sample

cells were used for the irradiations. After irradiation the solution was

transferred to a 0.5 cm quartz cell and the concentration of ferric ions

was determined by a Cary Recording Spectrophotometer. One

unirradiated sample (blank) was always run with each determination.

The energy absorbed by the solution is given by:

$$\frac{\text{Net O.D.} \times 6.023 \times 10^{22}}{T \times 2201 \times 15.6 \left[1 + 0.007(t - 25^{\circ})\right] \times 0.5} \qquad [1]$$

where Net O.D. is the optical density of the solution less the optical

density of the blank, T is the irradiation time in hours, t is the

temperature of the solution in degrees centigrade. The constants

used in the above are given in Allen (71); $G_{Fe^{+++}} = 15.6$ and $\epsilon_{Fe^{+++}}$

= 2201 at 25°C and 304 mμ. The dose rate values used are given in

Table II-4. These values were all standardized for decay of ^{60}Co to

January 1, 1967 for comparison using the following formula:

$$D = D_o e^{-\lambda t} \qquad [2]$$

TABLE II-4

Dosimetry Values

Source	Block	Position in block	Volume of solution (ml)	Energy Absorbed by Fricke solution x 10^{18} (ev/hr ml)
1	A	12	2	1.76
1	A	13	2	2.66
1	A	14	2	3.68
1	A	15	2	3.54
1	A	16	2	2.58
1	A	17	2	1.59
1	A	21	2	1.83
1	A	22	2	2.16
1	A	23	2	1.77
1	A	14	20	1.15
1	A	15	20	1.09
2	B	1	2	24.8*
2	B	3	2	24.5*
2	B	5	2	24.6*
2	B	8	2	24.6*
2	B	11	2	24.8*
2	B	13	2	25.2*

* These values were obtained by a coworker, D. Dugle.

where λ is 0.059 years^{-1}, D and D$_O$ are the dose rate after time t

and the initial dose rate, respectively, and t is the time (in years)

elapsed since the initial dose rate determination.

In calculating the dose received by the samples irradiated, it

was assumed that the dose rates were proportional to the electron

densities of the solutions being irradiated. The electron densities of

Fricke solution and MCP at 25°C were taken as 0.566 and 0.424 moles

of electrons/ml respectively.

2. Sample Preparation

a. Sample cells

The two types of samples cells used are pictured in Figure II-6.

Type A cells had rounded, thin bottoms. The average volume of these

cells would probably have been about 4 ml. These cells were used

for samples containing pure MCP and samples containing MCP with

liquid additives. They were made from Pyrex glass which had been

cleaned with a hot mixture of sulfuric and nitric acids and washed

several times with doubly distilled water.

Type B cells were flat, thin bottomed cells with small total

volumes. The total volumes of these cells varied from 2.1 ml to 2.8 ml.

They were used for samples containing MCP with gaseous additives.

The cells were blown first, rinsed with ethanol, then cleaned with

HNO_3 and rinsed several times with doubly distilled water. Both

types of cells were flamed while being evacuated after they were attached

Figure II-6

Sample Cells

LIQUID SAMPLE

METAL SAMPLE BREAKER

SAMPLE CELL

BREAKING TRAP

B

METAL SAMPLE BREAKER

SAMPLE CELL

LIQUID SAMPLE

BREAKING TRAP

A

to the system and before filling. In most cases the cells were filled within 48 hours after making them.

A third type of cell, similar to type A but larger in volume (about 25 ml) was used for two very low dose samples. These cells were cleaned as were type A.

b. Pure MCP samples

Samples containing pure MCP were made up by using the liquid sample system shown in Fig. II-2. Approximately 2 ml of liquid were measured by calibrated pipette and drained into the sample tube which was then attached to the system by a greased 12/30 ground glass joint. The liquid was frozen with liquid N_2. After evacuating the system, stopcock 29 was closed and the liquid allowed to warm up to room temperature, expelling trapped gases. This freezing, pumping, thawing cycle was performed 3 or 4 times until no deflection showed on the Pirani gauge when the system was opened to it. Then, with stopcocks 29 and 28 both open, the liquid was distilled into the trap which was cooled by liquid N_2. Following this, the sample was distilled into a sample cell with stopcock 28 closed and the sample was sealed off while the liquid was frozen by liquid N_2. These samples were used for the study of dose dependence of irradiated products.

c. MCP with liquid additives

The samples containing MCP and either benzene or 1,3-cyclo-hexadiene were also prepared on the system in Fig. II-2. In this case

the MCP and additive were each pipetted or syringed into the sample tube which was then attached to the system, degassed by the same freezing, pumping, thawing technique as for the pure MCP samples and sealed off in a similar manner. These samples all had total liquid volumes of about 2 ml.

d. MCP with gaseous additives

These samples were made up using the gas sample system shown in Fig. II-3. The MCP was purified as described on page 27 and distilled from the filling bulb into the liquid reservoir. After a number of degassing cycles, the liquid MCP was pumped on for a short time before the metal bellows valve was closed. When making samples, an excess of MCP was distilled into the calibrated measuring tube. After the MCP had melted, the excess MCP was distilled into the excess liquid tube until the desired volume of MCP remained. This MCP was then distilled into the sample cell and kept frozen until the gas had also been distilled into the cell, at which time it was sealed off. The gases were measured by allowing a portion to expand from the reservoir into the evacuated system with all stopcocks closed except those leading from the reservoir and to the desired calibrated bulb. The pressure of the gas in this calibrated volume was measured by the mercury manometer. After the stopcocks to the reservoir and calibrated bulb were closed, the excess gas was frozen into the excess gas tube and stopcock 31 opened. When the

whole system was thoroughly evacuated, stopcock 31 was closed and

the gas was distilled from the calibrated bulb into the sample cell.

In the case of the ND_3, the surface of the whole system,

excluding the filling bulb, was equilibrated with D_2O for 24 hrs and

evacuated before filling.

3. Sample Analysis

a. Gas chromatographic columns

A list of the gas chromatographic columns that were tried to

obtain optimum separation of the products of radiolysis and MCP is

given in Table II-5. With the exception of the charcoal, molecular

sieve and silica gel columns, the column packings were prepared by

dissolving the liquid phase in acetone, adding the solid support and

stirring on a steam bath while the acetone evaporated. All columns

were conditioned at temperatures several degrees higher than those

used during analysis. Various combinations of temperature and flow

rate of carrier gas were tried for each column.

b. Fractionation of products at -196°

After irradiation, the sample was placed in the breaking trap

as shown in Fig. II-6, with the metal breaker resting on the thin bottom

of the cell. The breaking trap was then attached to the analysis system,

shown in Fig. II-4, by a 24/40 ground glass joint. The whole of the gas

analysis system, with the exception of the portion from stopcock 18 to

22, was evacuated and with stopcock 25 closed, a "zero" reading was

TABLE II-5

Chromatographic Columns Tried for Product Separation

Column	Length (meters)	Product Separation Attempted
Charcoal	1	$\cdot H_2$, CH_4
Molecular Sieve	$2\frac{1}{2}$	H_2, CH_4, N_2, O_2, CO
Silica Gel	$2\frac{1}{2}$	C_6 - C_{12}
Tricresylphosphate 40% on Firebrick	$2\frac{1}{2}$	C_6
Squalane 25% on Firebrick	$2\frac{1}{2}$	C_6
Apiezon L 5% on Firebrick	$2\frac{1}{2}$	C_{12}
20% on Firebrick	$2\frac{1}{2}$	C_{12}
Silicone Grease 5% on Firebrick	$2\frac{1}{2}$	C_{12}
Silicone Oil 710 10% on Firebrick	$2\frac{1}{2}$	C_{12}
Silicone Rubber 28% on Firebrick	$2\frac{1}{2}$	C_{12}
Ucon 10% on Firebrick	$2\frac{1}{2}$	C_{12}
Di-n-decyl phthalate 10% on Firebrick	$2\frac{1}{2}$	C_6
Tris(cyano-ethoxy)propane 10% on Celite	$2\frac{1}{2}$	C_6

The composition referred to is grams of liquid phase per 100 grams solid.

taken on the Toepler-McLeod gauge. All stopcocks were then closed
and liquid N_2 placed around the two distillation traps. When the sample
contained a high pressure of gaseous additive, the breaking trap was
also liquid N_2 cooled. The sample cell was broken by raising the
metal breaker with a magnet and letting it fall onto the thin glass bottom
of the cell. Stopcock 23 was opened and then, after a few seconds,
stopcock 24. Pumping by the Toepler-McLeod was carried on until
all of the sample had distilled out of the breaking trap. Stopcock 24
was then closed and the liquid N_2 removed from the distillation traps.
The sample was allowed to distill back into the breaking trap. After
a second distillation into the distillation traps with stopcock 24 open,
the final constant volume and pressure of the gas collected in the
Toepler-McLeod was recorded. A portion of this gas, hereafter
called the -196° fraction, was then transferred to the evacuated gas
sampler G2. If the liquid portion of the sample was to be analyzed
the remainder of the sample was distilled from the distillation traps
into a side arm attached to the breaking traps and sealed off while
being cooled by liquid N_2.

c. -196° fraction

After a portion of these gases had been collected, the gas
sampler G2 was transferred to the Gow Mac gas chromatograph. The
first column used to analyze this gas mixture was the charcoal column.
It was used at a constant temperature of $50^\circ C \pm 2^\circ$ and flow rate of 57 to

64 ml helium per minute. This column was used for analysis of gases from samples that contained pure MCP and for MCP-liquid additive samples. The only products observed were H_2 and CH_4. The column was calibrated for CH_4 by measuring various quantities of the gas in the Toepler-McLeod, transferring a portion of the gas into gas sampler, G2, and injecting the gas onto the column in the same manner as for the irradiated sample. The calibration curve obtained for CH_4 was linear.

The charcoal column would not give separate peaks for O_2, N_2 and CO so that for the samples containing gaseous additives, except ND_3, it was replaced by the molecular sieve column which was also used on the Gow Mac chromatograph. A column temperature of $30^\circ C$ and flow rate of 60 ml helium per minute was used. Analysis, calibration of gases and calculation of H_2 yield were done in a manner similar to that used for the charcoal column.

The -196° fraction of the samples containing ND_3 was analyzed by mass spectrometry. Instead of collecting the gas in the gas sampler, G2, an adapter was made so that the gas could be transferred into a closed tube containing a vacuum stopcock on one end. This tube was fitted to the mass spectrometer by a 12-30 ground glass joint. The fraction of H_2, HD, D_2 and CH_4 in each sample was measured from the mass spectrum and the amount of each gas in the irradiated sample was calculated from the total amount of gas collected in the Toepler-McLeod. The mass spectrometer was calibrated for H_2, HD

and D_2 by using a sample of known composition of a mixture of these gases.

d. Liquid product analysis

The samples were analyzed for liquid products by injecting 100 μl of the sample onto the desired column. The columns used and their operating conditions are given in Table II-6.

TABLE II-6

Gas Chromatographic Columns Used for Quantitative Liquid Analyses

Column	Products Analyzed	Temperature Range ($^{\circ}$C)	Flow Rate of Carrier Gas (ml/min)
Silica Gel	C_6 - C_{12}	40 - 200	Helium (100)
Squalane	C_6	75	Helium (75)
Silicone Oil 710	C_{12}	40 - 200	Helium (60)

The identity of the peaks of the major liquid products was tentatively assumed from comparison to previous work (67) done by Freeman on methylcyclohexane radiolysis. Further identification of peaks was obtained by the following method. A 100 μl injection of irradiated sample was run on the chromatograph. A small amount of the suspected known compound was added to the sample and again 100 μl was injected onto the same column using identical conditions. Growth in peak height of the peak in question was taken as corroboration of the product identification. In this manner the peaks for 1-methylcyclo-pentene, 3-methylcyclopentene, and bimethylcyclopentyl were identified

and tentative identifications were assigned to hexene-1 and methyl-cyclopentylmethylcyclopentene.

The silica gel column gave three major C_6 peaks and two C_{12} peaks. Of the three C_6 peaks, two corresponded to 1-methylcyclopentene and 3-methylcyclopentene. The third C_6 was definitely not hexene-2, 4-methylpentene-2 or 4-methylpentene-1 and could quite possibly be hexene-1. It is quite possible, by analogy to Freeman's methylcyclohexane work (67), that the peak assigned to 1-MC also contained methylene cyclopentane and the peak assigned to 3-MC contained also 4-methylcyclopentene since these would probably have not been separated on the chromatographic column used. However, they will, in future, be referred to as the 1-MC and 3-MC peaks. The C_{12} peaks correspond to the two C_{12} peaks obtained from injections of bimethylcyclpentyl prepared as described on page 32. The larger of these two peaks is a saturated hydrocarbon and the smaller is unsaturated.

The peak obtained on the squalane column corresponds exactly to a hexene-1 peak and the group of very closely bunched peaks on silicone oil 710 column corresponds to peaks obtained on that column from injection of the bimethylcyclopentyl preparation containing C_{12} isomers.

The peak areas were calibrated by injection onto the column of 100 μl protions of solution prepared as follows. A stock solution containing

weighed amounts of MCP and the standard compound was made up.

This stock solution was then diluted several times to provide a series

of solutions of varying concentrations of standard compound. The

concentrations prepared ranged from less than to greater than the

concentration of the liquid product in the irradiated sample. Calibration

curves were then drawn by plotting calibration factors (C.F.) against

area ratios (A.R.) where

$$\text{C.F.} = \frac{\text{peak area of product / peak area of MCP}}{\text{moles of product / moles of MCP}} \qquad [3]$$

and

$$\text{A.R.} = \frac{\text{peak area of product}}{\text{peak area of MCP}} \qquad [4]$$

Calibration curves were determined with each set of samples analyzed.

Examples of typical calibration curves are given in Fig. II-7. The

compounds used for calibrating were 1-methylcyclopentene, 1-hexene,

bimethylcyclopentyl, 1,3-cyclohexadiene dimer and biphenyl. In the case of

both irradiated samples and calibration solutions, three injections

were made for each sample and an average taken for the areas of each

peak.

Figure II-7

Typical Calibration Curves for Liquid Products

A   1-Methylcyclopentene on silica gel column

B   1-Hexene on silica gel column

C   1-Hexene on squalane column

D   Bimethylcyclopentyl on silica gel column

E   Bimethylcyclopentyl on silicone oil 710 column

F   1,3-Cyclohexadiene dimer on silicone oil 710 column

III. RESULTS

A. Radiolysis of Pure MCP

With the exception of methane and hexene-1, the products measured were those resulting from C-H bond cleavage. These products were hydrogen, 1-methylcyclopentene (1-MC), 3-methyl-cyclopentene (3-MC), bimethylcyclopentyl (BMCP) and methylcyclo-pentyl methylcyclopentene (MCMC). In Figures III-1 to III-3 the product yields are shown as G values where G represents the molecules of product formed per 100 eV absorbed by the sample.

a. Hydrogen

The yield of hydrogen was determined by subtracting the methane yield from the total gas fraction collected which was volatile at -196°. The variation of yield with dose is presented in Figure III-1A and in Table III-1. The "initial yield" (G value extrapolated to zero dose), $G_i(H_2)$ is 4.5 ± 0.5 and the yield decreases sharply to 4.0 ± 0.1 at a dose of 5×10^{19} eV/gm. It remains constant at this G value up to a dose of 4×10^{20} eV/gm.

b. Methane

The yield of methane as a function of dose is shown in Figure III-1B and in Table III-1. The "initial yield" of methane is 0.12 ± 0.03. The yield of methane is independent of dose.

Figure III-1

Yields of Hydrogen and Methane as a Function of Dose

A: Hydrogen

B: Methane

TABLE III-1

Hydrogen Yields from Methylcyclopentane as a Function of Dose

Dose rate range (a) 4.5 to 6.9 (10^{18} eV/gm hr) (b) 3.8 to 5.2 (10^{19} eV/gm hr)

Dose (10^{19} eV/gm)	G (Hydrogen)	G (Methane)
0.33	4.76 b	0.09 b
0.34	4.50 a	0.10 a
0.67	4.35 b	0.08 b
1.01		0.13 a
1.33	4.17 a	0.12 a
1.34	4.17 b	0.12 b
1.35	3.93 b	0.13 b
1.43	4.23 b	0.12 b
1.44	4.02 b	0.12 b
1.74	3.91 a	0.14 a
2.08	4.26 b	0.13 b
2.68	4.29 b	0.12 b
3.14	3.93 a	0.13 a
4.99	3.93 b	
5.36		0.12 b
6.72	3.97 a	0.12 a
10.0	4.05 b	0.11 b
20.2	3.75 b	0.13 b
20.3	3.90 b	0.12 b
20.3	3.84 b	0.12 b
20.4	3.88 b	0.14 b
29.9	4.00 b	0.12 b
40.1	3.99 b	0.12 b
40.7	3.96 b	0.13 b

c. 1-Methylcyclopentene (1-MC)

The "initial yield" of 1-MC is 2.7 ± 0.1 and the yield decreases to a value of 2.2 which is independent of dose above 1×10^{20} eV/gm. The variation of yield with dose is given in Figure III-2A and Table III-2.

d. 3-Methylcyclopentene (3-MC)

The variation of yield of 3-MC with dose is shown in Figure III-2A. Although there is a great deal of scatter, the yield appears to be independent of dose with an "initial yield" of 0.8 ± 0.2. Results are also tabulated in Table III-2.

e. Hexene-1

The yield of hexene at various doses is shown in Figure III-2B. The "initial yield" is 1.0 ± 0.1 from which the yield decreases slightly to a constant value of 0.7 with increasing dose. The results are given in Table III-2.

f. Bimethylcyclopentyl (BMCP)

The variation of yield of the principal dimer with dose is shown in Figure III-3A and tabulated in Table III-3. This dimer is independent of dose and has an "initial yield" of 0.90 ± 0.10.

g. Methylcyclopentyl methylcyclopentene (MCMC)

The "initial yield" of MCMC from Figure III-3A is 0.20 ± 0.05. The yield increases with increasing dose. The results are given in Table III-3.

Figure III-2

Yields of 1-Methylcyclopentene , 3-Methylcyclopentene and Hexene

as a Function of Dose

A: ◯ 1-Methylcyclopentene

     ☐ 3-Methylcyclopentene

B: Hexene

TABLE III-2

Yield of C_6 Products as a Function of Dose

Dose (10^{20} eV/gm)	G		
	1-Methylcyclopentene	3-Methylcyclopentene	Hexene
0.134	2.53	0.55	0.95
0.200	2.59	0.69	0.87
0.333	2.56	1.00	0.95
0.469	2.53	0.94	0.89
0.669	2.43	0.74	0.69
0.676	2.46	0.89	0.84
0.996	2.27	0.75	0.66
1.36	2.21	0.71	0.66
1.68	2.31	0.74	0.68
2.00	2.23	0.59	0.49
2.02		0.85	0.70
2.03		0.77	0.61
2.03		0.92	0.86
2.39	2.35	0.62	0.54
2.69	2.32	0.84	0.67
3.00	2.18	0.83	0.68
3.36	2.34	0.98	0.76
3.67	2.17	0.82	0.65
4.03	2.20	0.91	0.74

Dose Rate Range for 1-Methylcyclopentene was 5.51 to 5.67 (10^{19} eV/gm hr).

Dose Rate Range for 3-Methylcyclopentene and hexene was 4.50 to 5.67 (10^{19} eV/gm hr).

Figure III-3

Yields of Bimethylcyclopentyl (BMCP), Methylcyclopentyl methylcyclo-

pentene (MCMC) and Total Dimer as a Function of Dose

A: ◯   BMCP

△   MCMC

B: Dimer

◯   Total Dimer (Silicone Oil 710)

△   BMCP + MCMC   (Silica gel)

TABLE III-3

Yields of Bimethylcyclopentyl (BMCP) and Methylcyclopentyl methylcyclo-

pentene (MCMC) as a Function of Dose

Dose (10^{20} eV/gm)	G	
	BMCP	MCMC
0.067	0.85 b	
0.134	0.80 a	
0.200	0.95 a	
0.268	0.87 b	
0.333	1.00 a	0.16 a
0.469	0.92 a	0.22 a
0.669	0.93 a	0.25 a
0.676	0.99 a	0.31 a
0.996	0.80 a	0.21 a
1.00	0.82 b	
1.36	0.76 a	0.29 a
1.68	0.83 a	0.29 a
1.96	0.86 b	
2.00	0.74 a	0.29 a
2.02	0.78 a	0.20 a
2.03	0.80 a	
2.04	0.83 a	
2.39	0.72 a	0.28 a

TABLE III-3:Continued

| Dose (10^{20} eV/gm) | G | |
	BMCP	MCMC
2.69	0.95 a	0.37 a
3.00	0.94 a	0.38 a
3.36	0.92 a	0.38 a
3.67	1.09 a	0.43 a
4.01	0.83 b	
4.03	1.09 a	0.43 a

Dose Rate Range (a) 4.50 to 5.67 (10^{19} eV/gm hr)

(b) 3.84 (10^{19} eV/gm hr)

h. Total Dimer

The yield of total dimer was obtained on the silicone oil 710 column. The values of G(Dimer) are given in Table III-4 and are compared with values of G(BMCP + MCMC) from the silica gel column. The yield as a function of dose is plotted in Figure III-3B. Except for the region below 1×10^{20} eV/gm, the agreement between the two is fairly good. The disagreement at low dose may be due, in part, to the inability to measure the small peaks accurately.

B. Radiolysis of MCP with Liquid Additives

Binary solutions of MCP with benzene and with 1,3-cyclohexadiene were irradiated. All these samples contained a total of 2 ml of liquid. The dose given the 1,3-cyclohexadiene/MCP samples was 3.43 ± 0.13 (10^{20} eV/electron mole) or 1.92 ± 0.03 (10^{20} eV/gm) and that given the benzene/MCP samples was 3.39 ± 0.18 (10^{20} eV/electron mole) or 1.88 ± 0.05 (10^{20} eV/gm).

For each product measured, the variation of the yield as a function of electron fraction, ε_a, of additive was observed. The electron fraction is defined by

$$\varepsilon_a = \frac{E_a \, W_a}{E_a W_a + E_s W_s} \qquad [1]$$

where E_a and E_s are the number of moles of electrons per gram of additive and substrate respectively and W_a and W_s are the weights of

TABLE III-4

Yield of Total Dimer as a Function of Dose

Dose (10^{20} eV/gm)	G	
	Dimer	BMCP + MCMC
0.134	0.78	
0.268	0.87	
0.333		1.16
0.469		1.14
0.536	0.70	
0.669	1.00	1.18
0.676		1.30
0.996	0.90	1.01
1.00	1.04	
1.36	1.07	1.05
1.68	0.98	1.12
1.96	1.06	
2.00	1.21	1.03
2.02	1.04	0.98
2.03	1.11	
2.39	1.17	1.00
2.69	1.02	1.32
3.00	1.07	1.32
3.36	1.14	1.30
3.67	1.10	1.52
4.01	0.99	
4.03	1.08	1.52

Dose Rate Range for Dimer was 3.84 to 5.67 (10^{19} eV/gm hr).

additive and substrate respectively in grams.

The dashed lines shown in the following Figures represent the yield expected, G_{ex}, in a binary system if the contribution of each part were proportional simply to the electron fraction of that component in the mixture.

1. Gaseous Products, Hydrogen and Methane

The yields of hydrogen and methane from 1,3-cyclohexadiene/ MCP mixtures are shown in Figure III-4A and Figure III-5A and the yields of these two products from benzene/MCP mixtures are shown in Figure III-4B and Figure III-5B. The results are tabulated in Tables III-5 and III-6. The 1,3-cyclohexadiene is more effective than benzene in inhibiting hydrogen and methane production at low additive concentrations. In these tables $\Delta g'(H_2)$ refers to the decrease in hydrogen yield corrected for hydrogen formed by the additive and based on the energy absorbed by MCP only.

2. Liquid Products from MCP

a. 1-MC

The yields of 1-MC from MCP with 1,3-cyclohexadiene added and with benzene added are shown in Figure III-6 and given in Tables III-7 and III-8 respectively. In the 1,3-cyclohexadiene/MCP solutions, the product could not be measured above an electron fraction of 0.03, whereas in the benzene/MCP solutions, this point was not reached until 0.20 ϵ_a. At higher concentrations of additive, the additive gas

Figure III-4

Yield of Hydrogen from Solutions

A: 1,3-Cyclohexadiene/MCP Solution

B: Benzene/MCP Solution

Figure III-5

Yield of Methane from Solutions

A: 1,3-Cyclohexadiene/MCP Solutions

B: Benzene/MCP Solutions

TABLE III-5

Yield of Hydrogen and Methane from 1,3-Cyclohexadiene/MCP

Solutions

ϵ a	Mole Percent	$G(H_2)$	$\Delta g'(H_2)$	$G(CH_4)$
0.00094	0.102	3.66	0.54	0.112
0.00293	0.320	3.32	0.87	0.084
0.00481	0.521	3.04	1.15	0.090
0.00973	1.06	2.65	1.52	0.075
0.0199	2.17	2.24	1.92	0.063
0.0297	3.24	2.05	2.09	0.062
0.0303	3.29	2.05	2.09	0.061
0.103	11.1	1.38	2.69	0.042
0.202	21.6	1.00	3.00	0.026
0.329	34.8	0.736	3.22	0.018
0.499	52.1	0.530	3.37	0.012
0.670	68.9	0.398	3.47	0.009
0.750	76.6	0.352	3.49	0.005
0.899	90.7	0.279	3.52	0.004
1.00	100	0.233	4.20	-----

Dose Rate $= 8.52 \pm 0.44$ (10^{19} eV/hr electron mole).

TABLE III-6

Yield of Hydrogen and Methane from Benzene/MCP Solutions

ϵ_a	Mole Percent	$G(H_2)$	$\Delta g'(H_2)$	$G(CH_4)$
0.0198	2.25	3.30	0.83	0.115
0.100	11.3	2.12	1.85	0.081
0.201	22.4	1.34	2.53	0.057
0.334	36.4	0.839	2.96	0.033
0.502	53.5	0.465	3.30	0.021
0.669	69.8	0.247	3.52	0.018
0.751	77.5	0.185	3.56	0.007
0.849	86.6	0.106	3.67	0.002
1.00	100	0.032	4.20	-----

Dose Rate = 7.903 ± 0.003 (10^{19} eV/hr electron mole)

Figure III-6

Yield of 1-Methylcyclopentene (1-MC) and 3-Methylcyclopentene (3-MC)

from Solutions

A: 1,3-Cyclohexadiene/MCP Solutions

B: Benzene/MCP Solutions

◯ 1-MC

△ 3-MC

TABLE III-7

Yield of 1-Methylcyclopentene (1-MC) and 3-Methylcyclopentene (3-MC)

from 1,3-Cyclohexadiene/MCP Solutions

ϵ_a	Mole Percent	G	
		1-MC	3-MC
0.00094	0.102	1.83	0.65
0.00293	0.320	1.81	0.59
0.00481	0.521	1.83	0.55
0.00973	1.06	1.66	0.50
0.0199	2.17	1.23	0.46
0.0297	3.24	1.29	0.42
0.0303	3.29	1.13	0.39
0.103	11.1		0.30

Dose Rate = 8.64 ± 0.32 (10^{19} eV/hr electron mole)

TABLE III-8

Yield of 1-Methylcyclopentene (1-MC) and 3-Methylcyclopentene (3-MC)

from Benzene/MCP Solutions

ϵ_a	Mole Percent	G	
		1-MC	3-MC
0.0198	2.25	1.85	0.80
0.0505	5.73	1.70	0.76
0.100	11.3	1.47	0.62
0.201	22.4	1.24	0.47

Dose Rate = 7.910 ± 0.003 (10^{19} eV/hr electron mole)

chromatographic peak interferred with the peak for 1-MC so that it was possible to measure this product only at the lower ϵ_a values.

b. 3-MC

The yields of 3-MC with varying concentrations of 1,3-cyclo-hexadiene and of benzene are tabulated in Tables III-7 and III-8 respectively. The graphical results are shown in Figure III-6. The product was measured only up to an electron fraction of 0.10 in 1,3-cyclohexadiene and 0.20 in benzene solutions because of interference at higher concentrations of additive between the product peak and the additive peak.

c. Hexene

The hexene yield was determined using two different columns, silica gel and squalane on firebrick. Figure III-7 graphically represents the results of the average for the two columns. The difference in the results for the two columns was less than 5%. The variation of yield with additive concentration is given in Tables III-9 and III-10 for 1,3-cyclohexadiene and benzene respectively.

d. BMCP

The only dimer measureable on the silica gel column in the presence of the two additives was BMCP. The BMCP yields for 1,3-cyclohexadiene and for benzene solutions of MCP are given in Tables III-11 and III-12 respectively and are shown in Figure III-8. In the 1,3-cyclohexadiene solutions, the yield was reduced to below the detection

Figure III-7

Yield of Hexene from Solutions

A: 1,3-Cyclohexadiene/MCP Solutions

B: Benzene/MCP Solutions

TABLE III-9

Yield of Hexene from 1,3-Cyclohexadiene/MCP Solutions

ϵ_a	Mole Percent	G
0.00094	0.102	0.703
0.00293	0.320	0.676
0.00481	0.521	0.589
0.00973	1.06	0.531
0.0199	2.17	0.508
0.0297	3.24	0.385
0.0303	3.29	0.379
0.103	11.1	0.229
0.202	21.6	0.150
0.329	34.8	0.082
0.499	52.1	0.059
0.499	52.1	0.064
0.670	68.9	0.047
0.750	76.6	0.021
1.00	100	-----

Dose Rate = 8.58 ± 0.44 (10^{19} eV/hr electron mole)

TABLE III-10

Yield of Hexene from Benzene/MCP Solutions

ϵ_a	Mole Percent	G
0.0198	2.25	0.573
0.0505	5.73	0.440
0.100	11.3	0.306
0.201	22.4	0.199
0.334	36.4	0.138
0.502	53.5	0.091
0.669	69.8	0.041
0.751	77.5	0.034
1.00	100	-----

Dose Rate $=$ 7.90 $\pm$ 0.01 (10^{19} eV/hr electron mole)

Figure III-8

Yield of Bimethylcyclopentyl (BMCP) and Dimer from Solutions

A: 1,3-Cyclohexadiene/MCP Solutions

B: Benzene/MCP Solutions

△BMCP

○Dimer

TABLE III-11

Yield of Bimethylcyclopentyl (BMCP) and Total Dimer from 1,3-Cyclo-hexadiene/MCP Solutions

ϵ_a	Mole Percent	G	
		BMCP	Dimer
0.00094	0.102	0.395	0.537
0.00293	0.320	0.284	0.408
0.00481	0.521	0.248	0.299
0.00973	1.06	0.213	0.285
0.0199	2.17	0.204	0.227
0.0297	3.24	0.171	0.142
0.0303	3.29	0.170	0.140
0.103	11.1		0.182

Dose Rate $= 8.64 \pm 0.32$ (10^{19} eV/hr electron mole)

TABLE III-12

Yield of Bimethylcyclopentyl (BMCP) and Total Dimer from Benzene/MCP

Solutions

		G	
ϵ_a	Mole Percent	BMCP	Dimer
0.0198	2.25	0.635	0.817
0.0505	5.73	0.304	0.323
0.100	11.3	0.322	0.460
0.201	22.4	0.192	0.358
0.334	36.4	0.081	0.107
0.502	53.5	0.027	0.047
0.669	69.8		0.052
0.751	77.5		0.024
0.849	86.6		0.012
1.00	100		- - - - -

Dose Rate $= 7.903 \pm 0.003 \ (10^{19} \ \text{eV/hr electron mole })$

limit (G $<$ 0.15) by an electron fraction of about 0.04 and for benzene solutions by an electron fraction of about 0.60.

e. Dimer

The total dimer yield from MCP only was measured on the silicone oil 710 column. The results are given in Tables III-11 and III-12 for 1,3-cyclohexadiene and benzene solutions respectively and are shown in Figure III-8. The results are similar to those obtained for BMCP on the silica gel column.

3. Liquid Products from Additives

a. 1,3-Cyclohexadiene dimer (1,4,4a,5,6,8a-hexahydro-1,4-

ethanonaphthalene)

This product was measured on two columns, silica gel and silicone oil 710. The results are given in Table III-13 and plotted in Figure III-9A and are the averages from the two columns. The yield reaches a maximum value of G = 6.5 at ϵ_a = 0.10, from which it decreases to a value of G = 3.4.

b. Biphenyl

In solutions containing benzene and MCP, biphenyl was formed at high benzene concentrations ($\epsilon_a > 0.70$). The results are plotted in Figure III-10A from which it may be seen that the biphenyl yield increases rapidly at high benzene concentrations. The G value in pure benzene is 0.11. The yields are listed in Table III-14.

Figure III-9

Yield of 1,3-Cyclohexadiene Dimer and Disappearance of 1,3-Cyclo-

hexadiene from Solutions

A: 1,3-Cyclohexadiene Dimer from 1,3-Cyclohexadiene/MCP

Solutions

B: Disappearance of 1,3-Cyclohexadiene from 1,3-Cyclo-

hexadiene/MCP Solutions

TABLE III-13

Yield of 1,3-Cyclohexadiene Dimer from 1,3-Cyclohexadiene/MCP

Solutions

ϵ_a	Mole Percent	$G_{av.}$
0.00094	0.102	0.312
0.00293	0.320	1.18
0.00481	0.521	1.85
0.00973	1.06	2.56
0.0199	2.17	3.02
0.0297	3.24	3.35
0.103	11.1	6.57
0.150	16.1	5.52
0.202	21.6	5.36
0.329	34.8	4.12
0.499	52.1	3.65
0.599	62.0	3.64
0.670	68.9	3.56
0.750	76.6	3.16
0.800	81.3	3.46
1.00	100	3.41

Dose Rate = 8.52 ± 0.40 (10^{19} eV/hr electron mole)

Figure III-10

Yield of Biphenyl, Dimer 1 (D1), Dimer 2 (D2) and Dimer 3 (D3) from

Benzene/MCP Solutions

A:　△ Biphenyl

　　　○ D1

B:　○ D2

　　　△ D3

TABLE III-14

Yield of Biphenyl and Unidentified Dimers from Benzene/MCP Solutions

ϵ_a	Mole Percent	Biphenyl	D1	D2	D3
0.0505	5.73		0.037	0.032	
0.100	11.3		0.066	0.072	
0.201	22.4		0.092	0.094	0.029
0.334	36.4		0.074	0.068	0.033
0.502	53.5		0.050	0.063	0.061
0.669	69.8		0.041	0.050	0.076
0.751	77.5	0.036	0.032	0.041	0.077
0.849	86.6	0.046	0.024	0.032	0.090
1.00	100	0.114			0.114

Dose Rate = 7.903 ± 0.004 (10^{19} eV/hr electron mole)

c. Unidentified Dimers

Three unidentified dimers were measured in benzene/MCP solutions. Two of these, D1 and D2, increased to a maximum yield of about 0.09 G units at an electron fraction of 0.20, then decreased with increasing benzene concentration. The other dimer, D3, increased steadily with increasing benzene concentration to G = 0.11 in pure benzene. The results are tabulated in Table III-14 and plotted in Figure III-10.

4. Disappearance of 1,3-Cyclohexadiene

The disappearance of 1,3-cyclohexadiene was measured at low concentrations of 1,3-cyclohexadiene. As can be seen from Figure III-9B, the rate of disappearance increased rapidly with increasing diene concentration. The results are given in Table III-15.

C. Radiolysis of MCP with Gaseous Additives

Samples containing MCP and a gaseous additive were irradiated. The gases used were HCl, CO_2, N_2O, SF_6 and ND_3. Each sample contained 2.01 ml of MCP and varying amounts of the dissolved additive. In the figures which follow the yields are plotted in g units, where g represents the molecules of product formed per 100 eV initially absorbed by the MCP only;

$$g = \frac{G}{\epsilon_{MCP}}$$

[2]

TABLE III-15

Disappearance of 1,3-Cyclohexadiene from 1,3-Cyclohexadiene/MCP

Solutions

ϵ_a	Mole Percent	G
0.00481	0.521	8.63
0.00973	1.06	16.5
0.0199	2.17	26.6
0.0297	3.24	37.9

1. Radiolysis of HCl/MCP Solutions

The yields of hydrogen and methane with varying concentrations of HCl are shown in Figure III-11 and tabulated in Table III-16. The hydrogen yield increases rapidly with the addition of HCl and appears to approach a limiting value of about 6.4 g units by the time 2 mole percent HCl has been added. The methane yield decreases gradually over the same concentration range. The total dose given was 2.08 ± 0.01 (10^{19}) eV/gm.

2. Radiolysis of CO_2/MCP Solutions

The total dose received by these samples was 2.06 ± 0.08 (10^{20}) eV/gm at a dose rate of 7.28 ± 0.01 $(10^{19}$ eV/hr electron mole). The mole percent CO_2 used was corrected for solubility of CO_2 in MCP using the Bunsen Coefficient for cyclohexane. The Bunsen Coefficient for MCP was not available.

a. Hydrogen

The hydrogen yield is decreased by the addition of CO_2 from an initial value of 4.20 g units to 2.60 g units at 10 mole percent CO_2. The results are plotted in Figure III-12 and given in Table III-17.

b. Methane

From Figure III-12, it may be seen that the methane yield is unaffected by CO_2 addition. The results are tabulated in Table III-17

c. Carbon Monoxide

CO was found in the products and its yield increases with

Figure III-11

Yield of Hydrogen and Methane from HCl/MCP Solutions

A: Hydrogen

B: Methane

TABLE III-16

Yield of Hydrogen and Methane from HCl/MCP Solutions

Mole Percent HCl	g(Hydrogen)	g(Methane)
0	4.19	0.127
0.839	6.16	0.121
1.648	6.35	0.056

Dose Rate $=$ 7.29 $\pm$0.01 (10^{19} eV/hr electron mole)

Figure III-12

Yield of Hydrogen, Methane and Carbon Monoxide from CO_2/MCP

Solutions

A: Hydrogen

B: ◯ Methane

△ Carbon Monoxide

TABLE III-17

Yield of Hydrogen, Methane and Carbon Monoxide from CO_2/MCP

Solutions

Mole Percent CO_2	g		
	H_2	CH_4	CO
0	4.20	0.125	-----
0.00988	3.94	0.119	0.002
0.0348	3.83	0.114	0.005
0.0901	3.63	0.103	0.009
0.192	3.46	0.121	0.019
0.267	3.42	0.082	0.017
0.601	3.18	0.122	0.033
1.12	3.05	0.120	0.045
1.79	2.93	0.124	0.068
3.34	2.79	0.126	0.089
5.12	2.67	0.119	0.115
5.84	2.67	0.130	0.156
10.54	2.55	0.092	0.178

increasing CO_2 concentration. The results are given in Figure III-12 and Table III-17.

d. 1-MC

The yield of 1-MC with increasing CO_2 concentration is shown in Figure III-13. It decreases from the initial value of g = 2.7 to g = 1.4 at 5 mole percent CO_2. The results are given in Table III-18.

e. 3-MC

CO_2 does not have as great an effect on the yield of this product as on the other two C_6 olefins measured. The yield, from Figure III-13, decreases by 28% from the initial value as compared to a 48% decrease for 1-MC and a 71% decrease for hexene. The results are tabulated in Table III-18.

f. Hexene

Hexene-1 is decreased in yield by the greatest amount of any of the C_6 olefins. It decreases from an initial value of 1.0 g units to 0.29 g units. The results are plotted in Figure III-13 and given in Table III-18.

g. BMCP

The yield of BMCP decreased by 20% from the initial yield when more than 2.5 mole percent CO_2 was added, as is shown in Figure III-14. The results are given in Table III-18.

h. MCMC

The yield of MCMC was reduced by 25% by the addition of 3 mole

Figure III-13

Yield of 1-Methylcyclopentene (1-MC), 3-Methylcyclopentene(3-MC)

and Hexene from CO_2/MCP Solutions

☐ 1-MC

○ 3-MC

△ hexene

Mole Percent CO_2

TABLE III-18

Yield of Liquid Products Measured from CO_2/MCP Solutions

Mole Percent CO_2	g					
	1-MC	3-MC	Hexene	MCMC	BMCP	Dimer
0	2.70	0.83	1.00	0.20	0.90	1.00
1.79	1.61	0.62	0.34	0.18	0.75	0.90
3.34	1.58	0.62	0.29	0.16	0.72	0.90
5.12	1.44	0.59	0.29	0.15	0.72	0.91
5.84	1.46	0.57	0.27	0.15	0.73	0.78

Figure III-14

Yield of Bimethycyclopentyl (BMCP), Methylcyclopentylmethylcyclo-

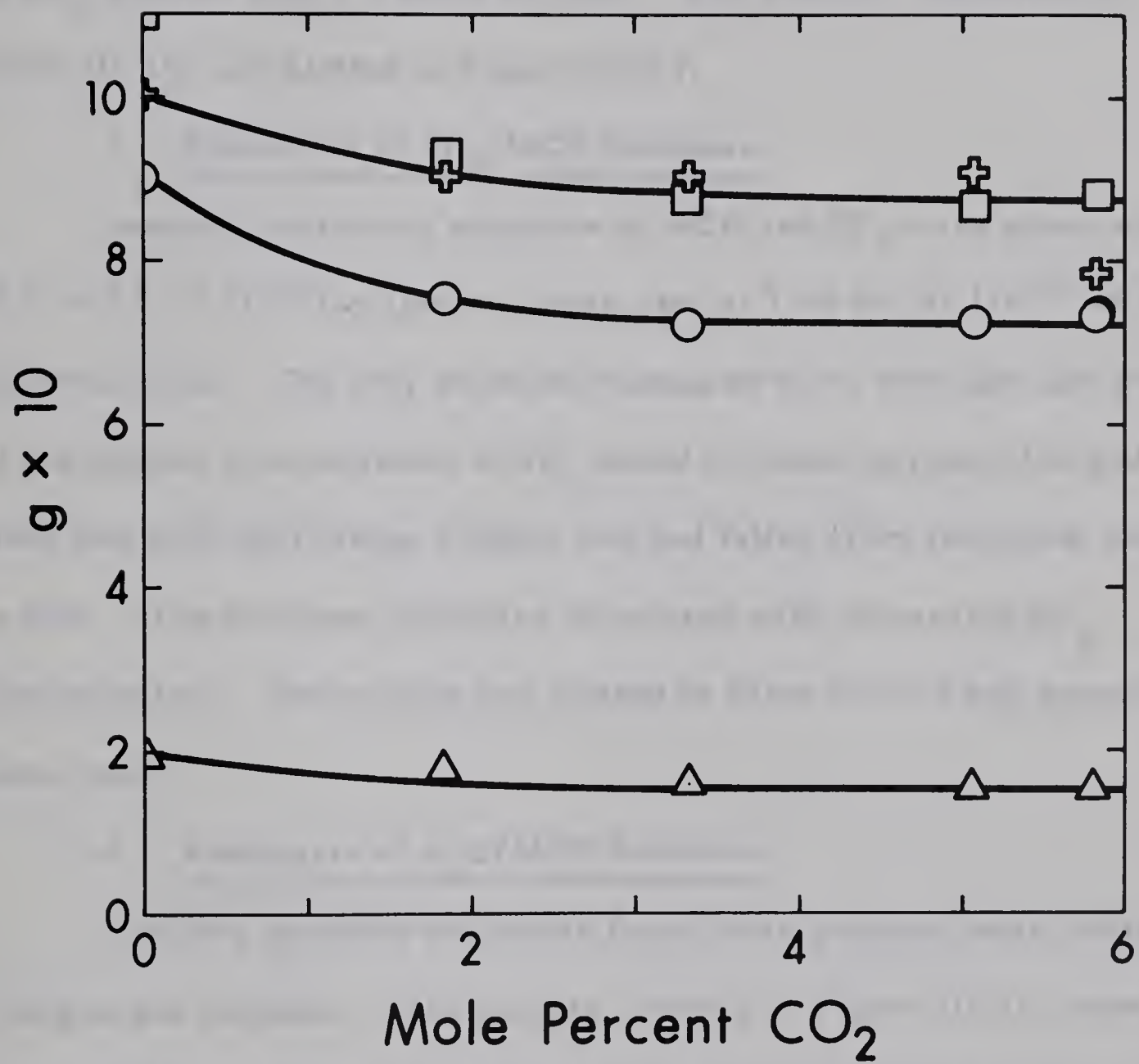pentene (MCMC) and Dimer from CO_2/MCP Solutions

◯ BMCP

△ MCMC

✚ Dimer (Silicone Oil 710)

☐ BMCP + MCMC

Mole Percent CO_2

$B \times 10$

percent or more of CO_2 (Figure III-14 and Table III-18).

i. Dimer

The yield of the total dimer measured on the silicone oil 710 column decreased by 13% from an initial g value of 1.00 with concentrations of CO_2 greater than 3.0 mole percent. The results, tabulated in Table III-18, are plotted in Figure III-14.

3. Radiolysis of SF_6/MCP Solutions

Samples containing solutions of MCP and SF_6 were given a dose of 2.18 ± 0.22 (10^{19}) ev/gm at a dose rate of 7.08 ± 0.05 (10^{19}) eV/hr electron mole. The only products measured were hydrogen and methane. At the highest concentration of SF_6 added (10 mole percent) the hydrogen yield was still decreasing slightly and had fallen from the initial yield by 53%. The methane yield also decreased with increasing SF_6 concentration. The results are plotted in Figure III-15 and given in Table III-19.

4. Radiolysis of N_2O/MCP Solutions

The only products measured from these samples were hydrogen, nitrogen and methane. The results, plotted in Figure III-16, show that while $g(H_2)$ decreases by 1.95 units at 13 mole percent nitrous oxide the nitrogen yield increases by 5.10 units, so that at this concentration of nitrous oxide $\Delta g(N_2)/ \Delta g(H_2) = 2.6$. The nitrogen yield was corrected for nitrogen formed by the direct radiolysis of nitrous oxide using $G(N_2) = 12.9$ for pure nitrous oxide.

Figure III-15

Yield of Hydrogen and Methane from SF_6/MCP Solutions

A: Hydrogen

B: Methane

TABLE III-19

Yield of Hydrogen and Methane from SF_6/MCP Solutions

Mole Percent SF_6	g	
	H_2	CH_4
0	4.20	0.125
0.00994	4.08	0.121
0.0497	3.84	0.128
0.100	3.67	0.118
0.499	3.04	0.116
1.05	2.54	0.123
2.54	2.38	0.097
4.99	2.14	0.088
7.52	2.02	0.076
10.0	1.98	0.087

Figure III-16

Yield of Hydrogen, Nitrogen and Methane from N_2O/MCP Solutions

A: ◯ Hydrogen

△ Nitrogen

B: Methane

The methane yield also decreased with increasing nitrous oxide concentration. Table III-20 gives the numerical results. These samples were given a dose of 2.11 ± 0.09 (10^{19}) eV/gm at a dose rate of 7.07 ± 0.12 (10^{19}) eV/hr electron mole.

5. Radiolysis of ND_3/MCP Solutions

a. H_2, HD, D_2 and CH_4 Yields

The samples for the measurement of the gaseous products non-condensable at $-196^{\circ}C$ were given a dose of 1.98 ± 0.03 (10^{19}) eV/gm at a dose rate of 6.87 ± 0.02 ($10^{19}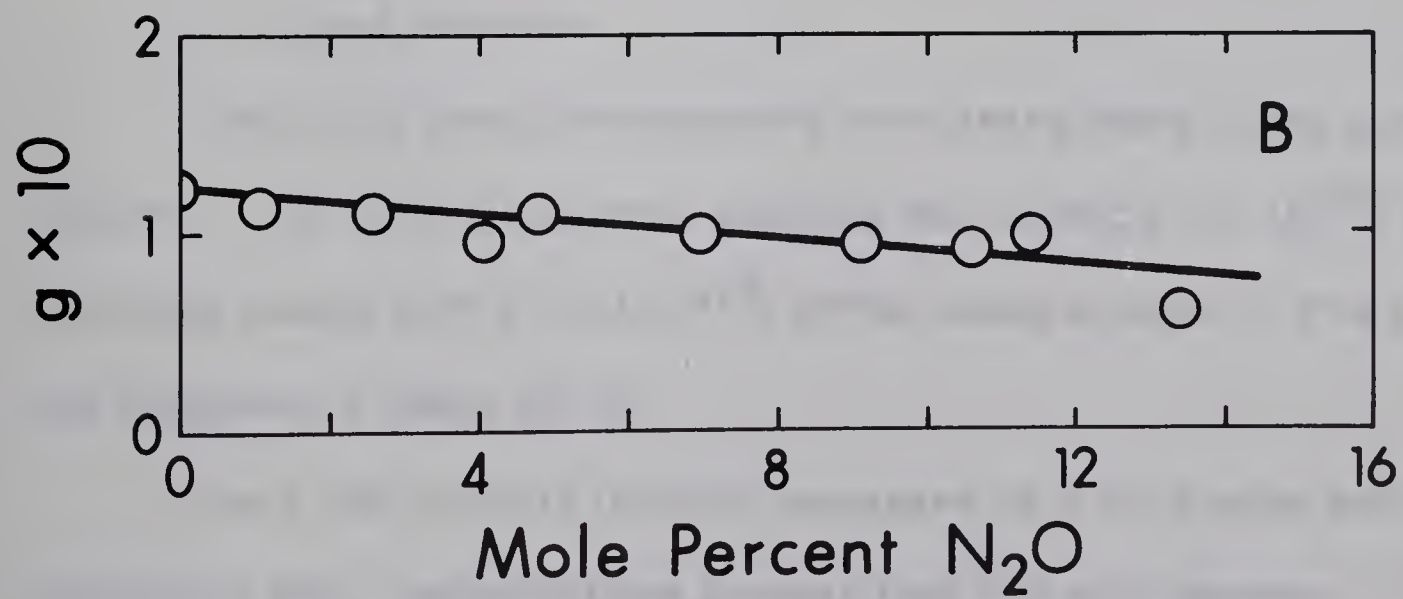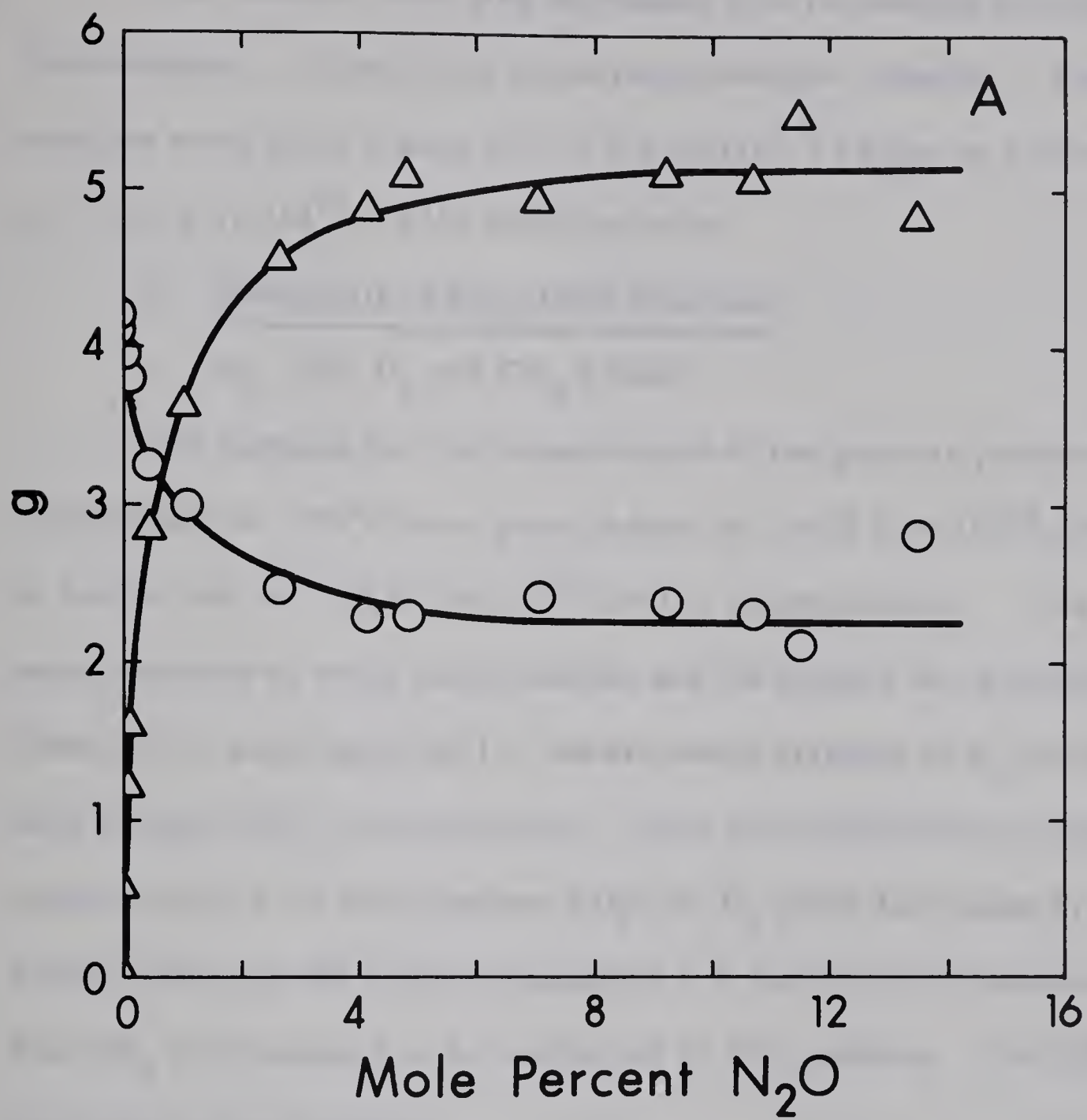$) eV/hr electron mole. The gases were analyzed by mass spectrometer and the results are given in Table III-21 and Figure III-17. Measureable amounts of D_2 were found only at higher ND_3 concentrations. Over the concentration range studied (up to 9.75 mole percent ND_3) the H_2 yield decreased by 0.8 g units while the HD yield increased by 1.6 g units over the same range. The CH_4 yield appears to be unaffected by ND_3 addition. No CH_3D was found in the products.

b. Liquid Products

The liquid products measured were those found in the pure MCP system. The dose given these samples was 1.98 ± 0.03 (10^{20}) eV/gm at a dose rate of 6.89 ± 0.01 (10^{19}) eV/hr electron mole. The results are tabulated in Table III-22.

The 1-MC yield is initially increased by 0.20 g units and remains constant at ND_3 concentrations greater than 0.5 mole percent. The

TABLE III-20

Yield of Hydrogen, Nitrogen and Methane from N_2O/MCP Solutions

Mole Percent N_2O	g		
	H_2	N_2	CH_4
0	4.20	0	0.125
0.00974	4.07	0.57	0.066
0.0528	3.86	1.22	0.125
0.100	3.79	1.59	
0.482	3.21	2.83	0.139
1.04	2.95	3.59	0.112
2.55	2.42	4.50	0.110
4.16	2.28	4.81	0.095
4.79	2.27	5.02	0.109
7.00	2.41	4.83	0.097
9.11	2.39	4 94	0.095
10.7	2.32	4 86	0.089
11.4	2.11	5.30	0.098
13.3	2.84	4.59	0.059

Figure III-17

Yield of H_2, HD, D_2 and Methane from ND_3/MCP Solutions

A: ◯ H_2

⊕ HD

△ D_2

B: CH_4

TABLE III-21

Yield of H_2, HD, D_2 and CH_4 from ND_3/MCP Solutions

Mole Percent ND_3	g			
	H_2	HD	D_2	CH_4
0	4.21	-----	-----	0.118
0.00927	4.29	0.025	-----	0.165
0.0294	4.38	0.073	-----	0.111
0.118	4.30	0.124	-----	0.112
0.281	4.12	0.171	0.003	0.113
0.949	4.05	0.410	0.003	0.138
2.85	3.87	0.900	0.009	0.120
6.64	3.70	1.38	0.029	0.076
9.75	3.51	1.58	0.049	0.103

TABLE III-22

Yield of Liquid Products from ND_3/MCP Solutions

Mole Percent ND_3	g					
	1-MC	3-MC	Hexene	BMCP	MCMC	Dimer
0	2.29	0.800	0.700	0.860	0.172	1.06
0.0100	2.32	0.916	0.743	0.896	0.234	1.11
0.0469	2.47	0.911	0.757	0.921	0.254	1.15
0.0949	2.63	0.963	0.745	0.925	0.242	1.10
0.487	2.56	0.924	0.718	0.995	0.249	1.09
0.990	2.60	0.984	0.646	1.05	0.249	1.16
4.71	2.55	0.984	0.478	1.10	0.219	1.29
9.52	2.49	0.944	0.399	1.26	0.221	1.44

3-MC yield also increased by 0.17 but not so rapidly, the constant value

being reached by the time 1 mole percent ND_3 had been added.   Hexene

decreased gradually from its initial yield. · These three products yields

are plotted in Figure III-18 A and B and tabulated in Table III-22.

Figure III-18 C and E show that the BMCP and total dimer yields

increased steadily with increasing ND_3 concentration.   The MCMC

yield increased by 0.07 g units when the ND_3 concentration was just

0.01 mole percent and then remained constant with increasing ND_3

concentration (Figure III-18D).

Figure III-18

Yield of Liquid Products from ND_3/MCP Solutions

A: 1-MC

B: ◯ 3-MC

☐ Hexene

C: BMCP

D: MCMC
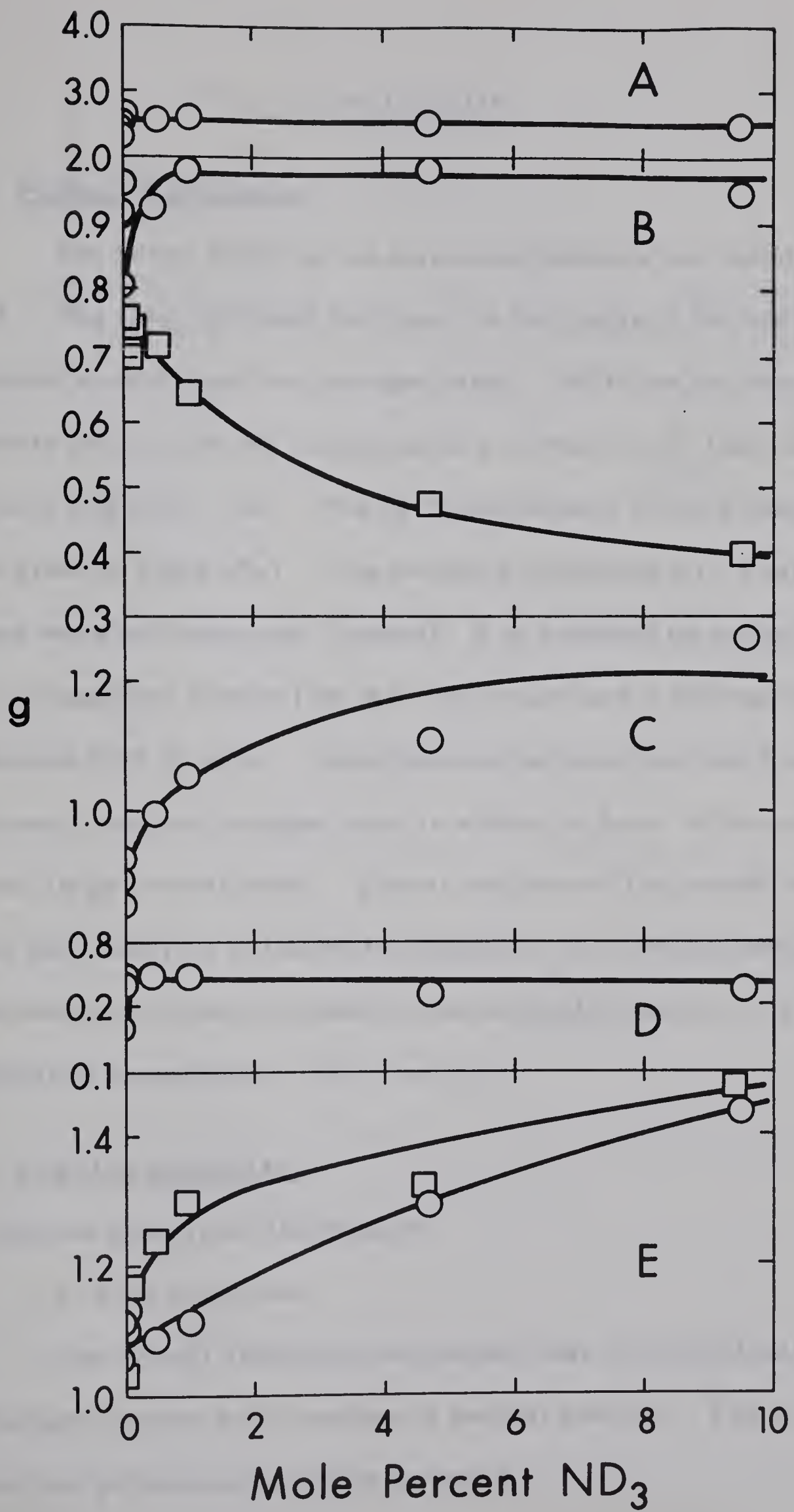
E: Dimer

◯ Total Dimer (Silicone Oil 710)

☐ BMCP + MCMC

g

4.0
3.0
2.0

A

0.9
0.8

B

0.7
0.6
0.5
0.4
0.3

1.2
1.0
0.8

C

0.2
0.1

D

1.4
1.2
1.0

E

0   2   4   6   8   10

Mole Percent ND$_3$

Mole Percent TiO$_2$

A

B

C

D

E

IV.   DISCUSSION

A.   Product Distribution

The initial yields of the measured products are listed in Table IV-1. The total hydrogen deficiency in the yields of the hydrocarbon products should equal the hydrogen yield. MCP has the empirical formula CH_2, so the H_2 equivalent of a product C_mH_n that has a G value of x is $x(n/2 - m)$. The hydrogen balance of the products is also given in Table IV-1. The products containing 2 to 5 carbon atoms were not measured, however, it is assumed by analogy with the cyclopentane system (64) that they would have a hydrogen equivalent of about $+ 0.24$ G units. The difference between the total hydrogen deficiency and the hydrogen yield is within the sum of the estimated rather large uncertainties. Kinetic analysis of the results obtained from the radiolysis of the MCP solutions of the various additives indicated that the most probable value of $G_i(H_2)$ was 4.2. The kinetic analysis is presented in a later section.

B.   Reaction Mechanism

1. General Radiolysis Mechanism

a. Pure Substrate

The overall radiolysis mechanism may be divided into reactions of charged species and reactions of neutral species. For a substrate A the charged species would be formed by

TABLE IV-1

Hydrogen Balance

Product	G_i	H_2 equivalent
CH_4	0.12 ± 0.03	$+0.12 \pm 0.03$
$C_2 - C_5$	a	$+0.24$[b]
1-MC	2.7 ± 0.1	-2.7 ± 0.1
3-MC	0.8 ± 0.2	-0.8 ± 0.2
Hexene	1.0 ± 0.1	0.0
BMCP	0.9 ± 0.1	-0.9 ± 0.1
MCMC	0.20 ± 0.05	-0.40 ± 0.10
Total		-4.4 ± 0.5
H_2	4.5 ± 0.5	$+4.5 \pm 0.5$

a. not measured

b. calculated by analogy with the results for cyclopentane obtained

by L. G. Walker (private communication).

$$A \xrightarrow{\sim\!\!\wedge\!\!\wedge\!\!\sim} [A^+ + e^-] \qquad\qquad [1]$$

The following reactions could then take place.

$$[e^- + mA] \longrightarrow [e^-_{solv}] \qquad\qquad [2]$$

$$[A^+ + e^-_{solv}] \longrightarrow [A^*] \qquad\qquad [3]$$

$$\longrightarrow A^+ + e^-_{solv} \text{ (free ions)} \qquad\qquad [4]$$

$$A^+ + e^-_{solv} \longrightarrow A^* \qquad\qquad [5]$$

The square brackets around reactants or products indicate that the

species are in the spurs.

Neutral reactive species will be formed by reactions $[3]$, $[5]$

and $[6]$ and will react according to reactions such as $[7]$ - $[11]$.

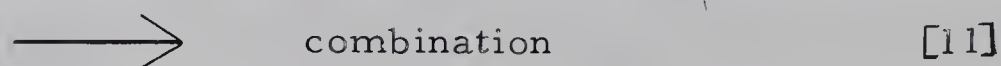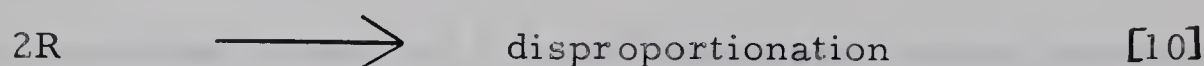$$A \xrightarrow{\sim\!\!\wedge\!\!\wedge\!\!\sim} A^* \qquad\qquad [6]$$

$$A^* \longrightarrow R_1 + R_2 \qquad\qquad [7]$$

$$\longrightarrow M_1 + M_2 \qquad\qquad [8]$$

$$R + A \longrightarrow RH + R_3 \qquad\qquad [9]$$

$$2R \longrightarrow \text{disproportionation} \qquad\qquad [10]$$

$$\longrightarrow \text{combination} \qquad\qquad [11]$$

where R is any radical, R_n is a specific radical and M is a molecule.

This general mechanism is in accord with the major products formed.

Dimers would be formed by reaction $[11]$, congruent olefins by

reactions $[8]$ and $[10]$, methane by reactions $[7]$ to $[9]$, and hydrogen

by reactions $[7]$ to $[9]$. In addition radicals may add to molecules to give

products.

b. Solutions

Reactive solutes, depending on their nature and concentration,

can interfere with reactions [2] , [3] , [5] and [7] to [11] . For

an electron scavenger, the reaction may be represented by

$$e^-_{solv} + S \longrightarrow S^-$$ [12]

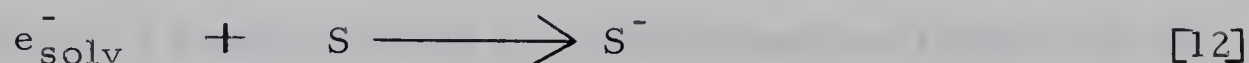Thus, if reaction [12] can compete with the recombination of electrons

and positive ions, the yield of A*, and thus of normal radiolysis products,

will decrease with increased solute concentration. The same would

be true for a positive ion scavenger. In this study, three electron

scavengers (nitrous oxide, sulfur hexafluoride and carbon dioxide) and

one positive ion scavenger (perdeutero ammonia) were used.

In addition to chemical reaction with a scavenger, positive ions

may lose their reactivity by charge transfer reactions such as

$$A^+ + B \longrightarrow B^+ + A$$ [13]

if the ionization potential of the solute, B, is lower than the recombin-

ation energy of the substrate A.

Radical scavengers (such as 1,3-cyclohexadiene) would interfere

with reactions [9] to [11] .

To simplify discussion of the MCP mechanism, the results will

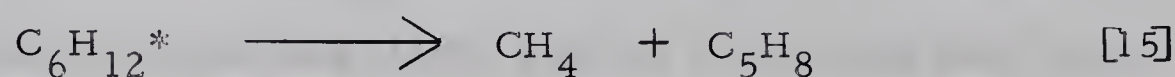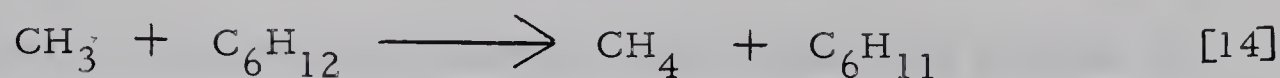be divided into two sections; products other than hydrogen and hydrogen.

2. Products Other than Hydrogen
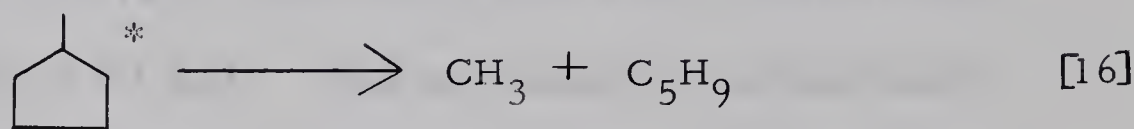
    a. Products Formed from MCP

    i. Methane

The methane yield $G(CH_4) = 0.12$, was independent of dose

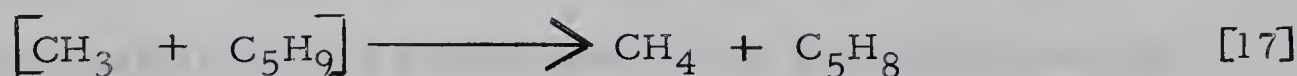(Figure III-1B). This value agrees well with the value found by

Hardwick (56), i.e. $G(CH_4) = 0.11$ and the value, $0.10 - 0.11$ G units,

calculated from the data of Schuler and Kuntz (32). It was decreased

to half its value by 3.25 mole percent 1,3-cyclohexadiene (Figure III-5A

insert) and by 22.4 mole percent benzene (Figure III-5B). These

results are consistent with methane formation by the reactions

$$CH_3 + C_6H_{12} \longrightarrow CH_4 + C_6H_{11} \qquad [14]$$

$$C_6H_{12}{}^* \longrightarrow CH_4 + C_5H_8 \qquad [15]$$

Methyl radical abstractions of hydrogen atoms from alkanes have been

reported in the literature (72). Methyl radicals may be formed by the

decomposition of an excited MCP molecule.

$$\longrightarrow CH_3 + C_5H_9 \qquad [16]$$

Hardwick (56) has proposed that a fraction of the methane may also be

formed by molecular detachment from one molecule, by means of a

disproportionation reaction between two radicals formed in the same

solvent cage

$$\left[CH_3 + C_5H_9 \right] \longrightarrow CH_4 + C_5H_8 \qquad [17]$$

Schuler and Kuntz (32) estimate that about half the methane is not

readily scavengeable, as would be the case for reactions [15] and [16].

No effect on the methane yield was observed when perdeutero ammonia

or carbon dioxide were added. Nitrous oxide linearly decreased the

yield to 0.09 when 10 mole percent was added (Figure III-17B) and

sulfur hexafluoride caused the methane yield to drop to 0.08 when 6

mole percent was added (Figure III-16B). At increased concentrations

of sulfur hexafluoride, the yield of methane remained constant. The

effects of these last two additives, however are small compared to

the effects produced by the radical scavengers.

ii. Congruent Olefins

The congruent olefins measured were 1-MC, 3-MC and hexene

although it must be remembered that the 1-MC yields may consist of

1-MC plus methylene cyclopentane (MEC) and the 3-MC yield may really

be 3-MC plus 4-MC (see page 55). The yield of 1-MC decreased by

17% and the yield of hexene decreased by 30% with increasing dose to a

dose of about 1×10^{20} eV/gm, after which they were constant with

increasing dose (Figure III-2A). This decrease to constant yield

would suggest that part of these products are readily scavengeable

and part not readily scavengeable. The 3-MC yield appeared to be

independent of dose.

It has been proposed for cycloalkanes that much of the cyclic

olefin and bicycloalkyl dimers are formed by the disproportionation

and combination of cycloalkyl radicals (reactions [10] and [11]).

For MCP these reactions would be

$$2 C_6H_{11} \longrightarrow C_6H_{10} + C_6H_{12} \qquad [18]$$
$$\longrightarrow (C_6H_{11})_2 \qquad [19]$$

For MCP there are four possible C_6H_{11} radicals which may be formed:

| I | II | III | IV |

For radicals of similar type, it seems true that the disproportion rate

is roughly proportional to the number of hydrogen atoms in β positions

to the radical site (74). With this in mind, and if each of the above

radicals had equal probability of being formed, then it would be expected

that Gi(1-MC + MEC)/Gi(3-MC + 4-MC) = 1.50 (MEC is methylene cyclo-

pentane). From the experimental results, Gi (1-MC)/Gi (3-MC) = 3.4,

which probably indicates that the tertiary radical, II, is the most favored

radical for formation or that the following reaction occurs

$$\text{I, III, or IV} \quad + \quad \text{MCP} \quad \longrightarrow \quad \text{MCP} + \text{II} \qquad [20]$$

This is not surprising since the tertiary C-H bond is the weakest C-H

bond in the molecule. MC may also be formed, along with hexene, by the

following reactions

$$[21]$$

$$[22]$$

$$[23]$$

The other possible disproportion and combination reactions from the

reactants in Equation [23] are

$$[24]$$

$$[25]$$

The two new products in reactions [24] and [25] were not found,

however their presence may have been hidden by other products or by MCP.

In addition to reactions [21] to [25], which may take place in

spurs or in the bulk medium, the following reactions may also take place

$$C_6H_{12} \longrightarrow C_6H_{12}{}^* \longrightarrow \quad \longrightarrow \qquad \text{[26]}$$

$$\longrightarrow \qquad \text{or} \qquad \text{[27]}$$

and in spurs only

$$\longrightarrow H_2 \ + \ C_6H_{10} \qquad \text{[28]}$$

$$\left[H \ + \ C_6H_{11} \right] \longrightarrow \left[H_2 \ + \ C_6H_{10} \right] \qquad \text{[29]}$$

From the reactions given, it would be expected that radical scavengers

would affect the yield of the olefin formed, especially in the bulk medium.

From the results (Figure III-6A), it may be seen that both 1-MC and

3-MC are reduced to half their initial values by 3.25 mole percent

1,3-cyclohexadiene. Benzene reduces 1-MC to 1/2 Gi by 22 mole

percent additive and also reduces 3-MC to 1/2 Gi by 30 mole percent

additive (Figure III-6B). Hexene was most efficiently scavenged,

decreasing its yield by half when only about one mole percent 1,3-cyclo-

hexadiene or 3.25 mole percent benzene were added. (Figure III-7)

Carbon dioxide, an efficient electron scavenger, also decreased

the yields of the congruent olefins. Again, the most efficiently scavenged

congruent olefin was hexene, which decreased by 72% on the addition of

3 mole percent carbon dioxide (Figure III-14). The 1-MC yield decreased

by 45% when 4 mole percent carbon dioxide was added and 3-MC decreased

by 25% when 3 mole percent was added. If carbon dioxide scavenges

only electrons, then the reaction being inhibited would be

$$C_6H_{12}^+ + e_{solv}^- \longrightarrow C_6H_{12}^* \qquad [30]$$

The addition of ND_3 also had an effect on the congruent olefin

yields (Figure III-19). The 1-MC yield increased by 0.2 units at 0.5

mole percent ND_3 and remained constant thereafter. The 3-MC yield

increased by 0.17 units at 1 mole percent and also remained constant

with continued increasing ND_3 concentration. Since the most probable

method of interaction of ND_3 is by proton transfer from the hydrocarbon

ions, the positive ions produced by radiolysis may react according to

the following reactions

$$RH^+ + ND_3 \longrightarrow R + ND_3H^+ \qquad [31]$$

$$ND_3H^+ + e^- \longrightarrow ND_3 + H \qquad [32]$$

$$\longrightarrow ND_2H + D \qquad [33]$$

$$C_6H_{12} + H \longrightarrow H_2 + C_6H_{11} \qquad [34]$$

$$C_6H_{12} + D \longrightarrow HD + C_6H_{11} \qquad [35]$$

producing one congruent olefin or dimer precursor for each RH^+

scavenged. In the absence of ND_3, it is possible that not all the positive

ions formed lead to congruent olefin or dimer precursors. When ND_3

is added, a large percentage of these positive ions is scavenged, leading

to the formation of a larger number of C_6H_{11} radicals and causing

the congruent olefin yield to increase. 1-MC and 3-MC increase more

rapidly initially than dimer increases or hexene decreases. This sudden

increase may be due to the elimination of certain positive ions by

scavenging which would, in the absence of ND_3, cause the 1-MC and 3-MC yields to decrease from secondary reactions.

Hexene may be formed by the ring cleavage of an excited MCP molecule or an excited C_6H_{11} radical. If these two precursors were formed mainly by reaction[30], then the scavenging of $C_6H_{12}^+$ ions by ND_3 would decrease the yield of hexene precursors. Experimentally, the yield of hexene decreased steadily to about half its initial value at 10 mole per cent ND_3.

In the radiolysis of the cyclopentane-ND_3 system Walker (64) found no decrease in ring opening products. It would have been interesting to observe the effect of ND_3 on any cyclohexane formed by MCP radiolysis however cyclohexane could not be separated analytically from MCP by the gas chromatographic columns used.

iii. Dimers

Two dimers were measured, bimethylcyclopentyl (BMCP) and methylcyclopentylmethylcyclopentene (MCMC). It is also possible that the peak measured as BMCP contains a small amount of a third dimer (see page 55). The yield of the most plentiful dimer, BMCP, is independent of dose and is 0.9 G units (Figure III-3A). The yield of MCMC increases with dose from an initial G value of 0.20 (Figure III-3A).

BMCP is most likely formed by the combination of two methyl-cyclopentyl radicals (reaction [18]). The MCMC is probably formed,

at least in part, by secondary reactions such as

$$C_6H_{10} \; + \; H \longrightarrow C_6H_9 \; + \; H_2 \qquad\qquad [36]$$

$$C_6H_9 \; + \; C_6H_{11} \longrightarrow MCMC \qquad\qquad [37]$$

As would be expected from its radical combination formation mechanism,

the yield of BMCP was decreased to half its initial value by only 0.1 mole

percent 1,3-cyclohexadiene or by 4.6 mole percent benzene (Figure III-8).

The MCMC yield in the presence of additives was too small to measure.

When 3 mole percent carbon dioxide was added, the BMCP yield

decreased by 19% and the MCMC yield decreased by 25% due to the

inhibition of reaction 30 (Figure III-15).

When the positive ion scavenger ND_3 was added, the BMCP yield

increased gradually to an apparently constant value of 1.2 units at 10 mole

percent ND_3 (Figure III-19C). Again, this may be explained by proposing

that a high percentage of the RH^+ ions are scavenged by ND_3, forming a

greater number of BMCP precursors than are present in pure MCP radio-

lysis. The MCMC yield increased very sharply initially by 0.07 units and

remained constant at this value with increasing concentration of ND_3

(Figure III-19D). An increase in C_6H_{10} due to increased C_6H_{11} from

reaction [31] would cause the MCMC yield in the presence of ND_3 to exceed

the yield in pure MCP as can be seen by the secondary reactions [36] and [37]

b. Products Formed from Additives

i. 1,3-Cyclohexadiene Dimer

The dimer from 1,3-cyclohexadiene was measured during the

analysis of the reaction products. The yield increases rapidly from

zero to a maximum of about 6.5 G units when 11 mole percent 1,3-cyclohexadiene was present, then decreases to a constant value of 3.3 G units independent of 1,3-cyclohexadiene concentration above about 70 mole percent 1,3-cyclohexadiene (Figure III-9A). Wakeford (37) found that when he added 1,3-cyclohexadiene to cyclohexene solutions he also obtained a maximum yield of the dimer of about 6.3 but at about 5 mole percent 1,3-cyclohexadiene. He attributed the high yield of dimer in the low concentration region to charge and/or excitation transfer from the activated substrate molecule. When 1,3-cyclohexadiene is added to cyclohexane, similar behavior is also observed. Schutte (73) proposes a chain mechanism for formation of the dimer involving charge transfer from an MCP molecule to a 1,3-cyclohexadiene (CHD) molecule.

$$MCP \longrightarrow MCP^+ + e^- \tag{38}$$

$$MCP^+ + CHD \longrightarrow MCP + CHD^+ \tag{39}$$

$$CHD^+ + CHD \longrightarrow DCHD^{+*} \tag{40}$$

$$DCHD^{+*} \longrightarrow DCHD^+ \tag{41}$$

$$DCHD^+ + CHD \longrightarrow DCHD + CHD^+ \tag{42}$$

where DCHD is the dimer from 1,3-cyclohexadiene.

ii. Benzene products

Several dimer type products were messured in MCP solutions containing benzene. One of these was identified as biphenyl and three were unidentified. Biphenyl, measureable at concentrations of benzene

greater than 80 mole percent, increased to G = 0.11 in pure benzene (Figure III-10A). One product, D_3, increased linearly over the whole concentration range from zero to 0.11 G units in pure benzene (Figure III-10B). The other two products D_1 and D_2 reached maxima of about 0.09 G units at 22 mole percent benzene and then gradually decreased with increasing benzene concentration (Figure III-10).

c. Disappearance of Additive from Solution

The comsumption of 1,3-cyclohexadiene was measured at low concentrations of the additive. The extremely rapid disappearance of 1,3-cyclohexadiene (Figure III-9B) compared with the smaller amount of dimer formed (Figure III-9A) at these low additive concentrations suggests that a large amount of polymerization takes place when 1,3-cyclohexadiene is present.

3. Hydrogen

The hydrogen yield may be divided into two portions, the readily scavengeable yield and the not readily scavengeable or residual yield. The readily scavengeable yield will be discussed in terms of nonhomogeneous kinetics.

a. Nonhomogeneous Kinetics

Freeman has devised a model to describe the scavenging of positive ions and solvated electrons in the radiolysis of liquids (57, 75). The model uses nonhomogeneous kinetics of charge neutralization in radiolytic saturated hydrocarbon systems.

The mechanism for the scavenging of positive ions may be written

$$A \longrightarrow\!\!\!\!\sim\!\!\!\!\sim\!\!\!\!\sim\!\!\!\!\longrightarrow \left[B^+ + C^- \right] \qquad\qquad [43]$$

$$\left[B^+ + C^- \right] \longrightarrow [D] \qquad\qquad [44]$$

$$\longrightarrow B^+ + C^- \quad \text{(free ions)} \qquad [45]$$

$$B^+ + C^- \longrightarrow D \qquad\qquad [46]$$

$$\left[B^+ + S \right] \longrightarrow \left[E^+ \right] \qquad\qquad [47]$$

$$B^+ + S \longrightarrow E^+ \qquad\qquad [48]$$

followed by $\left[E^+ + C^- \right] \longrightarrow [G] \qquad\qquad [49]$

$$E^+ + C^- \longrightarrow G \qquad\qquad [50]$$

where S is a scavenger which reduces the yield of product D and forms

a new product G.   Square brackets about reactants or products indicate

that the species are in a spur.   There exists a competition between C^-

and S for B^+ and this may be studied by measuring either the decrease

in D or the growth in G as a function of scavenger concentration.   For

a mathematical description of this competition it is necessary to know:

    i.   the initial relative spacial distribution of B^+ and C^-,

    ii.   the motions of B^+ and C^- under the influence of both the

        random diffusion forces and the force of their mutual

        electric field,

    iii.   the encounter radii for reactions [44] , [46] , [47] , and

        [48] and

    iv.   the encounter efficiencies of these same four reactions.

It is necessary to make approximations for these quantities since they

are not accurately known.

       i. The initial relative spacial distribution of positive ions and thermalized electrons can be crudely estimated. Using data given by Lea (76), Freeman (75) has constructed a spectrum of N(y) vs y where N(y) is the relative number of positive ion-thermalized electron pairs that have an initial separation distance y in water. It is necessary to correct this spectrum for the range of electrons in MCP. Assuming that the range is inversely proportional to $-(dT/dx)_{coll}$, the Bethe equation (Eq. 4 in Chapter I) may be used to determine the range in MCP in relation to that in water. The excitation potentials of the inner shell electrons of carbon and oxygen are about 280 and 520 eV, respectively. Thus the Bethe equation is valid only for electron energies above several hundred eV since it assumes that the energy of the secondary electron exceeds that of the orbital electrons. Since about 80% of ionization events have secondary electron initial kinetic energy of less than 100 eV (75), it is necessary to adjust the Bethe equation for use in this theory. Thus the valence electron densities and the first ionization potentials(gas phase) of MCP and water were used in the calculation. The relative ranges of 100 eV electrons in water and MCP were 1.00 and 1.28, respectively. Table IV-2 gives the N(y) vs y spectra for water, cyclohexane (75) and MCP.

TABLE IV-2

Spectra of Ion-pair Separation Distances

N(y)	$y \ (10^{-8} \ cm)$		
	H_2O	$c\text{-}C_6H_{12}$	$CH_3C_5H_9$
2150	14	17	18
1100	16	19	20
600	19	22	24
476	26	31	33
270	44	53	56
116	72	86	92
64	104	125	133
41	140	168	179
28	181	216	232
21	225	270	288
16	274	328	351
13	326	392	417
15	397	476	508
14	505	607	646
10	643	770	823
8	795	950	1018
6	960	1150	1229
8	1220	1460	1562
10	1650	1980	2112
34	2200	2600	2816

Total 5000

ii. The motions of the positive ion and solvated electron will be influenced by two opposing forces. The mutual electric field of the ion and electron will tend to cause their geminate recombination (Eq. [44]). Random diffusive forces will, however, tend to counteract this effect (Eq. [45]). In order to calculate the fraction of positive ions under-going geminate recombination that are scavenged, it is necessary to know the number, bn, of new molecules the ions meet before recombin-ation and the encounter efficiency, f_+, of reaction [47] . The average number, b of new neighbors met per jump depends on the ion-molecule effective encounter radius, the jump distance, the packing of the molecules in the medium and the diffusion coefficients of the molecules in the medium. The value of b for ordinary molecules or ions may be about 4. The number of diffusive jumps, n, made by the positive ion is given by (77)

$$n = t_{gr}/t_1 \tag{51}$$

where t_{gr} is the time required for geminate recombination

t_1 is the average time required for one diffusive jump

The expression for t_{gr} is found as follows. The relative drift velocity of a pair of monovalent ions in their mutual electric field is $300\ e(u_+ + u_-)/\epsilon r^2$

so

$$\frac{dt}{dr} = \frac{\epsilon r^2}{300 e(u_+ + u_-)} \tag{52}$$

where ϵ is the static dielectric constant of the medium

r   is the separation distance of the ions (cm)

e   is the charge on the ion (esu)

$(u_+ + u_-)$ is the sum of the mobilities of the ion and electron

Thus $$t_{gr} = \int_{r_o}^{y} \varepsilon r^2 dr / 300e(u_+ + u_-) \qquad [53]$$

$$= \varepsilon (y^3 - r_o^3)/4.32 \times 10^{-7} (u_+ + u_-) \qquad [54]$$

where y is the initial separations distance of the ion pair

and r_o is the center to center distance of B^+ and C^- at the instant of

the final electron jump.

Also, t_1 is given by (75)

$$t_1 = d \lambda^2 / 6D \qquad [55]$$

where d is a constant of about unity and is the same for all liquids

λ is the mean jump distance

and D is the diffusion coefficient of the species involved.

The equation that describes the fraction of positively charged ions

scavenged at a given scavenger concentration will now be derived.   If

N_s is the mole fraction of S in the solution, then the mole fraction of

all other species except S is $(1 - N_s)$.   The probability that B^+ will

encounter a species other than S in one diffusive jump is given statistically

by $(1 - N_s)^{b_+}$ where b_+ is the number of new neighbors B^+ meets per

diffusive jump.   For B^+ ions which undergo geminate recombination,

the probability that they will encounter a species other than S during

their lifetime is $(1 - N_s)^{b_+ + n_+}$, where n_+ is the number of diffusive jumps

taken before recombination with C^-.   Thus the probability that B^+ will

encounter one (or more) S during its lifetime is $\left[1 - (1 - N_s)^{b+n+}\right]$.
Since it is possible that a B^+ ion will not react with S on every encounter
it is necessary to take into account the encounter efficiency, f_+, of
reaction [47] where $0 \leq f_+ \leq 1$. If $f_+ < 1$, this is the same as decreasing
the effective value of N_s. Thus the probability that B^+ is scavenged
before geminate recombination occurs is given by $\left[1 - (1 - f_+ N_s)^{b+n+}\right]$.
This expression assumes that an encounter with x molecules of S in one
solvent cage is as effective as x encounters with one S molecule, and
that the scavenger and solvent molecules do not diffuse. If it is assumed
that S and solvent molecules diffuse and that B^+ does not move then the
probability that one of the diffusing molecules that encounters B^+ is a
scavenger is given by $\left[1 - (1-N_s)^{b_s n_s}\right]$ where b_s is the number of new
neighbors that S meets per diffusive jump and n_s is the number of
diffusive jumps made by S in time t_{gr}. If it is assumed that all species
in the medium diffuse, then the total probability that B^+ is scavenged
before geminate recombination is approximately

$$\phi_+ = 1 - (1 - f_+ N_s)^{b+n+ + b_s n_s} \qquad [56]$$

Using Eq. [51] to [55] to substitute in Eq. [56] gives

$$\phi_+ = 1 - (1 - f_+ N_s)^{\beta_+ \nu} \qquad [57]$$

where

$$\beta_+ \equiv \frac{1}{(u_+ + u_-)} \left[\frac{b_+ D_+}{\lambda_+^2} + \frac{b_s D_s}{\lambda_s^2} \right] \qquad [58]$$

$$\nu = 6 \epsilon (y^3 - r_o^3)/4.32 \times 10^{-7} d \qquad [59]$$

D_+ and D_s are the diffusion coefficients of B^+ and S,

λ_+ and λ_s are the mean jump distances of B^+ and S.

The fraction of ions which become free ions by reaction [45],
escaping geminate recombination is given by (78)

$$\phi_{fi} = e^{-\frac{r}{y}}$$ [60]

where $r = \epsilon^2/\epsilon kT$ and is the distance at which the mutual coulombic

energy of attraction between the ions equals kT

ϵ is the charge on the electron (esu)

k is the Boltzman's constant (erg/degree)

T is the temperature (°K)

Geminate recombination times are several orders of magnitude
shorter than the lifetimes of free ions at the dose rates used. Thus
at scavenger concentrations such that $k_{47}[S] \gg 1/t_{gr}$, all the free
positive ions will also be scavenged. Then the total probability of
scavenging all B$^+$ ions, both free and in spurs, is given by

$$\phi_+ = \phi_{fi} + \phi_+(1 - \phi_{fi})$$ [61]

ϕ_+ (and hence ϕ_+) is a function of f_+, N_s and the various
quantities in β_+ and y. Since f_+ and some of the quantities in β_+ are
not well known, these two may be treated as adjustible parameters in
the determination of ϕ_+.

The dependence of the yield of E$^+$ on N_s may be calculated, with
the aid of the N(y) vs y spectrum, by

$$G(E^+) = \frac{\sum N(y)\,\phi_+}{\sum N(y)} \times G(B^+)_o$$ [62]

where $G(B^+)_o$ is the initial yield of B$^+$ formed by reaction [43].

More frequently the decrease in a product, D, is measured as a function of the scavenger concentration so that

$$\Delta \, G(D) \; = \; \frac{\sum N(y) \, \phi_+}{\sum N(y)} \; X \; G(B^+)_m \qquad\qquad [63]$$

where $G(B^+)_m$ is the maximum yield of B^+ ions which would lead to the formation of D in the absence of scavenger.

Similar equations may be derived for negative ion (or electron) scavenging. In this case the following general reactions occur

$$\left[C^- + S \right] \longrightarrow \left[F^- \right] \qquad\qquad [64]$$

$$C^- + S \longrightarrow F^- \qquad\qquad [65]$$

followed by the formation of a new product by the reaction of F^-. In this case

$$\phi_- \; = \; \phi_{fi} + \phi_- (1 - \phi_{fi}) \qquad\qquad [66]$$

where

$$\phi_- \; = \; 1 \; - \; (1-f_- N_s)^{\beta - \nu} \qquad\qquad [67]$$

$$\beta_- \; = \; \frac{1}{(u_+ + u_-)} \left[\frac{b_- D_-}{\lambda_-^2} + \frac{b_s D_s}{\lambda_s^2} \right] \qquad\qquad [68]$$

b_-, D_- and λ_- are the average number of new neighbors met per jump, the diffusion coefficient and the average jump distance of C^-, respectively, and f_- is the encounter efficiency of reaction [64], $0 \leqslant f_- \leqslant 1$.

If $G(C^-)_0$ is the yield of initially formed C^- from reaction [43], then

$$G(F^-) \; = \; \frac{\sum N(y) \, \phi_-}{\sum N(y)} \; X \; G(C^-)_0 \qquad\qquad [69]$$

and

$$\Delta G(D) = \frac{\sum N(y) \phi_-}{\sum N(y)} \times G(C^-)_m \qquad [70]$$

where $G(C^-)_m$ is the maximum yield of C^- formed by reaction [43] which

reacts with B^+ in the absence of S to form D.

b. Application of Ion Scavenging Equations

The equations derived in the previous section were used to calculate

curves for the decrease in hydrogen yield and, in the case of N_2O addition,

the increase in nitrogen yield with increasing scavenger concentration.

In order to calculate ϕ_+ and ϕ_- in Eq. [61] and [66], respectively,

it was necessary to have values of β_+, β_- and $\mathcal{V}$. The values of

β_+ and β_- were varied until a curve was obtained which best fitted

the results. The fundamental quantities given in Table IV-3 are those

needed to give the values of β_+ and β_- determined in this manner.

In this table, values of D_+ and D_s (the diffusion coefficients of positive

ion and scavenger) were calculated from the following empirical

formula (50)

$$D = \frac{7.4 \times 10^{-10} \, T \, M^{0.5}}{\eta \, V^{0.6}} \quad cm^2/sec \qquad [71]$$

where T is the absolute temperature ($^\circ K$)

M is the molecular weight of the solvent (gms)

η is the viscosity (poise)

and V is the molar volume of the diffusing species (cc)

The value of the mobility of positive ions, u_+ was then calculated

TABLE IV-3

Fundamental Quantities

	$C_6H_{12}-N_2O$	$C_6H_{12}-SF_6$	$C_6H_{12}-CO_2$	$C_6H_{12}-C_6H_8$	$C_6H_{12}-C_6H_6$	$C_6H_{12}-ND_3$	Ref.
ϵ	$1.98(1-Ns)+1.61Ns$	$1.98(1-Ns)+2Ns$	$1.98(1-Ns)+1.60Ns$	$1.98(1-Ns)+2.25Ns$	$1.98(1-Ns)+2.28Ns$	$1.98(1-Ns)+15Ns$	79
$u_+(cm^2/Vsec)$	9.4×10^{-4}	9.4×10^{-4}	9.4×10^{-4}	9.4×10^{-4}	9.4×10^{-4}	9.4×10^{-4}	50
$u_-(cm^2/Vsec)$	4.5×10^{-3}	4.5×10^{-3}	4.5×10^{-3}	4.5×10^{-3}	1.8×10^{-3}	4.5×10^{-3}	75
b_+					4	4	
b_-	3	3	3	3			
$\lambda_+(cm)$					3.6×10^{-8}	3.6×10^{-8}	
$\lambda_-(cm)$	1.1×10^{-8}	1.1×10^{-8}	1.1×10^{-8}	1.1×10^{-8}			
$D_+(cm^2/sec)$	2.4×10^{-5}	2.4×10^{-5}	2.4×10^{-5}	2.4×10^{-5}	2.4×10^{-5}	2.4×10^{-5}	50
b_s	4	4	4	4	4	4	
$\lambda_s(cm)$	2.7×10^{-8}	2.7×10^{-8}	2.7×10^{-8}	2.5×10^{-8}	3.2×10^{-8}	3.2×10^{-8}	
$D_s(cm^2/sec)$	2.8×10^{-5}	2.8×10^{-5}	2.4×10^{-5}	2.2×10^{-5}	2.3×10^{-5}	3.6×10^{-5}	

from the equation (50)

$$u_+ = \frac{D_+ c}{kT}$$ [72]

where c is the charge on the ion and is equal to unity

k is Boltzman's constant (eV/deg)

T is the absolute temperature

Freeman (75) assumes that as a first approximation for cyclohexane

$$u_-/u_+ \approx 5$$ [73]

This value is equal to the average of the ratios of the mobilities of

solvated electrons and solvated sodium ions in water at 25° and in

liquid ammonia at -33°. The same approximation is made for MCP

in calculating u_-. The static dielectric constant for the solutions was

calculated from

$$\epsilon = \epsilon_A (1 - N_s) + \epsilon_s N_s$$ [74]

where ϵ_A and ϵ_s are the static dielectric constants of pure MCP

and pure liquid scavenger. The values of V were calculated using

Eq. [59] and [74] and the $N(y)$ vs y spectrum.

It was also found necessary to treat the maximum ion yield

leading to product as a variable. In order to use only two variables

in fitting the curves it was decided to treat f_+ and f_- as nonvariables,

giving them a value of unity throughout.

    i. Electron Scavengers

N_2O, CO_2 and SF_6

The equations for the reactions of charged species in the

MCP-N_2O system would be

$$C_6H_{12} \xrightarrow{\mathord{\sim\!\!\!\sim\!\!\!\sim}} \left[C_6H_{12}^+ + e^- \right] \qquad [75]$$

$$\left[e^- + mC_6H_{12} \right] \longrightarrow \left[e_{solv}^- \right] \qquad [76]$$

$$\left[C_6H_{12}^+ + e_{solv}^- \right] \longrightarrow \left[C_6H_{12}^* \right] \qquad [77]$$

$$\longrightarrow C_6H_{12}^+ + e_{solv}^- \text{ (free ions) } [78]$$

$$C_6H_{12}^+ + e_{solv}^- \longrightarrow C_6H_{12}^* \qquad [79]$$

$$\left[N_2O + e_{solv}^- \right] \longrightarrow \left[N_2O^- \right] \longrightarrow \left[N_2 + O^- \right] \qquad [80]$$

$$N_2O + e_{solv}^- \longrightarrow N_2O^- \longrightarrow N_2 + O^- \qquad [81]$$

$$\left[O^- + C_6H_{12}^+ \right] \longrightarrow \left[products \right] \qquad [82]$$

$$O^- + C_6H_{12}^+ \longrightarrow products \qquad [83]$$

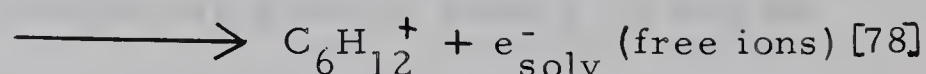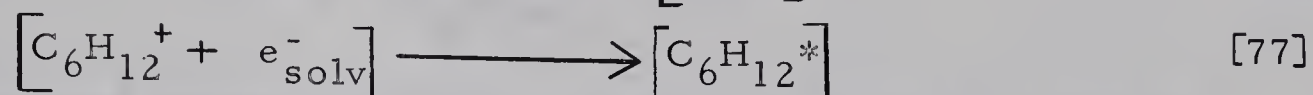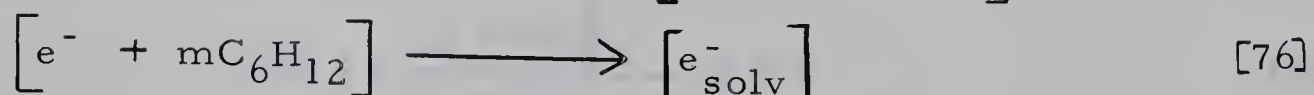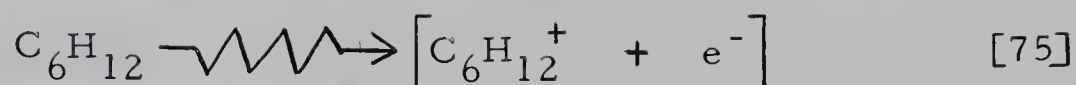where the square brackets around the reactants and products indicate

that the species are in spurs.

The neutral species formed by reactions [77] , [79] and [84]

will react according to reactions [85] to [89] .

$$C_6H_{12} \xrightarrow{\mathord{\sim\!\!\!\sim\!\!\!\sim}} C_6H_{12}^* \qquad [84]$$

$$C_6H_{12}^* \longrightarrow C_6H_{11} + H \qquad [85]$$

$$\longrightarrow C_6H_{10} + H_2 \qquad [86]$$

$$C_6H_{12} + H \longrightarrow C_6H_{11} + H_2 \qquad [87]$$

$$2\,C_6H_{11} \longrightarrow C_6H_{10} + C_6H_{12} \qquad [88]$$

$$\longrightarrow (C_6H_{11})_2 \qquad [89]$$

The maximum yield of N_2 would then correspond to the initial

yield of electrons formed by reaction [75] if the above reactions are

the only ones taking place. A curve of $g(N_2)$ vs $\log N_s$ may then be

constructed using the following equation which corresponds to the

general equation, Eq. [69]

$$g(N_2) = \frac{\sum' N(y)\, \phi_-}{\sum' N(y)} \times 5.0 \qquad [90]$$

The values used for the calculation are given in Table IV-4 and the

graph is shown in Figure IV-1. The circles represent experimental

values of $g(N_2)$, the nitrogen yield per 100 eV absorbed by MCP only.

The black circles are the N_2 yield corrected for N_2 formed by the

radiolysis of N_2O using $G(N_2) = 12.9$ for pure liquid N_2O. In the

gas phase various values have been reported for $G(N_2)$ from N_2O

ranging from 12.4 to 10.0 (82). In the liquid phase at $-88°C$ the

value $G(N_2) = 12.9$ has more recently been obtained (83). The maximum

value of $g(N_2)$ is 5.0. According to the mechanism given on the

preceeding page, this should also be the value of $G(e^-)$. However

if $G(e^-) \geqslant 5$ then the ion pair yield (W value) would be 20 eV or less.

In the gas phase W values are about 25 eV for hydrocarbons (43) thus

there probably exists another reaction by which nitrogen is formed.

Some of the nitrogen may be formed by the reaction

$$O^- + N_2O \longrightarrow N_2 + O_2^- \qquad [91]$$

This reaction has been proposed by Johnson and Warman (84) in the

gas phase and evidence for it has been found in the mass spectrometer.

In the cyclohexane-N_2O system, Sherman (41) has also suggested that

some excited cyclohexane molecules may transfer energy to nitrous

oxide to give N_2.

TABLE IV-4

Calculation of $g(N_2)$

N_s	$y(10^{-8}cm)$	$N(y)$	ϕ_{f_i}	βV	ϕ_-	$N(y)\phi_-$	$g(N_2)$
10^{-4}	18	2150	10^{-7}	80	0.0073	15.7	
	20	1100	10^{-6}	136	0.0125	13.7	
	24	600	10^{-5}	241	0.022	13.1	
	33	476	10^{-4}	630	0.056	26.8	
	56	270	0.007	3040	0.244	65.8	
	92	116	0.049	13700	0.717	83.1	
	133	64	0.122	40600	0.976	62.7	
	179	41	0.212	99400	0.999	41.0	
	232	28	0.303	214000	1.00	28.0	
	>250	155	>0.323	>258000	1.00	155.0	
Total		5000				505	0.51
10^{-3}	18	2150	10^{-7}	80	0.071	152	
	20	1100	10^{-6}	136	0.118	130	
	24	600	10^{-5}	241	0.199	119	
	33	476	10^{-4}	630	0.440	210	
	56	270	0.007	3040	0.939	254	
	92	116	0.049	13700	1.00	116	
	>100	288	>0.122	>16500	1.00	288	
Total		5000				1269	1.27

TABLE IV-4 (Continued)

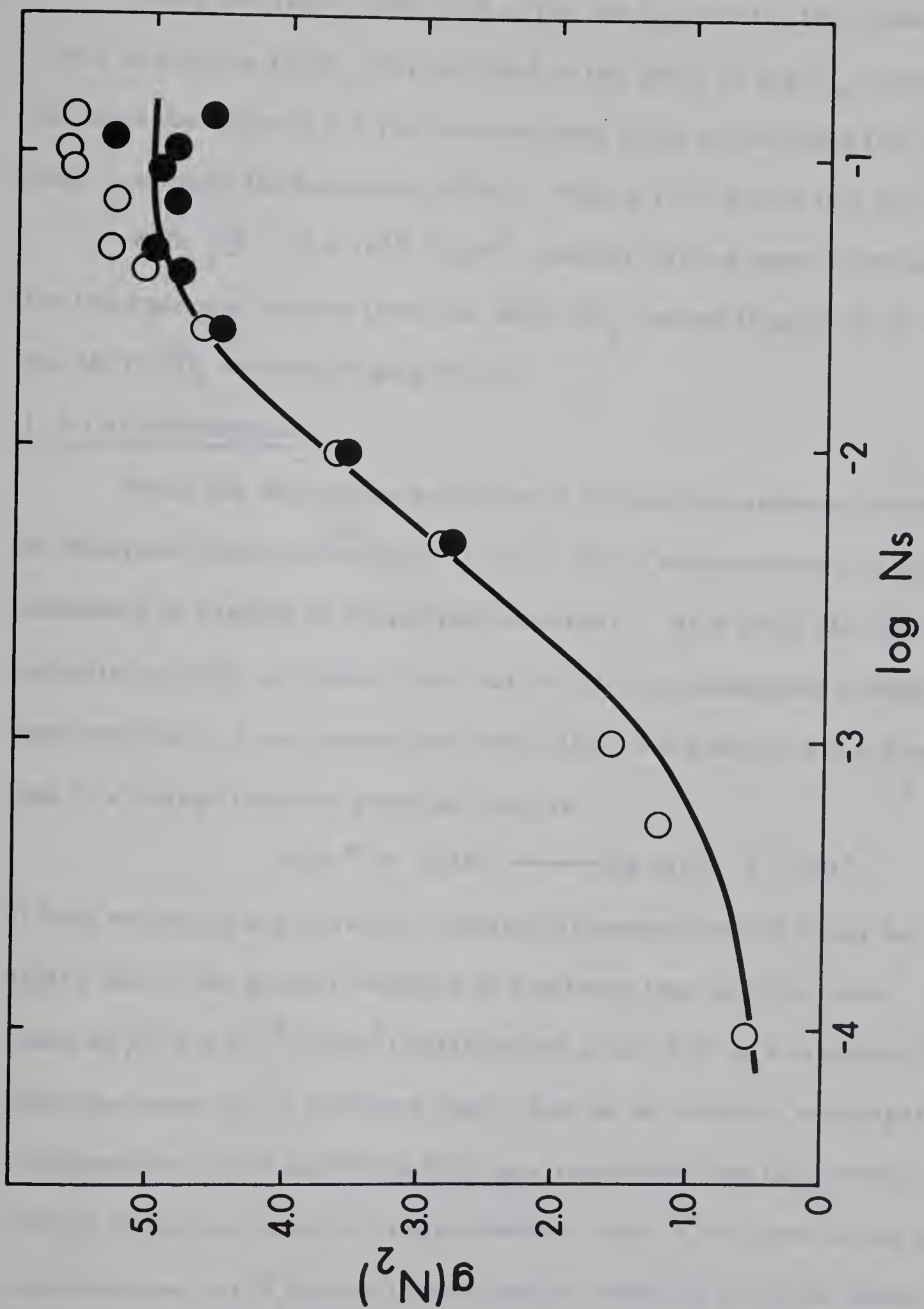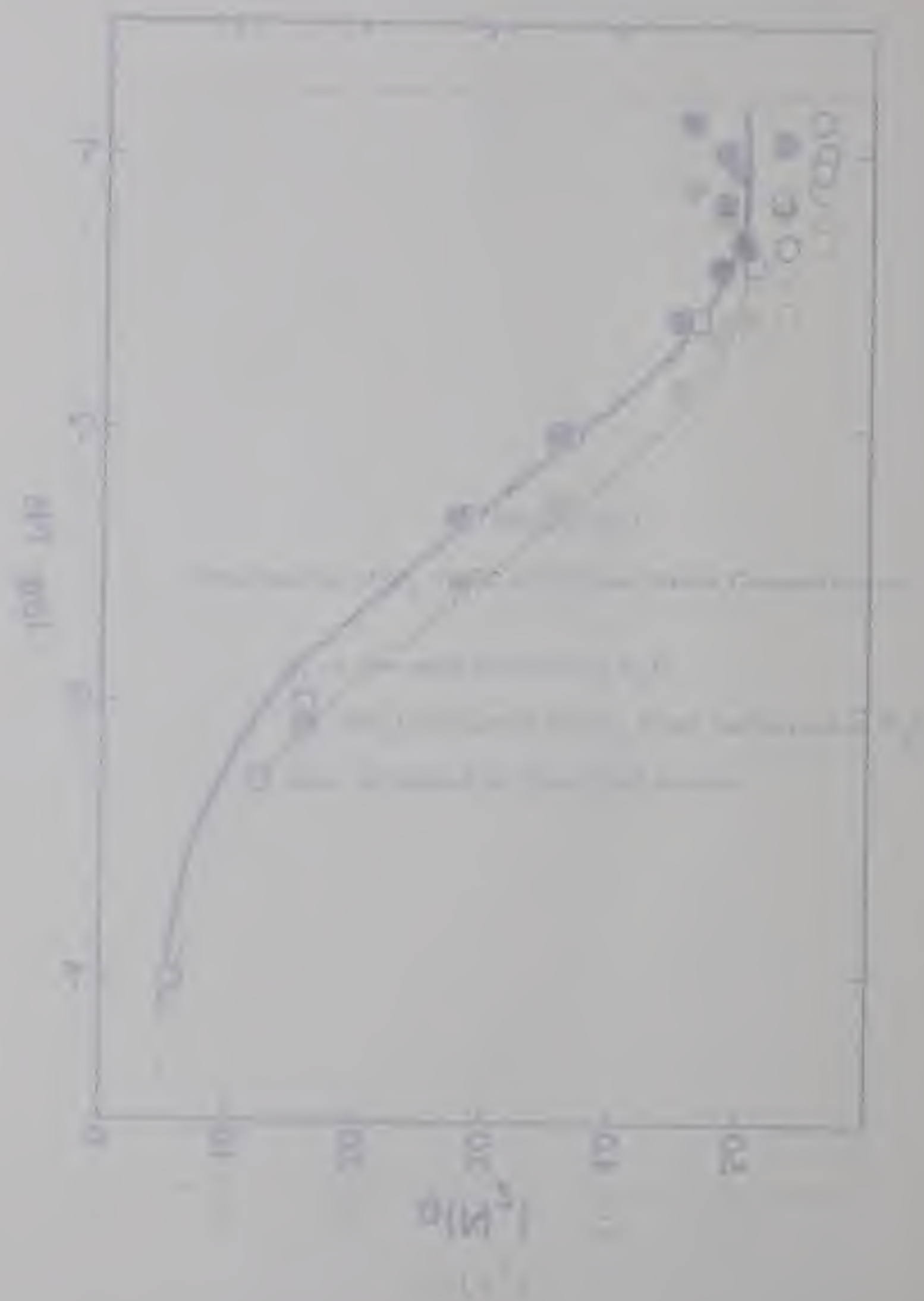| N_s	$y(10^{-8}$ cm)	$N(y)$	ϕ_{f_i}	$\beta\nu$	ϕ_-	$N(y)\phi_-$	$g(N_2)$
10^{-2}	18	2150	10^{-7}	80	0.554	1192	
	20	1100	10^{-6}	136	0.748	823	
	24	600	10^{-5}	241	0.913	547	
	33	476	10^{-4}	630	0.998	475	
	56	270	0.007	3040	1.00	270	
	>60	404	>0.049	>13700	1.00	404	
Total		5000				3711	3.71
10^{-1}	18	2150	10^{-7}	78	1.00	2150	
	>20	2850	$>10^{-6}$	>100	1.00	2850	
Total		5000				5000	5.00

Figure IV-1

Dependence of N_2 Yield on Nitrous Oxide Concentration

N_s is the mole fraction of N_2O

● $g(N_2)$ corrected for N_2 from radiolysis of N_2O

Line calculated as described in text

Using the same value of β as for the N_2 results, the theoretical curve of yield vs log N_s may be fitted to the $g(H_2)$ vs log N_s results if one uses the value of 1.8 for the maximum yield of electrons (or positive ions) leading to the formation of H_2.   Figure IV-2 shows this plot.

With $\beta_- = 6 \times 10^{14}$ V/cm^2, similar curves were constructed for the hydrogen results from the MCP-SF$_6$ system (Figure IV-3) and the MCP-CO$_2$ system (Figure IV-4).

1,3-Cyclohexadiene

From the absorption spectrum of 1,3-cyclohexadiene irradiated in methyltetrahydrofuran glass at -196° (85) it appears that 1,3-cyclo-hexadiene is capable of scavenging electrons.   Also since the ionization potential of MCP is greater than that of 1,3-cyclohexadiene it might be expected that 1,3-cyclohexadiene could also be a positive ion scavenger due to a charge transfer reaction such as

$$MCP^+ + CHD \longrightarrow MCP + CHD^+ \qquad [92]$$

If both reactions are possible, electron scavenging would likely be faster due to the greater mobility of electrons than positive ions.   The value of β (6×10^{14} V/cm^2) obtained for a curve fit at a maximum H_2 yield decrease of 1.8 indicates that it acts as an electron scavenger. Furthermore, Hush and Pople (86) have calculated that the electron affinity of another diolefin, trans-butadiene, was of the same order of magnitude as that of diphenyl which has an observed electron affinity of 0.41 eV in the gas phase.

Figure IV-2

Dependence of Hydrogen Yield on Nitrous Oxide Concentration

N_s is the mole fraction of N_2O
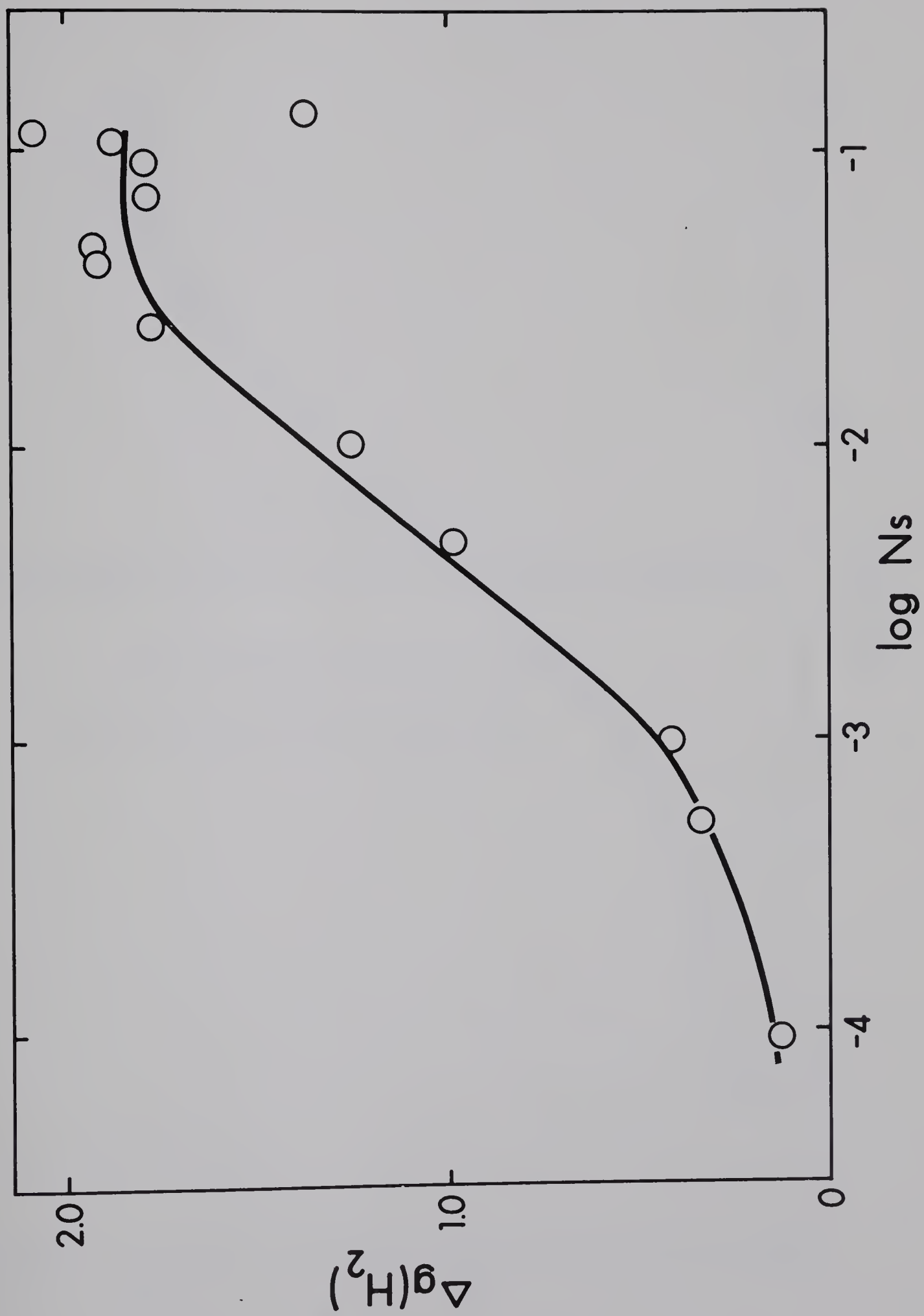
Line calculated as described in text

Figure IV-3

Dependence of Hydrogen Yield on the Sulfur Hexafluoride Concentratio

N_s is the mole fraction of SF_6

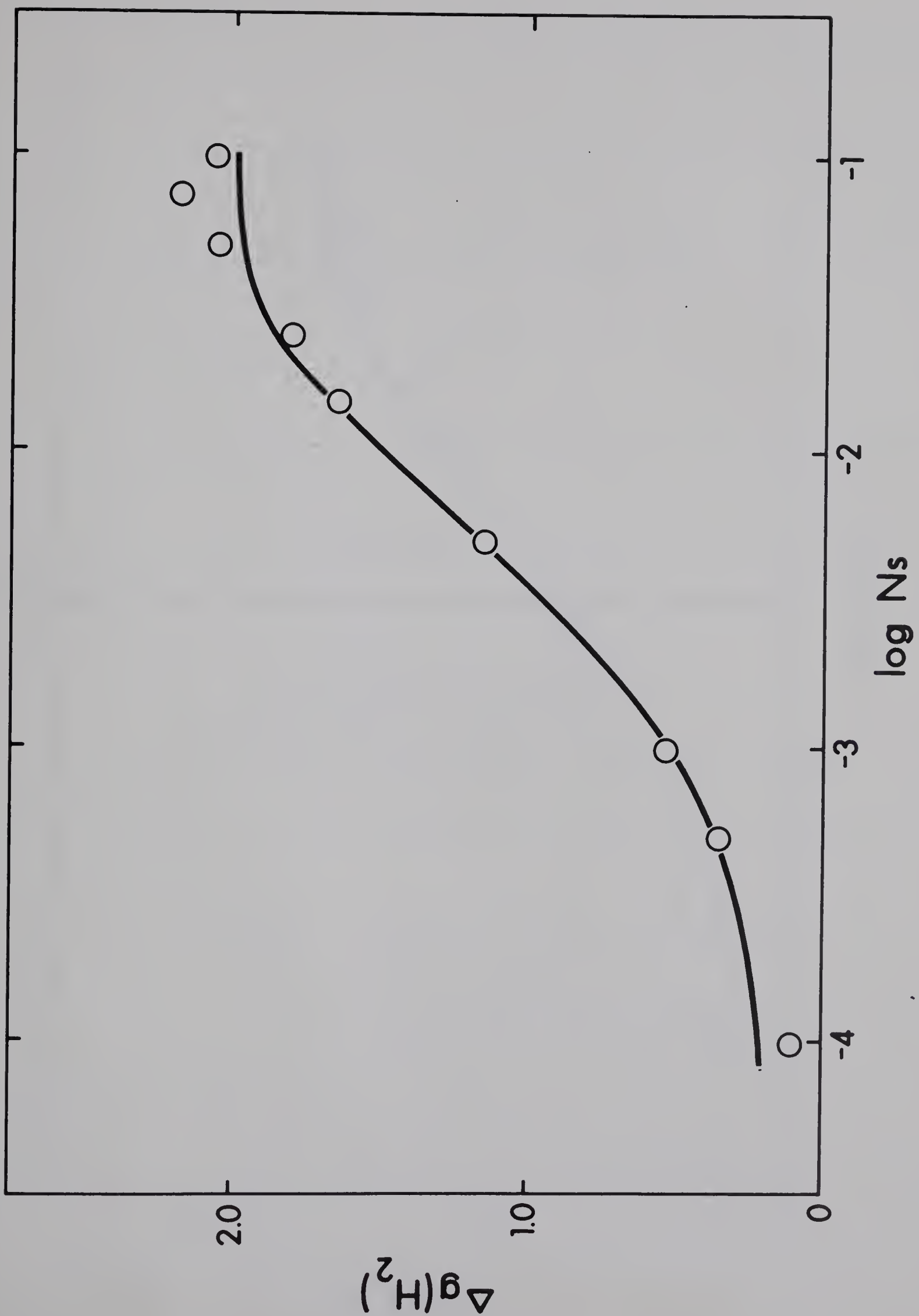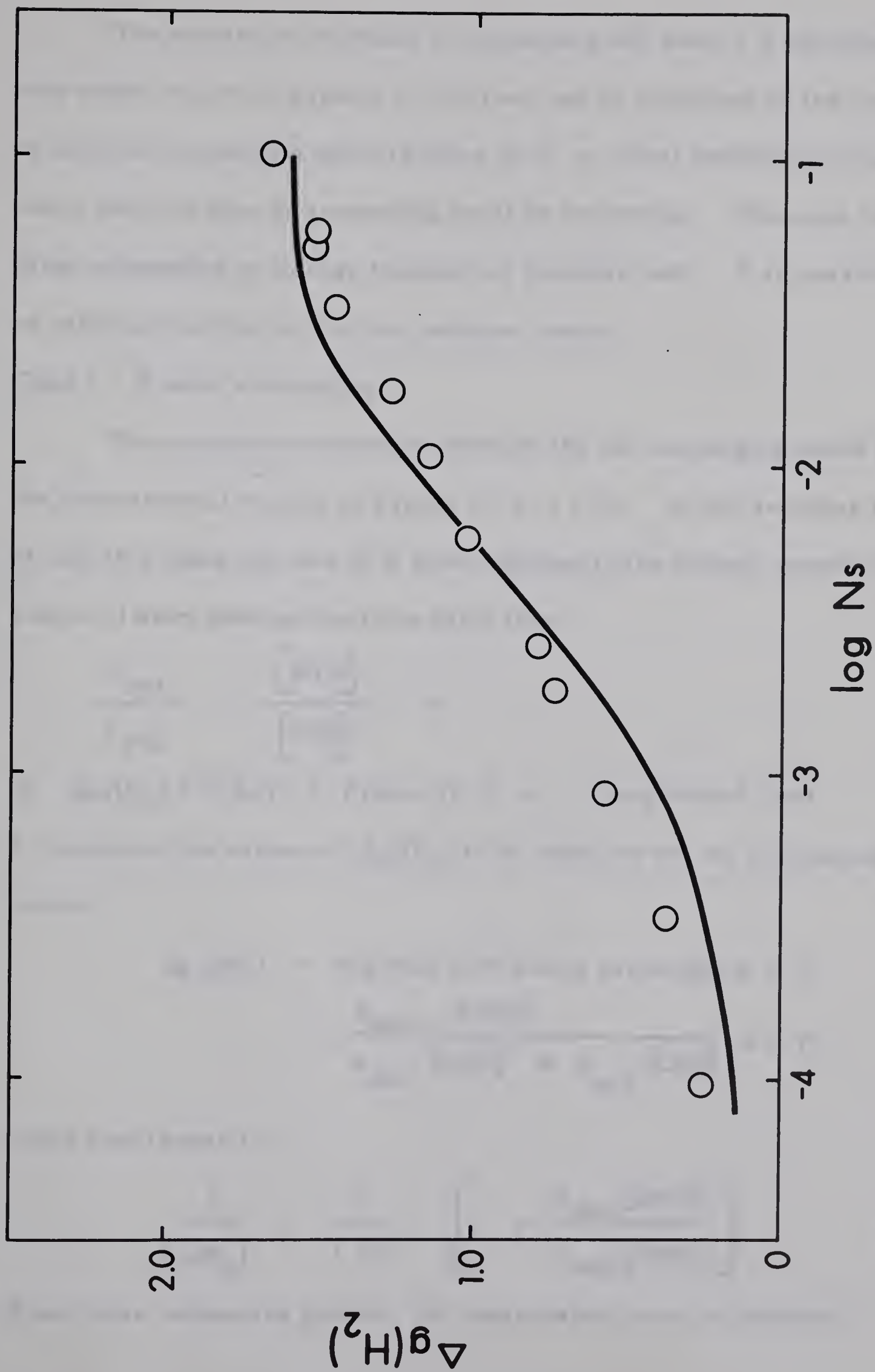Line calculated as described in text

Figure IV-4

Dependence of Hydrogen Yield on the Carbon Dioxide Concentration

N_s is the mole fraction of CO_2

Line calculated as described in text

The maximum decrease in hydrogen yield when 1,3-cyclohexadiene was added was much greater (3.52) than can be explained on the basis of electron scavenging alone (Figure IV-5 — short dashed line) thus more than one type of scavenging must be occurring. This may be H atom scavenging or energy transfer or possibly both. It is possible to calculate curves for the two extreme cases.

Case 1 - H atom scavenging

The maximum difference between the ion scavenging curve and the experimental results in Figure IV-5 is 1.72. If one assumes that at half this value the rate of H atom addition to the diolefin equals the rate of H atom abstraction from MCP then

$$\frac{k_{add}}{k_{abs}} = \frac{[MCP]}{[CHD]} = 9$$

at $\Delta g(H_2) = 0.86$ (c.f. Figure IV-5 — long dashed line).

To calculate the values of $\Delta g(H_2)$ to be added to the ion scavenging curves

$$\Delta g(H_2) = \text{fraction of H atoms scavenged} \times 1.72$$

$$= \frac{k_{add} [CHD]}{k_{abs} [MCP] + k_{add} [CHD]} \times 1.72$$

which rearranges to

$$\frac{1}{\Delta g(H_2)} = \frac{1}{1.72} \left[1 + \frac{k_{abs} [MCP]}{k_{add} [CHD]} \right] \tag{93}$$

When these values are plotted, the long-dashed curve is obtained
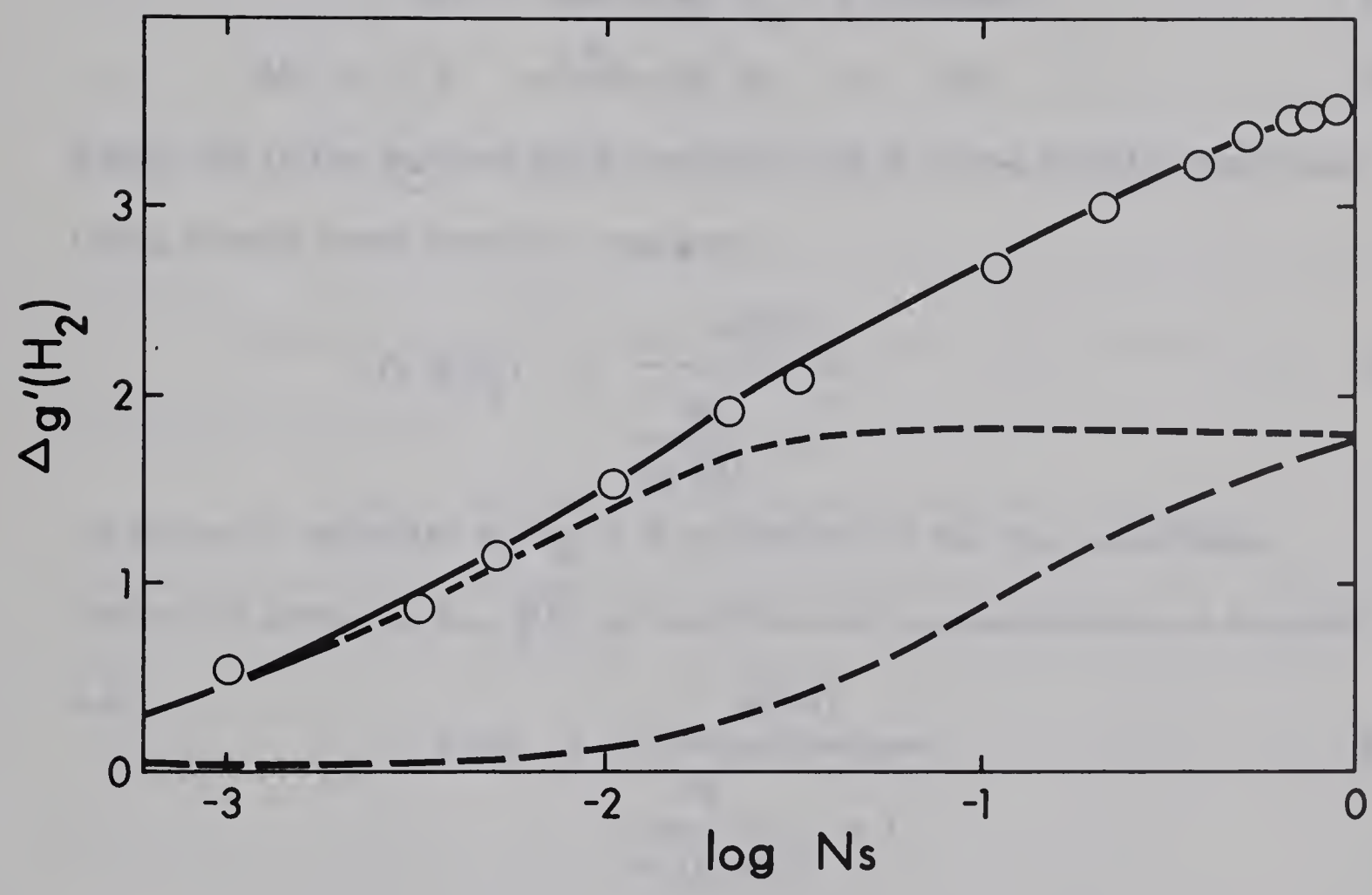
Figure IV-5

Dependence of Hydrogen Yields on the 1,3-Cyclohexadiene Concentration

- - - - - - -   Calculated ion scavenging curve

— — —   Calculated H atom scavenging or energy transfer cur

_____   Sum of the two calculated dashed curves

N_s is the mole fraction of 1,3-cyclohexadiene

$\Delta g'(H_2)$

log Ns

(Figure IV-5) which, when added to the ion scavenging curve, gives

the solid line.

Case 2 - Energy transfer

The energy transfer mechanism is a competition between Eq. [94]

and [95]

$$M* \xrightarrow{k_1} H_2 + product \qquad [94]$$

$$M* + S \xrightarrow{k_2} M + S* \qquad [95]$$

where M* is the excited MCP molecule and S is the diolefin molecule.

Using steady state kinetics, one gets

$$\Delta g(H_2) = \frac{g(M*)}{\dfrac{k_1}{k_2 [S]} + 1} \qquad [96]$$

In order to calculate k_1/k_2 it is necessary to fill two conditions.

These are given by Eq. [96] at two different concentrations of diolefin.

e.g.

$$0.86 = \frac{g(M*)}{\dfrac{k_1}{k_2(0.895)} + 1} \qquad [97]$$

and

$$1.72 = \frac{g(M*)}{\dfrac{k_1}{k_2(10.3)} + 1} \qquad [98]$$

Solving these two equations gives $k_1/k_2 = 1.07$ and $g(M*) = 1.9$. Using

these two constants it is then possible to plot the points which coincidently

fall on the same curve as was plotted for H atom scavenging, i.e. the

long-dashed curve in Figure IV-5. Thus it does not seem possible to choose between H atom scavenging or energy transfer to account for the excess H_2 decrease over ion scavenging at higher scavenger concentrations.

It is interesting to note that ion scavenging and H atom scavenging or energy transfer account for only 3.52 g units of H_2 of a total 4.20 g units initially formed. Thus 0.68 g units of H_2 are not scavengeable by any means in this system. If one chooses H atom scavenging rather than energy transfer as an explanation for the excess H_2 decrease after ion scavenging then possibly this unscavengeable H_2 is formed by a "molecular" process.

$$C_6H_{12} \xrightarrow{} C_6H_{12}^* \longrightarrow H_2 + C_6H_{10} \qquad [99]$$

It is impossible to compare this with a value obtained for the "molecular" olefin yield as the olefin yield could not be measured at high enough scavenger concentrations to reach a constant minimum olefin yield with increasing scavenger concentration.

ii. Positive Ion Scavengers.

ND_3 is generally considered to be a positive ion scavenger reacting by proton transfer from the initially formed positive parent ion RH^+. If, in the pure system, all positive ions eventually led to H_2 formation, then according to the mechanism given on page 117, the addition of ND_3 should give an HD yield equal to the decrease in H_2 yield. Experimentally, the decrease in H_2 yield is half the HD

yield at all concentrations of ND_3 studied (Figure IV-6). Thus ND_3 must be reacting with positive ions which would not, in its absence, give H_2 i.e.

$$C_6H_{12} \xrightarrow{\quad\quad} PH^+ + e^- \qquad\qquad [100]$$

$$\xrightarrow{\quad\quad} QH^+ + e^- \qquad\qquad [101]$$

$$PH^+ + e^- \longrightarrow PH^* \longrightarrow hydrogen \qquad\qquad [102]$$

$$QH^+ + e^- \longrightarrow QH^* \longrightarrow no\ hydrogen \qquad\qquad [103]$$

Three possible cases for these reactions may be considered.

Case 1

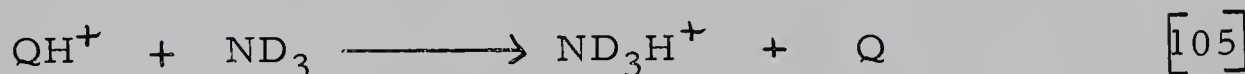From the results of added electron scavengers $g(PH^+)_{max} = 1.8$ (see page 138). If the addition of ND_3 gives the following

$$PH^+ + ND_3 \longrightarrow ND_3H^+ + P \qquad\qquad [104]$$

$$QH^+ + ND_3 \longrightarrow ND_3H^+ + Q \qquad\qquad [105]$$

followed by

$$ND_3H^+ + ND_3 \longrightarrow ND_2H + ND_4^+ \qquad\qquad [106]$$

$$ND_4^+ + e^- \longrightarrow ND_3 + D \qquad\qquad [107]$$

$$C_6H_{12} + D \longrightarrow HD + C_6H_{11} \qquad\qquad [108]$$

then $g(HD)_{max} = g(PH^+)_{max} + g(QH^+)_{max} = 2\ g(PH^+)_{max} = 3.6$ and $g(PH^+)_{max} = g(QH^+)_{max} = 1.8$. Thus for total exchange Eq. $[106]$, one would expect $g(H_2 + HD)_{max} = G(H_2)_0 + g(QH^+)_{max} = 4.20 + 1.8 = 6.0$. This value seems to be higher than one might expect for MCP.

Case 2

If one assumes no exchange and no isotope effect $(k_H/k_D = 1)$ we

Figure IV-6

Dependence of H_2 and HD Yields on the Perdeutero Ammonia Concentration

N_s is the mole fraction of ND_3

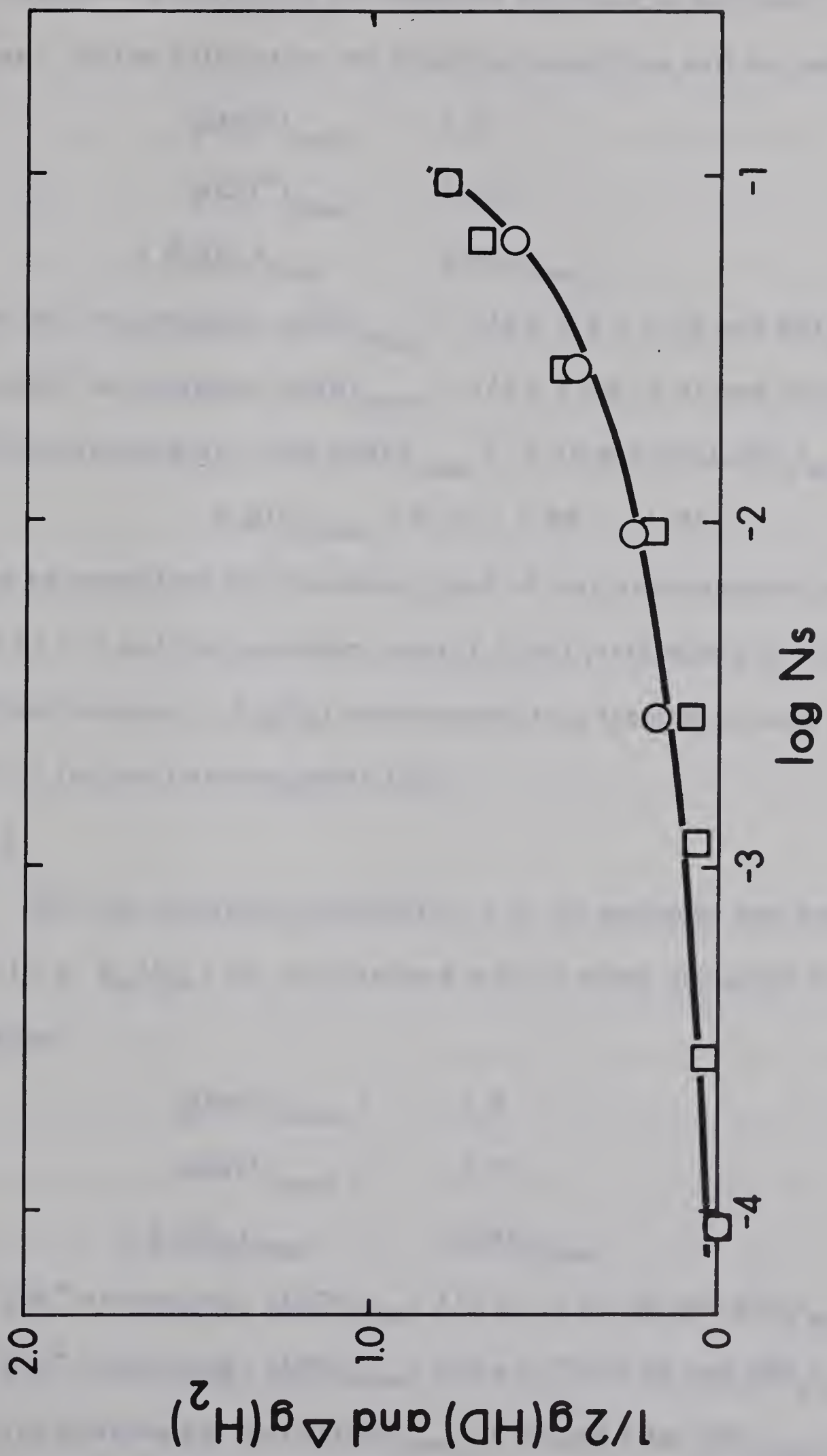$\bigcirc = \Delta g(H_2)$

$\square = \frac{1}{2} g(HD)$

The line is calculated as described in the text.

1/2 g(HD) and Δg(H$_2$)

2.0

1.0

0

-4

-3

-2

-1

log Ns

may calculate statistically the expected decrease in hydrogen yield due
to ions. In the calculation the following equalities will be used.

$$g(PH^+)_{max} = 1.8$$

$$g(QH^+)_{max} = 1.08$$

$$2\,\Delta g(H_2)_{max} = g(HD)_{max}$$

From PH^+ scavenging, $g(HD)_{max} = 3/4 \times 1.8 = 1.35$ and $g(H_2)_{max} = 0.45$

From QH^+ scavenging, $g(HD)_{max} = 3/4 \times 1.08 = 0.81$ and $g(H_2)_{max} = 0.27$

From ion scavenging, total $g(HD)_{max} = 2.16$ and total $g(H_2)_{max} = 0.72$

$$\Delta g(H_2)_{max} = 0.72 - 1.80 = -1.08$$

It may be noted that the maximum yield of ions scavengeable by ammonia

would be 2.9 and the maximum total $H_2 + HD$ yield would be 5.3. The

maximum value of $- \Delta g(H_2)$ corresponds to a fraction of only 1.08/2.9

$= 0.37$ of the total scavengeable ions.

Case 3

For the remaining possiblitiy, i.e. no exchange and some isotope

effect (e.g. $k_H/k_D = 2$), calculations may be made using the following

equalities:

$$g(PH^+)_{max} = 1.8$$

$$g(QH^+)_{max} = 0.77$$

$$2\,\Delta g(H_2)_{max} = g(HD)_{max}$$

From PH^+ scavenging, $g(HD)_{max} = 3/5 \times 1.8 = 1.08$ and $g(H_2)_{max} = 0.72$

From QH^+ scavenging, $g(HD)_{max} = 3/5 \times 0.77 = 0.46$ and $g(H_2)_{max} = 0.31$

From ion scavenging, total $g(HD)_{max} = 1.54$ and total $g(H_2)_{max} = 1.03$

$$\Delta\, g(H_2)_{max} = 1.03 - 1.80 = -0.77$$

Also the total ion yield is 2.6 and the total $g(H_2 + HD)_{max}$ is 5.0. It

may be seen, however, from the experimental results (Figure IV-6)

that at $N_s = 10^{-1}$ the decrease in hydrogen yield is already 0.8 and

there is no sign that the curve levels off at this point. Therefore it

is not likely that there is an isotope effect if no exchange is permitted.

It should be noted that the effect of allowing some exchange could be

compensated for by allowing some isotope effect since the two effects

work in opposite directions. Freeman (75) in his calculations on the

ND_3-cyclohexane results of Williams (54) assumed the conditions for

Case 2 i.e. no exchange and no isotope effect. If the values in Case 2

are used to determine the semi-empirical curve for MCP-ND_3 (Figure

IV-6) the value of β_+ needed to fit the results is 4×10^{13} V/cm^2.

Benzene

Since the ionization potential of benzene is lower than that of

MCP it is possible that benzene may scavenge positive ions by a charge

transfer reaction. A curve was calculated (Figure IV-7) which fitted

the experimental points at low scavenger concentration when β was a

maximum of 6×10^{13} V/cm^2 and a maximum H_2 yield decrease was 1.8.

For electron scavenging to be occurring, β should be ten times larger

according to the results of known electron scavengers. Thus it appears

that no electron scavenging occurs with benzene as an additive. The

values given in Table IV-3 which are consistent with this value of β_+,
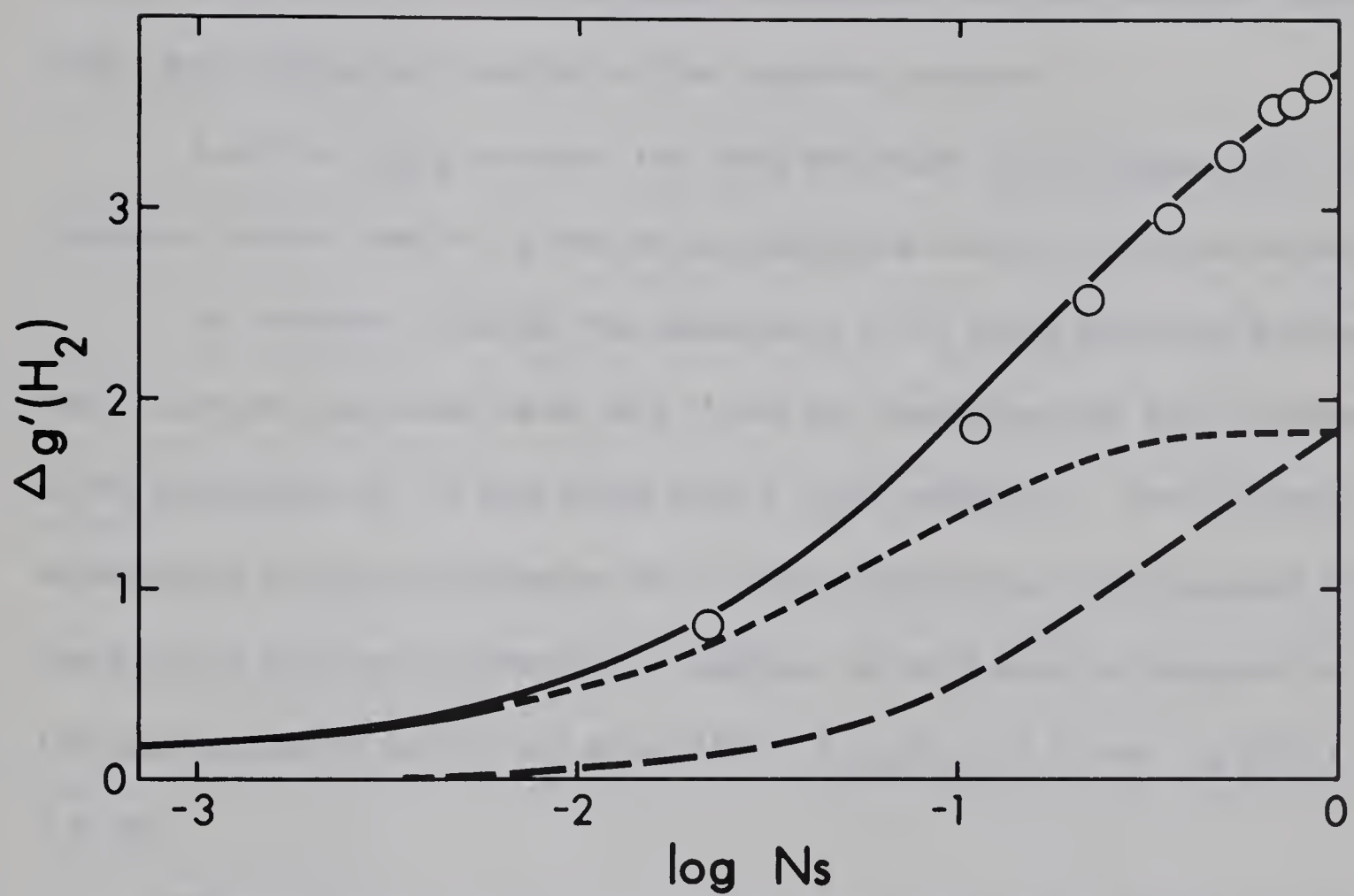
Figure IV-7

Dependence of Hydrogen (H_2) Yield on the Benzene Concentration

--------   Calculated ion scavenging curve

— — —   Calculated H atom scavenging or energy transfer

                   curve

———————   Sum of the two calculated dashed curves

N_s is the mole fraction of benzene

for benzene addition are the same as for the other positive ion scavenger,
ND_3 with the exception of the mobility of the electron, u_-. The mobility
is only 1.9 times that of u_+. Perhaps this is due to an interaction
between the solvated electron and a benzene molecule which is strong
enough so that the electron becomes associated with the benzene mole-
cule, decreasing the mobility of the negative species.

Like the C_6H_8 results, the total decrease in hydrogen yield with
benzene present was too great to be attributed solely to ion scavenging.

An attempt to assign the difference in H_2 yield decrease between
the observed maximum value of 3.7 and the maximum ion yield leading
to H_2 formation of 1.8 was made as for C_6H_8 addition. For H atom
scavenging a curve fit (Figure IV-7; long-dashed line) was obtained when
the ratio of the rate constants for addition of an H atom to benzene to
the abstraction of an H atom from MCP, $k_{add}/k_{abs} = 3.4$ at $\Delta g(H_2)$
$= 0.93$.

When a curve was calculated for energy transfer, a fit with the
curve obtained for H atom scavenging was again obtained using $k_1/k_2 =$
3.5 and $g(M^*) = 2.46$. Thus for benzene addition it is also not possible
to differentiate between H atom scavenging or energy transfer. Evid-
ence has been reported for H atom scavenging in the radiolysis of
cyclohexane-benzene mixtures (38) using tritium labelled cyclohexane.
Hardwick (35) has reported that for benzene in cyclopentane $k_{add}/k_{abs} \approx$
25 however the rate of abstraction of H atoms from tertiary carbons is

about 6 or 7 times as fast as the rate of abstraction from secondary

carbons. Thus it might be expected that $k_{add}/k_{abs} \approx 4$ for benzene

in MCP. This is not far from the value of 3.4 obtained above. Also

Yang (87) finds in the gas phase that

$$(k_{abs}/k_{add})_{1,3\text{-butadiene}} \approx (k_{abs}/k_{add})^2_{benzene}$$

From the rate constant ratio for benzene $(k_{abs}/k_{add})^2 \approx 11$ which is

nearly the same as the ratio obtained for 1,3-cyclohexadiene addition.

It should be noted however that since both of these authors were studying

radiolytic systems, ion scavenging is also occurring in both cases. Thus

a recalculation of their results with this in mind should probably be

made.

    c. Comparison of Parameters for Positive and Negative Ions.

    A summary of the values of β_+, β_-, $g(B^+)_0$ and $g(C^-)_0$

determined from the curves is given in Table IV-5 for the various

additives studied.

    N_2O, SF_6 and CO_2 are electron scavengers and it is probable

that C_6H_8 is also an electron scavenger. For these four, with $\beta_- = $

6×10^{14} V/cm^2, the maximum yield of electrons (or positive ions)

leading to hydrogen formation appears to be 1.8 ± 0.2.

    The values of β_+ and β_- differ by a factor of 10 or greater.

From Eq. $\boxed{58}$ or $\boxed{68}$, β is dependent on the sum of bD/λ^2 for

the positive ion or electron and $b_s D_s/\lambda_s^2$. Since the positive ion will

be similar in size to the scavenger, the values of the quantities in these

TABLE IV-5

Values of β_+, β_-, $g(B^+)_o$ and $g(C^-)_o$ Used to Fit Curves

Additive	$\beta_+(V/cm^2)$	$\beta_-(V/cm^2)$	$g(B^+)_o$	$g(C^-)_o$
N_2O		6×10^{14}		1.8
SF_6		6×10^{14}		2.0
CO_2		6×10^{14}		1.6
C_6H_8		6×10^{14}		1.8
C_6H_6	6×10^{13}		1.8	
ND_3	4×10^{13}		1.08*	

* $1.08 = 0.37 (1.8 + 1.1)$, see text

two terms will probably be approximately equal. It is possible that the average jump distance of the solvated electron is small compared to that of a positive ion since it has a relatively diffuse structure i.e. because it is not completely confined to a single cavity but might diffuse by small deformations of the local liquid structure. Thus $\lambda_- < \lambda_+$ or λ_s. Also since the mobility of a solvated electron is greater than that of a positive ion, the diffusion coefficient D_- will be greater than D_+. The effect of these two variations is to make $b_- D_-/\lambda_-^2 \gg b_+ D_+/\lambda_+^2$ or $b_s D_s/\lambda_s^2$ and thus $\beta_- > \beta_+$.

BIBLIOGRAPHY

(1) G. F. Friedlander and J. W. Kennedy, "Nuclear and Radio-chemistry", John Wiley & Sons, Inc., New York (1960) p. 419.

(2) F. P. Gowan in "Radiation Dosimetry", (G. H. Hine and G. L. Brownell, ed.) Academic Press, New York (1956) p. 878.

(3) A. Debierne, Compt. rend., 148, 703 (1909).

(4) S. C. Lind, "The Chemical Effects of Alpha Particles and Electrons", The Chemical Catalog Co., New York (1928).

(5) H. Eyring, J. D. Hirschfelder, and H. S. Taylor, J. Chem. Phys. 4, 479 (1936).

(6) F. Williams, J. Am. Chem. Soc. 86, 3954 (1964).

(7) A. O. Allen and A. Hummel, Disc. Faraday Soc. 36, 95 (1963).

(8) G. R. Freeman, Disc. Faraday Soc. 36, 247 (1963).

(9) R. L. Platzman, "Radiation Biology and Medicine", (W. D. Claus, ed.) Addison Wesley Reading, Mass, (1958) pp. 15-72.

(10) A. Kupperman, J. Chem. Ed. 36, 279 (1959).

(11) A. H. Samuel and J. L. Magee, J. Chem. Phys. 21, 1080 (1953).

(12) H. Fröhlich and R. L. Platzman, Phys. Rev. 92, 1152 (1953).

(13) J. W. T. Spinks and R. J. Woods, "An Introduction to Radiation Chemistry", J. Wiley and Sons, New York (1964) p. 50.

(14) G. R. White in "Radiation Dosimetry," (G. H. Hind and G. L. Brownell, ed.) Academic Press, New York (1956) p. 83.

(15) H. A. Bethe, Ann. Physik 5, 325 (1930).

(16)   L. M. Dorfman, J. Phys. Chem. 60, 826 (1956).

(17)   L. M. Dorfman, J. Phys. Chem. 62, 29 (1958).

(18)   P. Dyne, J. Phys. Chem. 60, 767 (1962).

(19)   R. R. Hentz, D. B. Peterson, S. B. Srivastava, H. C. Barzynski
         and M. Burton, J. Phys. Chem. 70, 2362 (1966).

(20)   M. Burton and W. N. Patrick, J. Phys. Chem. 58, 424 (1954).

(21)   R. B. Cundall and P. A. Griffiths, Disc. Faraday Soc. 36, 111(1963).

(22)   H. Pines, B. M. Abraham and V. N. Ipatieff, J. Am. Chem. Soc.
         70, 1742 (1948).

(23)   J. H. Futrell, J. Am. Chem. Soc., 81, 5921 (1959).

(24)   R. Barker, W. H. Hamill, and R. R. Williams, J. Phys. Chem.
         63, 825 (1959).

(25)   A. A. Scala, S. G. Lias and P. Ausloos, J. Am. Chem. Soc.
         88, 5701 (1966).

(26)   T. J. Hardwick, J. Phys. Chem. 66, 2132 (1962).

(27)   J. A. Stone, A. R. Quirt and O. A. Miller, Can. J. Chem. 44,
         1175 (1966).

(28)   T. J. Hardwick, "Actions Chimiques et Biologiques des Radiations"
         (ed. M. Haissinsky) Masson & Cie., Paris (1966).

(29)   R. H. Schuler and G. A. Muccini, J. Am. Chem. Soc. 81, 4115
         (1959).

(30)   H. A. Dewhurst, J. Phys. Chem. 63, 813 (1959).

(31)   R. A. Holroyd, J. Phys. Chem. 65, 1352 (1961).

(32)   R. H. Schuler and R. R. Kuntz, J. Phys. Chem. 67, 1004 (1963).

(33)   T. J. Hardwick, J. Phys. Chem. 64, 1623 (1960).

(34)   T. J. Hardwick, J. Phys. Chem. 66, 117 (1962).

(35)   T. J. Hardwick, J. Phys. Chem. 65, 101 (1961).

(36)   D. L. Dugle, Ph. D. Thesis, University of Alberta (1964).

(37)   B. R. Wakeford, Ph. D. Thesis, University of Alberta (1963).

(38)   J. Y. Yang, B. Scott and J. G. Burr, J. Phys. Chem. 68, 2014 (1964).

(39)   G. R. Freeman, J. Chem. Phys. 33, 957 (1960).

(40)   G. Scholes and M. Simic, Nature 202, 895 (1964).

(41)   W. V. Sherman, J. Chem. Soc. 599 (1966).

(42)   R. Blackburn and A. Charlesby, Nature 210, 1036 (1966).

(43)   S. Sato, R. Yugeta, K. Shinsaka and T. Terao, Bull. Chem. Soc. Japan 39, 156 (1966).

(44)   R. A. Lee and D. A. Armstrong, Nature 200, 552 (1963).

(45)   S. Gordon, E. J. Hart, M. S. Matheson, J. Rabine and J. K. Thomas, Disc. Faraday Soc. 36, 193 (1963).

(46)   E. J. Hart, J. K. Thomas and S. Gordon, Radiation Research Supp. 4, 74 (1964).

(47)   J. P. Keene, Y. Raef and A. J. Swallow, "Pulse Radiolysis" (ed. M. Ebert et al) Academic Press, New York (1965) pp. 99-106.

(48)   E. P. Kalyazin and V. I. Makarov, Neftekhimiya 3, 227 (1963).

(49)   E. P. Kalyazin, Yu. D. Perfil'ev, N. A. Bakh and An. N. Nesmeyanov, Neftekhimiya 6, 582 (1966).

(50)   G. R. Freeman, J. Chem. Phys. 39, 988 (1963).

(51)   G. R. Freeman, J. Chem. Phys. 39, 1580 (1963).

(52)   R. M. Noyes, J. Am. Chem. Soc. 77, 2042 (1955).

(53)   W. R. Busler, D. H. Martin and F. Williams, Disc. Faraday
        Soc. 36, 102 (1963).

(54)   T. J. Hardwick, J. Phys. Chem. 66, 291 (1962).

(55)   G. R. Freeman, J. Chem. Phys. 43, 93 (1965).

(56)   T. J. Hardwick, J. Phys. Chem. 66, 1611 (1962).

(57)   M. A. Dillon and M. Burton, "Pulse Radiolysis" (ed. M. Ebert
        et al) Academic Press, New York (1965) pp. 259-277.

(58)   R. E. Bühler and T. Gäumann, "Pulse Radiolysis" (ed. M. Ebert
        et al) Academic Press, New York (1965) pp. 279-284.

(59)   J. P. Keene, E. J. Land and A. J. Swallow, J. Am. Chem. Soc.
        87, 5284 (1965).

(60)   S. K. Ho and G. R. Freeman, J. Phys. Chem. 68, 2189 (1964).

(61)   P. J. Dyne and W. M. Jenkinson, Can. J. Chem. 38, 539 (1960).

(62)   A. R. Lepley, Anal. Chem. 34, 322 (1962).

(63)   B. M. Hughes and R. J. Hanrahan, J. Chem. Phys. 69, 2707 (1965).

(64)   L. G. Walker, University of Alberta, private communication.

(65)   G. A. Muccini and R. H. Schuler, J. Phys. Chem. 64, 1436 (1960).

(66)   P. J. Dyne and J. Denhartog, Can. J. Chem. 41, 1794 (1963).

(67)   G. R. Freeman, J. Chem. Phys. 36, 1534 (1962).

(68)   G. R. Freeman, J. Chem. Phys. 36, 1542 (1962).

(69)   M. Schlochauer and H. E. Gunning, J. Chem. Phys. $\underline{19}$, 474 (1951).

(70)   E. H. Farmer and C. G. Moore, J. Chem. Soc., 131 (1951).

(71)   A. O. Allen, "Radiation Chemistry of Water and Aqueous Solutions",
        D. Van Nostrand Co., Inc., Princeton, N. J. (1961) pp. 21-22.

(72)   E. W. R. Steacie, "Atomic and Free Radical Reactions", (2nd
        Edition), Vol. 2, Reinhold Publishing Co., New York (1954) p. 498.

(73)   R. Schutte, University of Alberta, private communication.

(74)   J. W. Kraus and J. G. Calvert, J. Am. Chem. Soc. $\underline{79}$, 5921
        (1957).

(75)   G. R. Freeman, J. Chem. Phys. $\underline{46}$, 2822 (1967).

(76)   D. E. Lea, "Actions of Radiation on Living Cells", 2nd Edition,
        Cambridge University Press, (1955) pp. 24-27.

(77)   J. W. Buchanan and F. Williams, J. Chem. Phys. $\underline{44}$, 4377 (1966).

(78)   G. R. Freeman and J. M. Fayadh, J. Chem. Phys. $\underline{43}$, 86 (1965).

(79)   Handbook of Chemistry and Physics, (R. C. Weast, ed.) The
        Chemical Rubber Co., Cleveland, Ohio (1965-66) 46th Edition.

(80)   International Critical Tables, (E. W. Washburn, ed.), McGraw-
        Hill Book Co., Inc., New York (1926).

(81)   R. D. Kleeman, "A Kinetic Theory of Gases and Liquids", John
        Wiley and Sons, New York (1920) p. 132.

(82)   F. T. Jones and T. J. Sworski, J. Phys. Chem. $\underline{70}$, 1546 (1966).

(83)   M. G. Robinson, University of Alberta, private communication.

(84)   G. R. A. Johnson and J. M. Warman, Trans. Faraday Soc. $\underline{61}$,
        1709 (1965).

(85)   T. Shida and W. H. Hamill, J. Am. Chem . Soc. <u>88</u>, 5371

         (1966).

(86)   N. S. Hush and J. A. Pople, Trans. Faraday Soc. <u>51</u>, 600 (1955).

(87)   Kang Yang, J. Am. Chem. Soc. <u>84</u>, 3795 (1962).